2019

Mechanistic Studies of TGFβ-induced Cancer Stem Cell Formation and Mammary Tumorigenesis through an ILEI/LIFR Signaling Axis

Alec N. Woosley
Medical University of South Carolina

Mechanistic Studies of TGFβ-induced Cancer Stem Cell Formation and Mammary Tumorigenesis through an ILEI/LIFR Signaling Axis

Alec N. Woosley

A dissertation submitted to the faculty of the Medical University of South Carolina in partial fulfillment of the requirements for the degree of Doctor of Philosophy in the College of Graduate Studies

Department of Biochemistry and Molecular Biology

2019

Approved by:

Chairman, Advisory Committee _____

Philip H. Howe

_____

Dennis K. Watson

_____

Steven A. Rosenzweig

_____

Vamsi K. Gangaraju

_____

Shaun K. Olsen

_____

David T. Long

Table of Contents:

List of Abbreviations

Akt: Protein Kinase B

α-SMA: alpha Smooth Muscle Actin

BAT: Beta-Activated Translation

BCSC: Breast Cancer Stem Cell

CD24: Cluster of Differentiation 24

CD44: Homing Cell Adhesion Molecule

CSC: Cancer Stem Cell

CNTF: Ciliary Neurotrophic Factor

CT-1: Cardiotrophin 1

CTC: Circulating Tumor Cell

E1KD: E1 Knock-Down

eEF1A1: eukaryotic Elongation Factor 1A1

EGF: Epidermal Growth Factor

EMT: Epithelial-Mesenchymal Transition

Erk: Extracellular-signal-related kinase

FAM3C: Family with sequence similarity member 3C

FGF: Fibroblast Growth Factor

gp130: glycoprotein 130

HMLE: Human Mammary epithelial Cell

IHC: Immunohistochemistry

hnRNP: heterogenous ribonucleoprotein

IL-6: Interleukin-Like 6

ILEI: Interleukin-like EMT inducer

Jak: Janus Kinase

LIF: Leukemia Inhibitory Factor

LIFR: Leukemia Inhibitory Factor Receptor

MAPK: Mitogen-activated protein kinase

MaSC: Mammary Stem Cell

MET: Mesenchymal-Epithelial Transition

MEC: Mammary Epithelial Cell

NMuMG: Normal Murine Mammary Gland

OSM: Oncostatin-M

SCCs: Somatic Stem Cells

STAT3: Signal Transducer and Activator of Transcription 3

TGFβ: Transforming Growth Factor Beta

TIC: Tumor Initiating Cell

TMA: Tumor Microarray

List of Tables

List of Figures

Acknowledgements

I would first and foremost begin by giving tremendous thanks to my friends and family, especially my mother Kathy, my father Greg, and my sister Regan. You have been an integral part of this tremendous journey every step of the way, and I would not have been able to do it without your unconditional love and support through it all. I want to next give thanks to my thesis committee: Drs. Philip Howe, Shaun Olsen, Vamsi Gangaraju, Dennis Watson, Steve Rosenzweig, and David Long. Your guidance throughout my graduate training has given me great confidence as an independent thinker and as a scientist. Phil, thank you for taking me in as a trainee and for being my mentor, I will always owe you a tremendous debt of gratitude for allowing me the opportunity to train in your lab. I carry tremendous respect and admiration for my current and former lab mates: Drs. Bidyut Mohanty, Yong Jiang, Andrew Brown, George Hussey, Annamarie Dalton, Breege Howley, Simon Grelet, Laura Link, and Toros Dincman. As a young and eager graduate student, I laid emphasis on learning as much as I could from those who surrounded me day-to-day in the lab, and there could not have been a better group of colleagues that I had the privilege to work beside and forge relationships with. Special emphasis goes to thanking Drs. George Hussey and Annamarie Dalton, who worked with me extensively during our work on discovering the ILEI/LIFR signaling pathway. I would like to extend thanks to the NIH, the Hollings Cancer Center, MUSC, MUSC-CGS and specifically Dr. Cynthia Wright for giving me the opportunity to pursue my Ph.D. Lastly, I want to thank all of those who strive to make our world a better place through scientific discovery and innovation.

Abstract

ALEC N. WOOSLEY. Mechanistic Studies of TGFβ-induced Cancer Stem Cell Formation and Mammary Tumorigenesis through an ILEI/LIFR Signaling Axis. (Under the direction of PHILIP H. HOWE)

The dual functionalities of Transforming Growth Factor Beta (TGFβ) as either a tumor promoting or suppressing cytokine is highly dependent on cellular context, specifically during malignant transformation and metastatic progression of normal mammary epithelial cells. Our lab has extensively studied the pathologic function of TGFβ in mammary tumorigenesis and metastasis through its role in activating epithelial-mesenchymal transitions (EMT) and cancer stem cell (CSC) phenotypes. We have demonstrated that TGFβ induces EMT and CSC phenotypes in mammary epithelial cells through a non-canonical, translational regulatory mechanism involving an hnRNP complex containing hnRNP E1 that inhibits translation of a cohort of mRNAs. We hypothesized that TGFβ-mediated EMT and CSC formation through hnRNP E1 functional silencing is dependent on ILEI translation and its downstream functional output. Through extensive *in vitro* biochemical, biophysical and cell/molecular analysis we identified a novel mechanism of ILEI signaling through its extracellular ligand-binding and activation of Leukemia Inhibitor Factor Receptor (LIFR). LIFR is highly implicated in embryonic stem cell maintenance through coordination of several key signaling pathways such as Erk/MAPK, PI3K/Akt, and Jak/STAT. We determined that mammary epithelial cells confer EMT and CSC properties through elevated STAT3 activity by TGFβ-induced ILEI translation and subsequent autocrine LIFR

activation. Disruption of this pathway by shRNA silencing of ILEI or LIFR in tumorigenic cell lines results in *in vivo* abrogation of tumorigenesis and metastasis. Interestingly, we can also demonstrate that TGFβ transcriptionally upregulates LIFR in mammary epithelial cells through both canonical (SMAD3) and non-canonical (ILEI/STAT3) pathways in a kinetically coordinated manner. Cellular studies indicate that disruption of either TGFβ/SMAD and/or TGFβ/ILEI/STAT3 pathways alters LIFR transcription and stemness properties that are correlated with enhanced proliferation, invasion, and migration phenotypes. In total, we have established a cellular mechanism by which TGFβ induces mammary EMT and CSC programs in a feed-forward manner through the upregulation of both a ligand (ILEI) and its extracellular receptor (LIFR). These findings provide a novel platform for targeted therapies against mammary tumorigenesis and metastatic spread.

Chapter 1

Introduction

Invasive breast carcinoma is the most common type of cancer among women, with roughly 252,000 new cases arising throughout 2018 in the United States alone [1]. Out of this population of new diagnoses, roughly 40,000 women will succumb to mortality, validating the disease as a major public health issue [1]. Although primary breast cancers can be treated through surgical intervention and targeted therapies that result in a 99% 5-year relative survival rate, metastasis and invasion from the mammary epithelium into secondary sites decreases this rate to roughly 25%, validating a critical need for therapies that specifically target metastases[1]. At the cell and molecular level, breast cancers are categorized into several subtypes and morphologic profiles that ultimately dictate pathology, prognosis and therapeutic strategy [2,3]. Immunohistochemistry (IHC) analysis of estrogen receptor (ER), progesterone receptor (PR), and human epidermal growth factor receptor (HER2), as well as clinical features such as tumor grade, size and nodal pathology are a current standard for assessing clinical management and prognosis [4,5]. These receptors are critical in regulating growth and survival of mammary cell populations and are highly implicated in treatment strategies. Cell-to-cell communication by extracellular receptors is critically abrogated or enhanced during mammary tumorigenesis, resulting in misregulation of downstream transcriptional and phenotypic outputs. In addition to hormone receptor function in mammary epithelial cell survival and proliferation, maintenance of the development and morphogenesis of the mammary epithelium is also highly

regulated by cytokines such as several Interleukins, tumor necrosis factor alpha (TNFα), and transforming growth factor beta (TGFβ) [6–8].

The TGFβ superfamily encompasses 30 growth factor genes in mammals including 3 TGFβ isoforms (TGFβ 1-3) that are similar in their biological activities *in vitro* but encoded and expressed in a tissue-specific, regulatory manner [9]. Evolutionarily, there is evidence of the major TGFβ signaling network genes found in primitive metazoans such as *Trichoplax adhaerens* [10]. In humans, TGFβ1 mRNA is enriched in endothelial, hematopoietic and connective-tissue cell populations; TGFβ2 mRNA is detected in epithelial and neuronal cells, and TGFβ3 mRNA is primarily found in mesenchymal cells [9,11]. During the normal lifespan of mammals, TGFβ1 and TGFβ3 are expressed and heavily utilized during early morphogenesis, while TGFβ2 is critical for the maturing and differentiating epithelium [9,12] . Thus, cellular mechanisms controlled by TGFβ account for major developmental programs that dictate not only early development but also cell behavior and fate within the mature organism. Originally discovered in the early 1980s, TGFβ was first purified from human platelets, placenta, and bovine kidney extracts [13–16]. TGFβ was initially observed to enhance anchorage-independent growth in normal fibroblastic cell populations by cell stimulation assays [17–19]. As mentioned above, TGFβ isoforms are ubiquitously expressed in almost all cell types with the highest levels being derived from platelet populations [17–20] . TGFβ serves many biologic roles during both normal cell homeostasis as well as during disease onset and progression that is highly dependent on cell-state. For example, TGFβ is highly implicated in the differentiation and self-renewal properties of both embryonic stem

cells (ESCs) and Somatic stem cells (SCCs) through tight the control of transcriptional programs during development [21]. TGFβ 1-3 is synthesized as a homodimeric molecule containing an N-terminal propeptide region that gives a total molecular weight of 75kD (termed pro-TGFβ) [22]. The dimeric propeptide regions, termed the latency-associated proteins (LAPs), are enzymatically cleaved from the active 24kD TGFβ dimer. Tight control of TGFβ concentrations in the extracellular space is mediated by pro-TGFβ being tethered to the extracellular matrix (ECM) by the latent TGFβ binding proteins (LTBPs) [22]. This results in TGFβ "sensing" that allows for stringent control of cytokine activation through rapid temporal modulation by the cell [22]. Activated TGFβ functions through coordination and high-affinity binding to a subset of cell-surface receptors broadly termed the type I (signal propagating, TGFβR1) and type II (activating, TGFβRII) TGFβ receptors [9]. Seven type I and five type II receptors exist in humans in addition to several extracellular regulators that dictate receptor activation potential as well as available ligand concentration [6,23]. Activation of the TGFβ receptor complexes induces downstream transcriptional outputs canonically through the SMAD family of transcription factors [24]. These factors were originally discovered in type I TGFβ receptor activation results in its kinase activity upon the regulatory SMADs (R-SMADs) 1, 2, 3, 5, and 8 on their extreme C-terminal regions [25]. This phosphorylation event allows for R-SMADs to form as dimers or in complex with the common mediator SMAD4 [24,25]. R-SMAD complexes containing SMAD4 are then able to translocate to the nucleus and directly regulate the enhanced or abrogated transcription of target genes [25,26] . Since the SMADs alone do not bind

with high affinity to DNA, several R-SMAD/SMAD4 complexes will further associate with additional non-SMAD transcription factors in the nucleus to confer sufficient DNA-binding capability as well as added complexity to the transcriptional output [26]. SMAD3 has been demonstrated to form transcriptional complexes with master regulators of mouse ESC maintenance such as Oct4, Nanog and Sox2 [27,28]. SMAD3 has also been shown to accumulate at "super-enhancer" regions that regulate genes controlling cell identity [28,29]. In addition to canonical SMAD signaling, TGFβ also regulates the activation of several major signaling modalities such as the MAP kinase, Rho-like GTPase, and phosphatidylinositol-3-kinase/Akt pathways [30–33].

In the context of epithelial cancers TGFβ serves paradoxical roles by functioning as both a tumor suppressor gene during pre-malignancy and remarkably switching to a pro-oncogenic role during late tumor progression and metastasis [6,34,35]. This dual functionality is linked to altered cellular responses to TGFβ during tumor progression that "hijack" its signaling pathways in order to facilitate oncogenic transformation and downstream metastatic events [34,35]. One cellular mechanism that may be guided by aberrant TGFβ signaling during malignant transformation is the epithelial-mesenchymal transition (EMT) [36–38]. Under normal homeostatic conditions, EMT is utilized by TGFβ during early embryogenesis, tissue remodeling, and wound healing [38,39]. The EMT program induces a functional alteration of several transcriptional factors (ZEBs, SNAIL, SLUG, TWIST, Wnt/β-catenin), regulation of cytoskeletal remodeling (E/N-cadherin switching), functional non-coding RNAs, and epigenetic modifications

that result in dramatically transformed cellular phenotypes [39–41]. All of the molecular processes that induce EMT are highly dynamic and reversible as during the mesenchymal-epithelial transition (MET) [36,42]. The misregulation of the highly transient EMT/MET process is implicated during fibrosis, inflammation, and cancer progression through altered cellular acquisition of invasive and migratory phenotypes [34,35,42].

It has been postulated that reducing the rate at which primary breast cancers form metastatic derivatives can be accomplished through targeting the molecular switches that guide EMT programs that subsequently enrich fibroblasts that harbor stem cell phenotypes. It has been extensively demonstrated that the TGFβ pathway is instrumental in maintaining self-renewal and differentiation capabilities of ESCs [21]. The presence of cancer cells that are phenotypically similar to stem cells, also termed tumor initiating cells (TICs), has been shown in several cancer types including breast, skin, and brain malignancies [43–46]. These cell populations were originally discovered in hematologic cancers, whereby isolation an analysis of circulating tumor cells (CTCs) revealed surface marker expression profiles remarkably similar to hematopoietic stem cells [43,47,48]. Breast TICs, termed breast cancer stem cells (BCSCs), are thought to serve as molecular “seeds” for secondary tumor formation due to their ability to potently induce tumorigenesis, self-renew, and differentiate [39,48,49]. These phenotypes derived from single cell populations may explain the presence of complex cellular hierarchies and the heterogenous nature of solid tumors [48,50]. Cells that have undergone an EMT are tumorigenic, capable of forming mammospheres, and possess surface markers

and gene expression profiles similar to both mammary stem cells (MaSCs) and other CSC types [51,52]. Weinberg and his colleagues performed experiments that enriched mammary epithelial cells that had undergone EMT by TGFβ stimulation and probed their surface marker expression patterns to see any similarities to MaSCs. Indeed, tumorigenic epithelial cells that had undergone an EMT acquired a $CD24^{low}/CD44^{high}$ profile that is characteristic of MaSCs [51]. Isolation of these subsets of cells followed by mammary fat pad injection demonstrated potent tumor initiating frequencies when compared to populations with a non stem-like $CD24^{high}/CD44^{low}$ profile [51]. The role of TGFβ-mediated EMT in metastasis and BCSC formation has been established by several groups who demonstrate that within the normal mammary gland as well as other epithelial organs, an EMT program is utilized in order to enter a BCSC state [53–55]. An important aspect of BCSCs generated from neoplastic cells having undergone an EMT is their ability to resist the efficacy of several chemotherapeutic drugs that target bulk epithelial cell populations within primary tumors [56,57].

TGFβ is a potent inducer of EMT and promotes loss of cell-cell adhesions and concomitant acquisition of an invasive, migratory phenotype during late tumor progression [18,35,58]. Our lab has shown a non-canonical mode of TGFβ-mediated EMT induction through a tumor suppressor ribonucleoprotein (mRNP) complex containing heterogeneous nuclear ribonucleoprotein E1 (hnRNP-E1) and eukaryotic elongation factor 1A1 (eEF1a1) [59,60]. This complex binds a structurally conserved 3'UTR or BAT element (TGFβ activated translation) and inhibits translation of several mRNAs involved in EMT. TGFβ stimulation initiates the non-

canonical Akt2 kinase cascade and promotes complex release from mRNA, resulting in restored protein translation and EMT [59,60]. Using a genome-wide combinatorial approach by expression profiling and RIP-Chip analysis, our lab revealed a cohort of over 30 mRNAs that are controlled by this 3'-UTR BAT mechanism of translational regulation by TGFβ [59–61]. One gene of importance discovered to be translationally regulated by this mechanism is FAM3C *Interleukin-like EMT* Inducer (ILEI) [59–61]. ILEI is a secreted factor that was discovered after structure-based analysis of novel four-helical bundle cytokines that adopt conformations similar to Interleukin-6 (IL-6), Leukemia Inhibitory Factor (LIF), Oncostatin-M (OSM) [62–65]. belonging to the FAM3 family of cytokine-like molecules and is involved in EMT, tumor progression, and retinal laminar formation [66–68]. Stable overexpression of ILEI promotes tumorigenesis in mouse models using xenograft implantation [66]. These observations remain as the only biological assay for ILEI function, due primarily to the past inability to generate recombinant protein that is biological active for *in vitro* studies. Although there is little known regarding the signaling mechanism of ILEI, its designation as a potent inducer of EMT and tumor progression validates it as an attractive target for drug development [66–68].

An important aspect of elucidating an ILEI signaling pathway is characterizing the extracellular receptor that mediates its functional output. The work within aimed to understand these processes through a cohort of *in vitro* and *in vivo* analyses into potential ILEI signaling modalities. Many extracellular cytokines utilize Leukemia inhibitory factor receptor (LIFR) for cell signaling, regulating a variety of downstream functions including stem cell maintenance and

self-renewal properties through ligand-binding to Leukemia inhibitory factor (LIF) [69,70]. The mechanism of signal transduction through LIFR has traditionally required ligand-induced heterodimer formation with the shared receptor gp130, a founding member of the tall receptors that is also involved in the IL-6/IL-12 signaling cascade through ligand-induced homodimerization [71]. Heterodimerization of gp130 with LIFR activates cytoplasmic tail-bound Janus kinases (JAKs) via auto- and trans-phosphorylation [71,72]. This activation subsequently enables the formation of cytoplasmic docking sites for several downstream signaling effectors including STAT proteins and components of the MAPK and PI3K pathways [72,73]. LIFR/gp130 signaling through LIF-binding is reported to have a role in mediating induction and maintenance of embryonic stem cells through Jak/STAT activation [69]. Within the context of cancer progression, LIFR serves dual roles as a tumor suppressor and promoter similar to that of TGFβ. Studies have shown that LIFR suppresses metastasis through activation of the Hippo-YAP pathway in breast malignancy [74]. Another group demonstrated tumor dormancy phenotypes in breast cancer being controlled by LIFR signaling [75]. Within other cancer types such as hepatocellular carcinoma and pancreatic malignancy, LIFR has been shown to inhibit metastasis [76,77]. As a tumor promoting factor, LIFR has been shown to stimulate melanoma cell migration and associate with an unfavorable prognosis [78]. It has been also demonstrated to enhance metastasis in prostate cancer through epigenetic activation by KMT2D histone methyltransferase activity [79]. Given the paradigm of LIFR signaling in tumorigenesis and metastasis, a truly defined mechanism that

dictates cellular phenotypes downstream of LIFR activation is driven by several variables including ligand availability and cell-type.

The studies highlighted within this work indicate that ILEI serves as a binding partner to LIFR via yeast-two-hybrid screening, giving a potential ILEI receptor candidate. Although ILEI plays an important role in mammary epithelial EMT and tumorigenesis, a mechanism describing ILEI function and downstream signaling modalities has remained elusive due to inability to produce bioactive material. Although this aspect of the work is not extensively shown in the forthcoming chapters, the time and effort it took to reach the goal of bioactive, purified ILEI in large yields was extremely challenging. It is therefore extremely important to highlight detailed purification strategies that were performed that led to the discovery of the biologically active ILEI protein. Figure 1 demonstrates a general overview of the strategies implemented in the enrichment of bioactive protein through several expression/purification systems (Fig 1). As mentioned above, ILEI is translated after hnRNP E1 phosphorylation or silencing as a 25kD protein containing 25 amino acid signaling sequence and 17 amino acid pro-peptide region (Fig 1A). Amino acids 1-43 are cleaved upon the release of the mature ILEI cytokine into extracellular space [80]. Traditional overexpression systems in *E.coli*, mammalian, and yeast cells yielded varying amounts of pure protein that did not induce signaling activity when treated on cells (Fig 1B). Since ILEI is a secreted factor, mammalian purifications had to be executed out of the conditioned medium. We also isolated an endogenous ILEI gene product using traditional protein chemistry methods in WM9 melanoma cell conditioned media.

This protein induced LIFR phosphorylation and STAT3 activation *in vitro* but could only be produced in minimal yields. It was not until recent structural findings highlighting the importance of ILEI dimerization that we discovered scaled up purification schemes of the active molecule. A current understanding of the ILEI structure describes a disulfide-mediated dimerization mechanism that results in "domain swapping" of two ILEI monomers [81].. Interestingly, only a small fraction of the total protein is dimeric, suggesting a potential co-factor that may enhance dimer stability in the extracellular space [81]. Since we often observed biological activity in long-term assays in cell culture conditions, we hypothesized that dimers are formed at higher temperature over time. With this knowledge, we first designed recombinant ILEI chimeras as well as optimized *E. Coli* expression system parameters with the goal of enriching the dimer species. This protein did not display any activity. We optimized a purification protocol that included an incubation test at different temperatures to attempt to facilitate dimerization (Fig 1C). Polyacrylamide electrophoresis analysis of purified ILEI derived from multiple sources shows that dimerization depends on intact disulfide bridges, as the dimeric species becomes monomeric in the presence of beta mercaptoethanol (Fig 1D-E). Ultimately, two factors controlled the dimerization phenomenon in *E. Coli* : (1) temperature of protein storage and (2) salt concentration of the buffer system used throughout the purification process (Fig 1D). In summary, we optimized a protocol of ILEI purification in *E. Coli* that produces high amounts of bioactive material (Refer to Figure 1 and the methods section for an overview of the ILEI purification protocol out of *E. Coli*.).

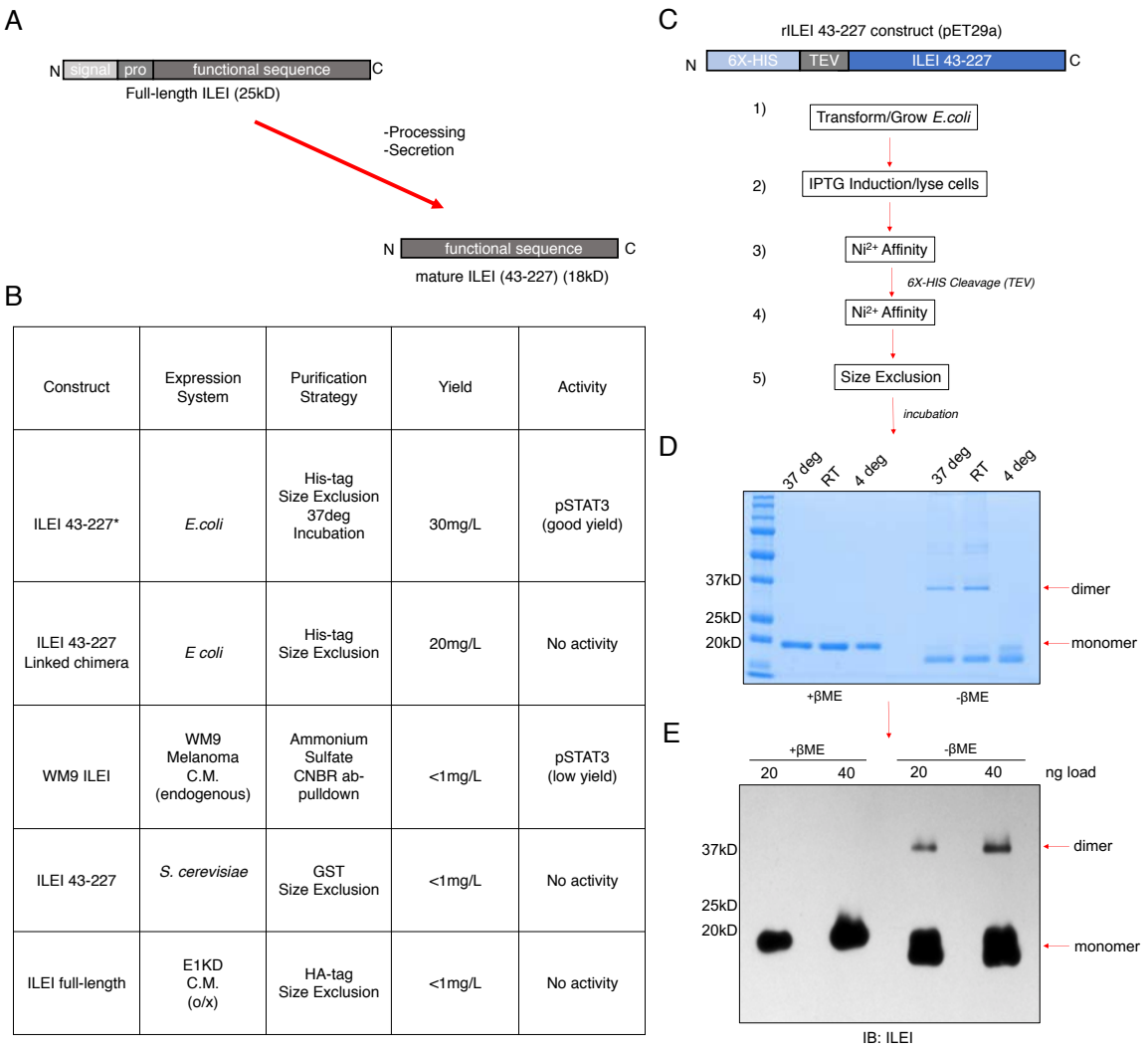

Construct	Expression System	Purification Strategy	Yield	Activity
ILEI 43-227*	*E.coli*	His-tag Size Exclusion 37deg Incubation	30mg/L	pSTAT3 (good yield)
ILEI 43-227 Linked chimera	*E coli*	His-tag Size Exclusion	20mg/L	No activity
WM9 ILEI	WM9 Melanoma C.M. (endogenous)	Ammonium Sulfate CNBR ab- pulldown	<1mg/L	pSTAT3 (low yield)
ILEI 43-227	*S. cerevisiae*	GST Size Exclusion	<1mg/L	No activity
ILEI full-length	E1KD C.M. (o/x)	HA-tag Size Exclusion	<1mg/L	No activity

Fig 1. ILEI purification strategies. (A) ILEI construct diagram demonstrating post-translation processing to the mature form ranging amino acids 43-227. (B) Table depicting constructs worked with throughout the duration of this project. (C) Active ILEI purification strategy derived for ILEI 43-227*. (D) Coomassie-stained SDS-PAGE gel analyzing rILEI after purification and incubation for 24 hours in temperatures ranging from 37deg-4deg in the presence and absence of beta mercaptoethanol. (E) Immunoblot analysis of rILEI in the presence and absence of beta mercaptoethanol.

The data presented in this dissertation represent a potential novel signaling mechanism that plays a role in BCSC phenotypes through a non-canonical mode of TGFβ signaling. Neoplastic mammary epithelial cells that have undergone an EMT are established as possessing significantly increased metastatic activity and

resistance to chemotherapeutics, due primarily to conventional therapies targeting bulk populations without effectively targeting subpopulations of BCSCs that possess enhanced mesenchymal traits. Elucidating the mechanism of ILEI function through the identification of its signaling receptor is of high impact due to the importance of ILEI in EMT and BCSC formation. These observations will provide a blueprint for development of novel therapeutics that selectively target ILEI-mediated EMT and BCSC formation. Our molecular studies involving receptor/ligand interactions will represent an immediate logical basis for small molecule design focused on antagonizing ILEI ligand-binding and activation of STAT pathway activation through LIFR.

Chapter 2

Materials and Methods

Cell Culture, Treatments and Cell Manipulations

NMuMG (ATCC), HMLE, HEK293 (ATCC) and HEK293t (ATCC) cells were maintained at 37°C, 5% v/v CO_2 in a humidified incubator. NMuMG, HEK293 and HEK293t cells were cultured in DMEM (Corning) high glucose supplemented with 10% fetal bovine serum (Atlanta Biologicals) and 1% antibiotic/antimycotic solution (penicillin G, streptomycin, amphotericin B) (ThermoFisher). HMLE cells were isolated for trypsin resistance and sorted by FACS as previously described [82]. HMLE cells were cultured in DMEM:F12 supplemented with 5% calf serum (VWR), 0.5 µg/ml hydrocortisone, 10 µg/ml insulin, 20 ng/ml epidermal growth factor (Corning) and 1% antibiotic/antimycotic. TGFβ treatments were conducted using 5 ng/mL recombinant TGBβ2 (Genzyme) for the indicated durations. Phase contrast cell images were obtained using a Leica DM IL LED Inverted Phase Contrast microscope. Lentiviral constructs were obtained from the shRNA core at MUSC or cloned into the pLKO.1-neo construct (Addgene) using EcoR1/Age1 sites. Sequences for the shRNA hairpins are listed in Table 1. HEK293t cells were grown to 60-70% confluence and transfected with the pLKO.1 shRNA plasmid containing the targeted hairpins, psPAX2 and pMD2.G packaging plasmids using Lipofectamine 3000 in OPTI-MEM. Media was changed after overnight incubation to fresh culture media. Virus was collected and filtered at 24 and 48 hours through a 0.22 µm sterile filter. For transduction, 1:5 to 1:2 ratios of virus containing media to culture

media was incubated on the target cells with 8 μg/mL polybrene overnight. Culture media was changed to include either 1 μg/mL puromycin (ACROS Organics) or 2 mg/mL G418 (Invivogen) for NMuMG derivative cells. Resistant pools were collected for experimentation. For experiments utilizing siRNAs, cells were transfected at 60-70% confluence using Lipofectamine 3000 in OPTI-MEM for 24 hours before analyzing RNA and whole cell lysates for successful knock-down. Cells transfected with siRNA for mammosphere assays were monitored over the course of ten days post-transfection in order to observe steady knockdown during the experiments (siRNA sources below in Table 1). For inhibitor studies, cells were treated with either Stattic (Santa Cruz) or SIS3 (Millipore Sigma) at indicated concentrations.

MTT Assay

Cell lines were seeded at 1×10^3 cells per well in a 96-well plate and cultured overnight prior to any drug treatments. MTT assay was performed by addition of 20 μl of a 5 mg/ml MTT solution and incubation for 3 h at 37 °C. To stop the reaction, 100 μl MTT stop mix (40% dimethyl formamide, 20% sodium dodecyl sulfate (SDS)) was added and plates were incubated for 1 h at room temperature with shaking. The reduction of yellow MTT to purple formazan by viable cells was detected by reading absorbance at 590 nm using a Wallac Victor3 plate reader.

Mammosphere Assay

NMuMG wild-type and derivative cell lines were cultured either in the presence or absence of 5 ng/mL TGFβ for 9 days and were trypsinized from 2D adherent

culture plates. Cell suspensions were diluted to 2,500 cells/mL and seeded into a 96-well non-adherent plate (500 cells/well) containing DMEM (Corning), 20 ng/mL epidermal growth factor (Corning), 20 ng/mL fibroblast growth factor (Corning) and B27 supplement (Gibco). After 7-9 days, spheroids from each cell line (n=5) were quantified under phase-contrast microscopy. For passaging, the mammospheres were pooled, trypsinized, and passed through a 0.22 micron filtered syringe before re-seeding into a fresh 96-well non-adherent plate. After an additional 7-9 days, spheroids that self-renewed were again quantified under phase-contrast microscopy with a Leica DM IL LED Inverted Phase Contrast microscope. Cell growth was considered a mammosphere at 100μm diameter for all mammosphere assays.

Human lung cancer cell line A549 shRNA constructs was cultured in adherent conditions in RPMI 1640 medium (HyClone, Logan, UT) supplemented with 10% FBS (Atlanta Biologicals, Flowery Branch, GA), 1X antibiotic–antimycotic (ThermoFisher, Waltham, MA), and prophylactic plasmocin (InvivoGen, San Diego, CA) at 37 °C and in 5% CO_2. After 3-4 days, cells were detached using 1X trypsin-EDTA (ThermoFisher, Waltham, MA). Following a wash in 1X PBS (Fisher Scientific, Fair Lawn, NJ), cells were resuspended in serum free DMEM/F12 with 1x B-27 supplement (ThermoFisher, Waltham, MA), 20ng/ml human recombinant EGF, 20ng/ml mFGF, 1X antibiotic–antimycotic, and 0.25% methyl cellulose (Sigma-Aldrich, St. Louis, MO) to reduce cell aggregation. Cells were plated at 1000 cells/ml in anchorage-independent conditions using a 6 well ultra-low

attachment plate. Spheres were grown for 10 days at 37 °C and in 5% CO_2 and then counted under light microscopy. Images were obtained at 5x magnification.

Western Blotting

Whole cell lysates were extracted as follows: Appropriate volumes of Tris-Triton lysis buffer (20 mM Tris pH 7.5, 1% Triton X-100, 10% glycerol, 137 mM NaCl, 2 mM EDTA, and Halt Protease and Phosphatase Inhibitor cocktail (ThermoFisher) was added to cell plates. Cells were immediately scraped, incubated on ice for 30 minutes, and cleared by centrifugation for 20 minutes at 16,000 x g. Protein concentrations were measured with Bradford Protein Assay (BioRad). For conditioned medium immunoblots, cells were serum starved overnight in serum-free DMEM. Medium was collected and precipitated using trichloroacetic acid/acetone. Protein samples were denatured by incubating at 95° for 5 minutes with 1x Laemmli reducing denaturing sample buffer (60 mM Tris-Cl pH 6.8, 1% SDS, 10% glycerol, 5% BME). 1–100 µg of whole cell lysate was resolved on a 8, 10, or 12% polyacrylamide SDS gels and transferred onto PVDF membrane. Membranes were blocked for 1h at RT in 5% skim milk/Tris-buffered saline with 0.01% Tween-20 (TBST) and incubated overnight at 4° on primary antibody + 5% skim milk/TBST. The following primary antibodies were used: ILEI (ab72182; Abcam; 1:1,000), hnRNP E1 (#M01, Abnova; 1: 1,000), E-Cadherin (#610181; BD biosciences; 1:5,000), N-Cadherin (#610920; BD Biosciences; 1:5,000), alpha smooth muscle Actin (ab5694; Abcam; 1:1,000), LIFR (sc-659, Santa Cruz; 1:1,000), FLAG (#2368, Cell Signaling Technologies; 1:1,000), pSTAT3 (#9145,

Cell Signaling Technologies; 1:1,000), STAT3 (#4904, Cell Signaling Technologies; 1:5,000), gp130 (sc-376280, Santa Cruz; 1:1,000), pTYR (#9416, Cell Signaling Technologies; 1:5,000), pSMAD3 (#9520, Cell Signaling Technologies; 1:500), SMAD3 (sc-101154, Santa Cruz; 1:1,000), GAPDH (sc-32233; Santa Cruz; 1:10,000), and HSP90 (sc-13119; Santa Cruz; 1:10,000). After primary antibody incubation, membranes were washed 4x 15 minutes in TBST and incubated for 1h at RT on secondary antibody + TBST. The following secondary antibodies were used: Goat anti-Mouse IgG (31430; ThermoFisher; 1:10,000) and Goat anti-Rabbit IgG (31460; ThermoFisher; 1:10,000). After secondary antibody incubation, membranes were washed 4x 15 minutes in TBST and detected using Luminata Forte Western HRP substrate (EMD Millipore) and HyBlot CL Autoradiography Film (Denville) or CCD camera (BioRad ChemiDoc System; BioRad).

Bacterial Protein Purification

Bacterial protein preparation was initiated using a construct that spans human amino acids 43-227 with an N-terminal TEV-cleavable hexahistidine tag for purification. BL21 transformed bacterial cells were induced with IPTG for 4 hours. After centrifugation at 8,000 rpm for 15 minutes, the resulting bacterial pellets were resuspended in 20mM Tris-HCl pH 8, 20% sucrose. Cell suspensions were flash frozen and subsequently slow thawed in a circulating ice bath. Lysis Buffer (350mM NaCl (VWR), 10mM Imidazole, 100µg/L Lysozyme (MP Biomedicals), and 1mM BME) was added to the thawing cells suspension then centrifuged at 35,000 rpm for 1 hour at 4°C in a SW40 rotor using a Beckman UltraCentrifuge (Optima LE-80K). His-tagged ILEI was separated from the clarified lysate using

HisPur NiNTA resin (Thermo Scientific). The histidine tag was removed using a his tagged TEV protease. Cleavage was conducted overnight at 4°C and the digested his tag and TEV protein was separated from ILEI using HisPur NiNTA resin. rILEI was further purified by gel filtration on a SD75 16/60 column to greater than 95% purity (GE Healthcare).

Flow Cytometry

HMLE cells were cultured in normal growth media to 70% confluence in 6cm dishes (Denville). Cells were trypsinized, washed 2 times with PBS and resuspended in 1 mL 4% paraformaldehyde (Alfa Aesar) in PBS for 10 minutes at 37°C and one minute on ice. After fixation, cells were washed 3 times in PBS + 1% BSA (Fisher). Cells were incubated with PE conjugated anti-human CD24 antibody (1:400) (Biolegend) and FITC conjugated anti-human CD44 primary antibody (1:400) (Biolegend) in 100µL PBS + 1% BSA for 1 hour at room temperature. Cells were washed 3 times in PBS + 1% BSA, resuspended in 500µL PBS and filtered through a 40µm mesh strainer. Flow cytometry was performed on a BD Fortessa X-20 Analytic Flow Cytometry and analyzed using the BD Diva software. The ALDEFLUOR assay was conducted according to manufacturer's instructions (Stem Cell Technologies) in NMuMG shScr and E1KD cells modulated for ILEI and LIFR. Briefly, cells were grown to 70% confluence, trypsinized, washed in PBS, and resuspended at a concentration of $1*10^6$ cells per mL in ALDEFLUOR buffer. 5µL ALDEFLUOR reagent was added to 1mL suspended cell solution. 500µL of the suspension was immediately transferred to a tube containing 5µL DEAB. All solutions were incubated for 45 minutes at room

temperature. Subsequently, cells were pelleted, resuspended in 500µL ALDEFLUOR buffer and filtered through a 40µm mesh strainer. Flow cytometry was performed on 30,000 event counts using a BD Fortessa X-20 Analytic Flow Cytometry and analyzed using FlowJo software (FlowJo, LLC).

Yeast Two-hybrid Screening

ILEI ORF (corresponding to amino acid 42-227) was cloned into the yeast two-hybrid DNA-binding domain vector pGAD424 (Clontech) and transformed into the yeast strain PJ69-4A [83]. The strain was mated with the yeast strain Y187 containing a normalized library of HeLa cell cDNAs cloned into a GAL4 AD vector (Clontech, Takara). The resulting library in the diploid strain was screened for activation of the *ADE2* reporter gene on yeast minimal medium lacking leucine, tryptophan and adenine. The positive clones were confirmed for interaction by further tests in PJ69-4A strain and plasmid DNA sequenced to identify the interacting genes.

Protein Binding Experiments

Recombinant human ILEI protein (Sino Biologicals) and recombinant human LIF protein (R&D) were radio labeled with ^{125}I (Perkin Elmer) using Iodobeads (Peirce) as described by the manufacturer. Briefly, Iodobeads were washed twice with PBS pH 7.2 and air dried. 5µg BSA (Fisher), rLIF, or rILEI was dissolved in 200µL PBS pH 7.2 with one washed Iodobead and 0.6mCi Na^{125}I (Perkin Elmer). The reaction mixture was incubated for 15 minutes at room temperature. Solution was removed from the Iodobead to quench the reaction and radiolabeled protein was separated from free Na^{125}I using PD-10 prepacked gravity columns (GE Healthcare).

HEK293 cells were transiently transfected with either empty pcDNA3.1 (Addgene) vector or pcDNA3.1-LIFR-flag using Lipofectamine 3000 (ThermoFisher) where indicated. Binding experiments were conducted 24 hours after transfection where applicable. Transiently transfected HEK293 or untransfected E1KD cells were cultured to 90% confluence in a 6 well dish, washed with PBS and incubated with radiolabeled protein or unlabeled protein for western blotting for 2 hours at 4°C with gentle rocking. 1mM bis(sulfosuccinimidyl)suberate (BS3) (ThermoFisher) was added to the well and incubated at room temperature for 30 minutes before quenching the crosslinking reaction with 20mM Tris pH 7.5 for 15 minutes at room temperature. Cell lysates were analyzed by 8% SDS-PAGE gel electrophoresis. Gels were dried, exposed to a phosphorImager screen and observed using a Typhoon FLA 1900 PhosphorImager or transferred to PVDF (BioRad) for western blotting analysis.

PCR analysis

Total RNA was isolated using TRIzol (ThermoFisher Scientific). cDNA synthesis was performed using qScript cDNA synthesis kits with 1ug of total RNA (Quantabio). Semi-quantitative PCR was conducted on 10 ng of cDNA using Maxima Hot Start PCR Master Mix (ThermoFisher Scientific). Real-time quantitative PCR was conducted using iQ SYBR Green Supermix (Bio-Rad) using CFX384 Real-Time System (Bio-Rad). Reactions were conducted on 50 to 10 ng of cDNA. Primers are listed in Supplementary Table 2. Relative gene expression was calculated using RFX Manager software, and genes were normalized to GAPDH internal control.

Tissue Microarray and immunohistochemistry

TMA sample identification is listed in Table S2. 5 μm FFPE sections were routinely deparaffinized in xylene, rehydrated in alcohol, and processed as follows: The sections were incubated with target retrieval solution (Dako S1699) in a steamer (Oster CKSTSTMD5-W) for 10 minutes and then 3% hydrogen peroxide solution for 10 minutes and protein block (Dako X0909) for 20 minutes at room temperature. FAM3C (Sigma HPA050548) 1:1,600, incubation in a humid chamber at 4^{o}C overnight followed by biotinylated secondary antibody for 30 minutes and ABC reagent (Vector PK-6101) for 30 minutes. Immunocomplexes of horseradish peroxidase was visualized by DAB (Dako K3468), and sections were counterstained with hematoxylin before mounting. Samples were imaged using a using Leica DM IL LED Inverted Phase Contrast microscope and scored blindly 0-3 for staining intensity by three independent researchers and averaged for the final IHC score. Images representing scores 0-3 are shown in Fig. S4a. Student's t-test statistical analysis was performed using Prism 7 (Graphpad).

Mammary Fat Pad Clearance Assay

Mammary fat pad clearance surgery was performed on 3-week old NOD/SCID (Breeders obtained from Jackson Labs) according to the minimally invasive protocol [84]. Briefly, mice were anesthetized using isoflurane and prepared for surgery by shaving the region around the 4th nipple, scrubbed the sight with betadine and alcohol wipes alternating three times each and applied topical lidocaine. A small incision around the 4th nipple was made, adjacent fat pad was

separated from skin and surrounding muscle, and excised. 5,000 cells as indicated in 10μL of PBS suspension was injected into the visible cleared fat pad using a pointed Hamilton Syringe. Reconstituted fat pads were excised after a 6-week period. After extraction, fat pads were spread on a glass slide, allowed to air dry briefly to prevent future dissociation from the slide and placed in Carnoy's Fixative (60% ethanol, 30% CHCl3, and 10% glacial acetic acid) overnight at 4°C. Slides were washed in 70% ethanol, 50% ethanol, 30% ethanol and water, each step for 20 minutes at room temperature. After hydration, slides were placed in Carmine stain overnight at room temperature. Carmine stain was prepared as follows: Place 1g carmine (Sigma C1022) and 2.5g aluminum potassium sulfate (Sigma A7167) in 500mL dH_20 and boil 20 min. Adjusted final volume to 500mL with H_20. Filtered and refrigerated. Once stained, fat pads were dehydrated in sequential ethanol washes at 70%, 95% and 100% for 15 minutes each at room temperature. Fat was cleared using toluene overnight and slides were mounted using Permount (Fisher). Slides were visualized for Carmine stain by bright field imaging, and RFP and GFP fluorescent signal using a 1.25x objective on an Olympus BX61 Fluorescent Microscope with an Olympus DP72 8-bit RGB camera and Cellsens software in the Laboratory Core in the Center for Oral Health Research at MUSC.

Serial Dilution Mammary Fat Pad Injection Studies

8 week old NOD.CB17-Prkdc^{scid}/J mice (Jackson Labs) were injected with 100μL PBS cell suspension using E1KD shScr, E1KD shILEI or E1KD shLIFR cells at 1,000, 10,000 or 100,000 cells per fat pad. Mice were evaluated weekly using

calipers to assess tumor volume. Mice were sacrificed and tumors and lungs were extracted at 13-14 weeks. Final tumor volumes were weighed and lungs were stained for H&E. Briefly, lungs were formalin-fixed and paraffin-embedded in the Biorepository and Tissue Analysis Core at MUSC. Paraffin-embedded lungs were cut into 5 μm sections and stained with hematoxylin and eosin. H&E stained lungs were imaged using a 1.25x objective on an Olympus BX61 Microscope with an Olympus DP72 8-bit RGB camera and Cellsens software in the Laboratory Core in the Center for Oral Health Research at MUSC. Two-way Anova statistical analysis for volume measurements over time and Student T-test analysis of final tumor weights and metastatic tumor burden were performed using Prism 7 (Graphpad).

Table 1: si/shRNA sources and sequences

shRNA and siRNA	Referred to herein as	Sequence	Source
Scramble siRNA	siSCRAM/scarm	#6568	Cell Signaling Technologies
Mouse/human hnRNP E1 shRNA	E1KD	CCGGCCATGATCCAACTGTGTAATTCTC GAGAATTACACAGTTGGATCATGGTTTT TG (TRCN0000120937)	MUSC Hollings Cancer Center shRNA Shared Resource Technology
Mouse shILEI	shILEI	CCGGGAACAGCACATAAAGAACAATCT CGAGATTGTTCTTTATGTGCTGTTCTTT TTTG (TRCN0000191798)	MUSC Hollings Cancer Center shRNA Shared Resource Technology
Mouse siILEI 1	siILEI 1/siILEI	D057098-01-002	Dharmacon Inc
Mouse siILEI 2	siILEI 2	D-057098-02-002	Dharmacon Inc
Human shILEI 1	shILEI 1	CCGGATGTTGGAAGAGGGATCAATGCT CGAGCATTGATCCCTCTTCCAACATTTT TTG (TRCN0000298583)	MUSC Hollings Cancer Center shRNA Shared Resource Technology
Human shILEI 2	shILEI 2	CCGGGAGGAGATGTGGCACCATTTACT CGAGTAAATGGTGCCACATCTCCTCTT TTTG (TRCN0000298584)	MUSC Hollings Cancer Center shRNA Shared Resource Technology
Human shILEI 3	shILEI 3	CCGGCTTGGTGTGTGCATGAGTATTCT CGAGAATACTCATGCACACACCAAGTT TTTG (TRCN0000293815)	MUSC Hollings Cancer Center shRNA Shared Resource Technology
Mouse shLIFR	shLIFR	CCGGGCAGAGATACAGCTTAGTAAACT CGAGTTTACTAAGCTGTATCTCTGCTTT TTG (TRCN0000065613)	MUSC Hollings Cancer Center shRNA Shared Resource Technology
Mouse siLIFR 1	siLIFR 1/siLIFR	D-040750-01-002	Dharmacon Inc
Mouse si LIFR 2	si LIFR 2	D-040750-02-002	Dharmacon Inc
Mouse siSMAD3	siSMAD3	D-040706-01-0002	Dharmacon Inc
Mouse siSTAT3	siSTAT3	D-040794-01-0002	Dharmacon Inc

Table 2. RT and qPCR primers

Primers (5' → 3')	Forward	Reverse
RT mouse LIFR	CCTCAAGACAAAGTGGTGCT	GAGGATAGCCTGCAAAGACC
qPCR LIFR	GGAGCCGAGGATTCAACTTA	TCAGAACTCCACTCTCTCCA
RT mouse GAPDH	GGTTGTCTCCTGCGACTTCA	TAGGGCCTCTCTTGCTCAGT
RT mouse BMI	GGCTCGCATTCATTTTATGCTG	ATGAAGTACCC TCCACACAG
RT mouse Nanog	CTTCAGATAGGCTGATTTG GT	AATTCGATGCTTCCTCAGAAC
RT mouse Snail	TCTGAAGATGCACATCCGAAGCCA	AGGAGAATGGCTTCTCACCAGTGT
RT mouse Slug	AGATGCACATTCGAACCCAC	GTCTGCAGATGAGCCCTCAG
RT mouse ILEI	GAGCT GCAAAGTTGGTAGTG	TAGAACGAATGGCTGAGTCC

Chapter 3

TGFβ promotes breast cancer stem cell self-renewal through an ILEI/LIFR signaling axis

3.1 Introduction

Breast cancer is the third leading cause of cancer-related deaths in the US with approximately 40,000 fatal outcomes each year. Breast cancer patients with late-stage metastasis have a 27% 5-year relative survival rate, a significant decrease in comparison to patients with localized disease (99% 5-year survival) [1]. Metastases derived from primary breast lesions (commonly targeted to the bone, brain, liver, lung, and distant lymph nodes) require the coordination of several cellular and molecular processes, including the epithelial-mesenchymal transition (EMT) [85,86]. Under normal conditions, EMT is utilized during embryonic development and tissue regeneration where cells undergo a highly dynamic switch between epithelial and mesenchymal phenotypes [36,38]. Mammary epithelial cells acquire migratory and invasive properties upon EMT activation, thereby implicating EMT regulatory mechanisms in breast malignancies [37,87]. EMT is facilitated by an array of transcriptional reprogramming, epigenetic modification, and differential expression patterns of epithelial/mesenchymal-specific cell adhesion and cytoskeletal proteins [4]. It has also been suggested that the reverse process of EMT, the mesenchymal-epithelial transition (MET), is executed once cancer cells have reached their metastatic niche in order to promote secondary colonization and tumorigenesis [36,88].

The current understanding of EMT in cancer progression has recently shed

light on the existence of undifferentiated mammary stem cells known as tumor initiating cells (TICs) or breast cancer stem cells (BCSCs) that are derived from basal mammary epithelial cells (MECs) undergoing EMT and subsequent self-renewal/differentiation, dissemination, and secondary tumorigenesis [46,50,52]. The cells have been extensively characterized due to their role in tumor progression and chemoresistance [50,89]. BCSCs are identified by functional assays and differential regulation of established stem cell markers, including CD44/CD24, BMI1, aldehyde dehydrogenase activity, and Nanog [52,90–92].

The link between EMT and BCSC formation has been extensively investigated by groups focused on the pleotropic cytokine transforming growth factor β (TGFβ) and its signaling modalities [41,51,58]. These studies collectively demonstrate the role of TGFβ-induced EMT and BCSC formation within the mammary epithelium. It is therefore important to characterize the molecular mechanisms defining TGFβ-induced BCSCs for the development of new therapies targeting breast cancer metastasis. Studies from our lab uncovered a master regulator of the mesenchymal proteome during TGFβ-induced EMT. We identified a tumor suppressor ribonucleoprotein (mRNP) complex containing heterogeneous nuclear ribonucleoprotein E1 (hnRNP E1) and eukaryotic elongation factor 1A1 (eEF1a1) that binds a structurally conserved 3'-UTR or BAT element (TGFβ activated translation) and inhibits translation of several mRNAs involved in EMT [59,60]. TGFβ signaling initiates a non-canonical kinase cascade that results in Akt2-mediated phosphorylation of hnRNP-E1 at serine 43. Subsequently, hnRNP E1 complexes are released from EMT related mRNA transcripts, translation is

restored, and EMT progresses. Using a genome-wide combinatorial approach by expression profiling and RIP-Chip analysis, our lab revealed a cohort of over 30 mRNAs that are controlled by the 3'-UTR BAT mechanism of translational regulation by TGFβ [61]. Knockdown of hnRNP E1 within normal mammary epithelial cells results in a transition to a mesenchymal, invasive and migratory state, and drives spontaneous tumor formation in mice [60]. Analysis of the mRNAs translationally regulated by hnRNP E1 revealed FAM3C, also known as interleukin-like EMT inducer (ILEI), a cytokine analyzed for its role in EMT and tumorigenesis.

ILEI is a member of the FAM3 family of secreted cytokines and was discovered through a sequence based search for predicted four-helical bundle cytokines [62]. ILEI has been shown to play a role in a variety of biological processes including Alzheimer's disease, retinal laminar formation, and bone density regulation [68,93,94]. In the context of epithelial tumorigenesis, ILEI serves an essential role in EMT activation and metastatic progression after translational upregulation by TGFβ. Subsequent N-terminal processing and secretion results in the full-length 25kD molecule being reduced to a 18kD variant that functions within the extracellular space [66,67,80]. Although these studies demonstrate an important role for ILEI in disease, mechanistic studies and identification of the extracellular receptor mediating ILEI function has yielded little progress. The previously described role of ILEI in EMT and tumorigenesis gives rise to its possible function in BCSC formation and self-renewal. Indeed, it has been demonstrated that secreted inflammatory cytokines such as interleukins 6 and 8 (IL-6/IL-8) play

important roles in BCSC enrichment and chemoresistance [95–97]. These findings present an interesting possibility that ILEI may also function in a similar capacity within the context of TGFβ-mediated EMT and BCSC formation.

The IL-6 family of secreted cytokines, that adopt four-helical bundle structures such as leukemia inhibitory factor (LIF), cardiotrophin-1 (CT-1), ciliary neurotrophic factor (CNTF), and oncostatin M (OSM), all utilize leukemia inhibitory factor receptor (LIFR) in complex with glycoprotein 130 (gp130) for downstream signal transduction [98,99]. The gp130/LIFR signaling platform is involved in many important cell biological processes including inflammation, bone-remodeling, reproduction, cardiac function, neuromuscular function, the hematopoietic system, and embryonic stem cell (ESC) homeostasis [98]. The wide realm of functionality for the gp130/LIFR axis is due to the activation of several major cell-regulatory pathways including the Jak/STAT, Erk/MAPK, and Akt/PI3K signaling pathways [98]. In the context of breast cancer progression, LIFR and its ligands have been implicated in both the enhancement and repression of oncogenesis, metastatic progression, and dormancy phenotypes [74,75,100].

Herein, we aimed to understand the molecular mechanism underlying the TGFβ/hnRNP E1 pathway in the regulation of MEC self-renewal. We determined that loss of hnRNP E1 from normal MECs is sufficient to induce a transition to a BCSC state. Reduction of ILEI levels in hnRNP E1 knockdown cells reduces the tumor initiating properties of these cells both *in vitro* and *in vivo*. Additionally, leukemia inhibitory factor receptor (LIFR) and STAT3 were identified as effectors of ILEI signaling in BCSCs. Our data indicates that TGFβ induces the self-renewal

capacity of BCSCs through hnRNP E1-dependent induction of ILEI and the subsequent activation of JAK-STAT signaling through LIFR.

3.2 Results

TGFβ-mediated functional silencing of hnRNP E1 in mammary epithelial cells induces BCSC formation and self-renewal

hnRNP E1 has been shown to regulate the migratory and invasive potential of cells undergoing TGFβ-mediated EMT [59]. To determine whether hnRNP E1 regulates any of TGFβ's effects in BCSC self-renewal, we utilized a normal murine mammary gland epithelial cell line (NMuMG) with or without shRNA-guided knockdown of hnRNP E1 (Fig 2A). These cell lines will be referred throughout as E1KD cells as demonstrated by successful silencing of hnRNP E1 (Fig 2A). We also utilized human mammary epithelial cells (HMLE) that were sorted into epithelial (HMLE-Epi) and mesenchymal (HMLE-Mes) populations through differential trypsin sensitivity and silenced hnRNP E1 within the epithelial pool (Fig 2B). The NMuMG lines were passaged from two-dimensional cultures into non-adherent, serum-free conditions in the presence of limited growth factors to test their capacity to grow and self-renew as spheroid structures or mammospheres. Parental NMuMG cells do not form mammospheres without a 9-day pre-treatment with TGFβ. Upon attenuation of hnRNP E1 (E1KD cells), mammosphere formation is significantly enhanced even in the absence of TGFβ pre-treatment (Fig 2C). To test self-renewal capacity, both NMuMG and E1KD mammospheres were trypsinized, resuspended, and passaged up to three times. E1KD mammospheres displayed increased self-renewal capacity sustained over multiple passages when

compared to the NMuMG spheres, validating hnRNP E1 as an important factor mediating stem cell phenotypes in these lines (Fig 2D-E). To test the contribution of hnRNP E1 to the self-renewal of human mammary cells *in vitro*, we performed FACS analysis of CD44/CD24 stem cell surface marker expression in HMLE-Epi, HMLE-Mes, and HMLE-Epi cells silenced for hnRNP E1. Knockdown of hnRNP E1 in the HMLE-Epi population results in a switch to a more mesenchymal-like $CD44^{high}/CD24^{low}$ profile (Fig 2F).

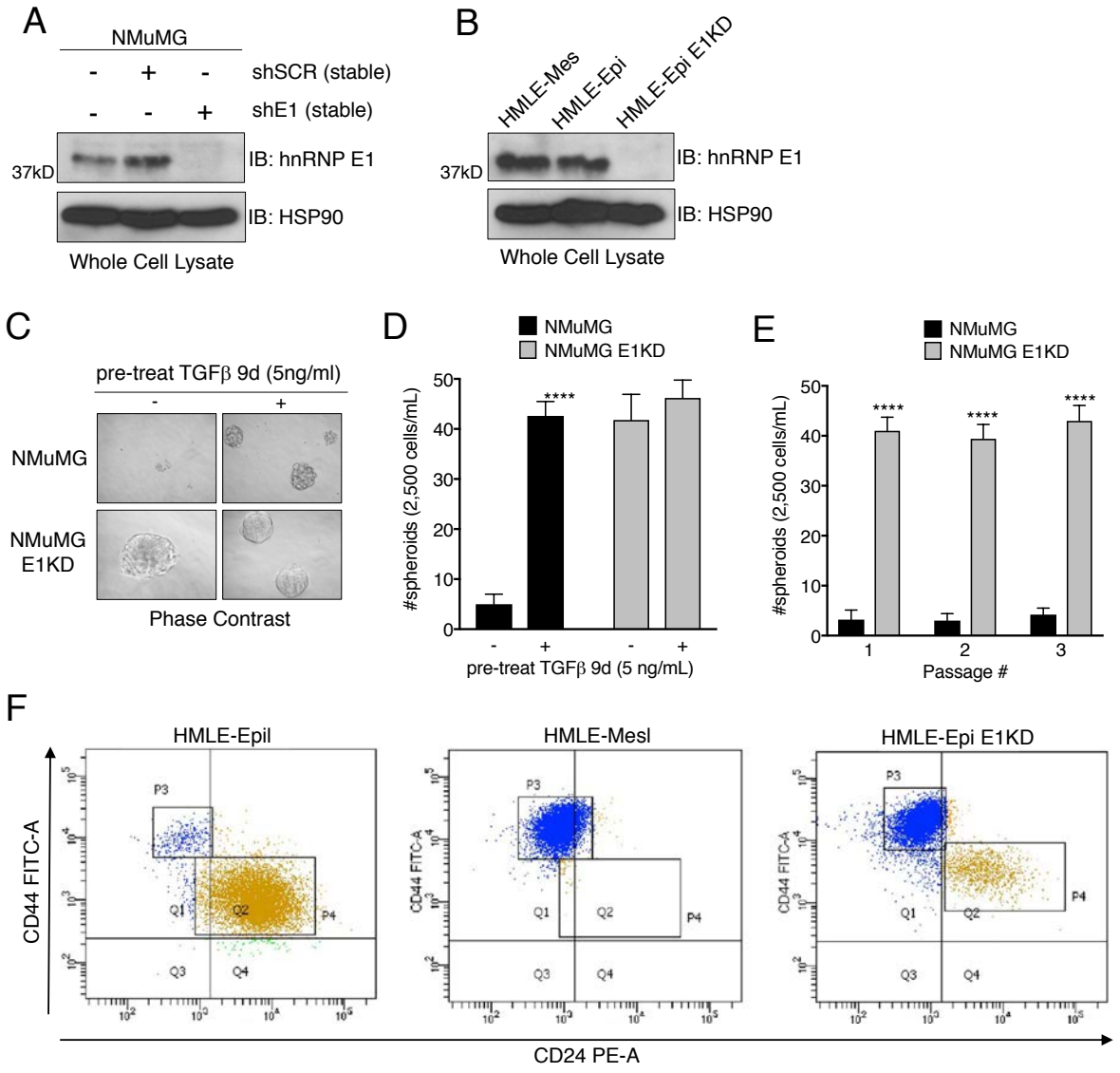

Fig 2. TGFβ-mediated functional silencing of hnRNP E1 in mammary epithelial cells induces BCSC formation and self-renewal. (A) Immunoblot analysis of hnRNP-E1 protein levels in parental NMuMG cells stably transduced with either scramble control shRNA or shRNA targeting hnRNP-E1. (B) Immunoblot analysis of trypsin-selected and FACS sorted (CD44/CD24) HMLE mesenchymal, HMLE epithelial, and HMLE epithelial cell lines silenced for hnRNP E1. (C) Phase contrast images and (D) quantification of mammosphere formation by NMuMG and NMuMG shE1 (E1KD) cells with or without 9-day TGFβ pre-treatment (error bars represent mean +/- SD; n=5; ****p <0.0001, unpaired Student's t-test). All mammospheres were counted at a minimum diameter of 100μm. (E) Quantification of sequentially passaged mammospheres from NMuMG and E1KD cells (error bars represent mean +/- SD; n=5; ****p <0.0001, unpaired Student's t-test). (F) FACS analysis of CD44/CD24 surface marker expression in HMLE epithelial, mesenchymal, and epithelial E1KD populations (HMLE epi P3: 3.4%, P4: 92.7%; HMLE mes P3: 98.0% P4: 0.7%; HMLE epi E1KD P3: 80.8%, P4: 12.5%)

TGFβ/hnRNP E1 induces BCSC Self-Renewal through a Secreted Factor

Our initial observations indicated that TGFb signaling and/or hnRNP E1 silencing induces stem-like phenotypes in both murine and human mammary epithelial cells. In order to investigate the capacity of E1KD cells to exhibit either myoepithelial or luminal phenotypes suggesting differentiation potential, we stained E1KD mammospheres for either basal (CK5 and CK14) or luminal (CK8 and CK18) cytokeratins (Fig 3A). We demonstrate that E1KD cells can exhibit both myoepithelial and luminal epithelial cell phenotypes (Fig 3A) [101]. Additionally, Red Fluorescent Protein (RFP)-expressing NMuMG cells were capable of mammosphere growth upon co-culture with Green Fluorescent Protein (GFP)-expressing E1KD cells in a dose-dependent manner, with both cell types exhibiting co-localization within the spheroids (Fig 3B quantification, Fig 3C for RFP-NMuMG and GFP-E1KD co-culture images by immunofluorescence). To delineate between self-renewal induced by E1KD generated cell surface proteins and secreted factors, conditioned media (CM) collected from 7-day E1KD mammospheres was cultured with the NMuMG parental cell line. The CM from E1KD cells was sufficient to increase, in a dose-dependent manner, the mammosphere growth of RFP-expressing NMuMG cells (Fig 2D quantification; Fig 3E for NMuMG-RFP mammosphere immunofluorescence upon E1KD conditioned media treatment). Therefore, a secreted factor derived from modulation of hnRNP E1 may play a critical role in TGFβ-induced BCSC formation and self-renewal.

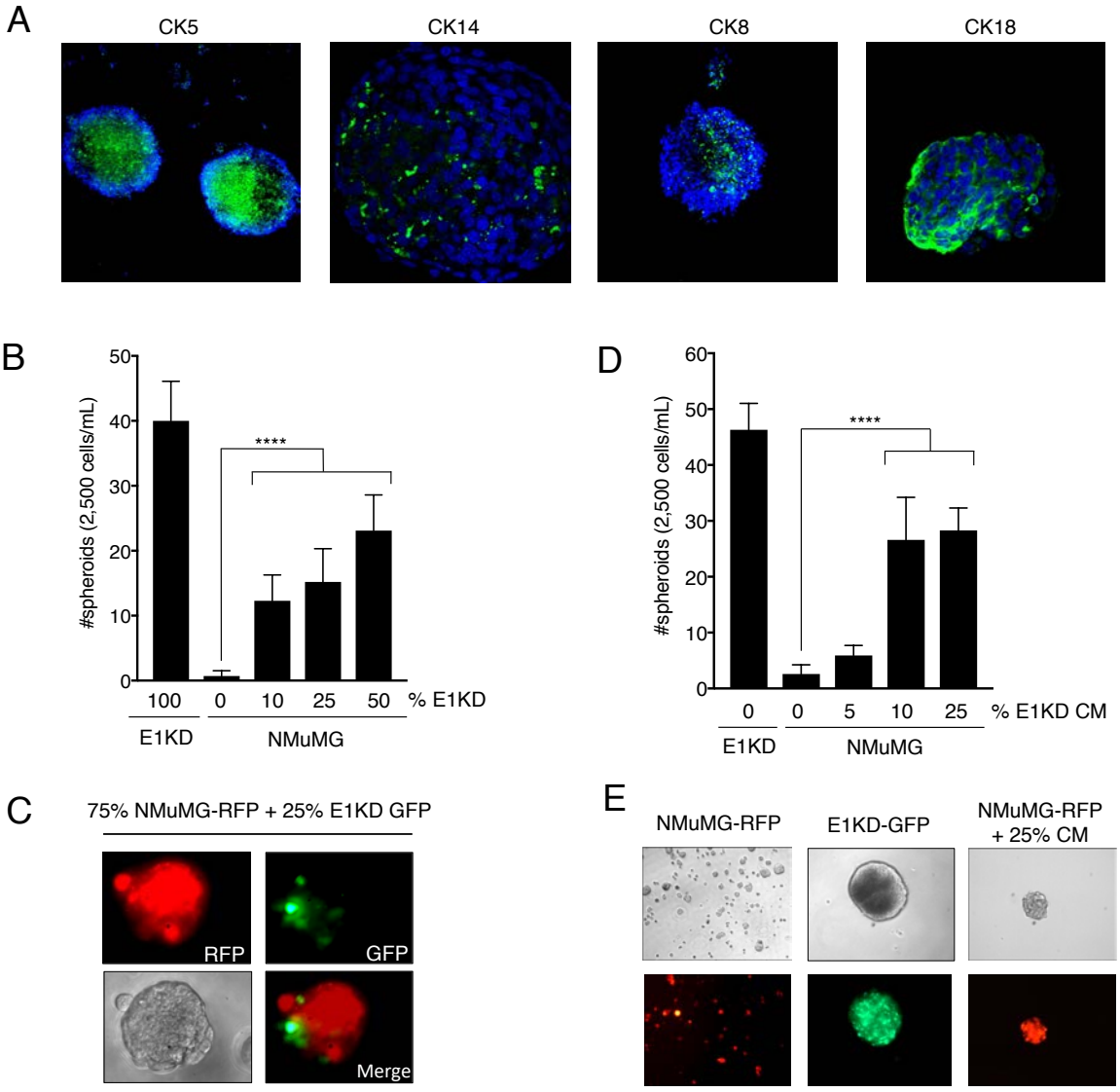

Fig 3. **TGFβ/hnRNP E1 induces BCSC Self-Renewal through a Secreted Factor.** (A) E1KD mammospheres stained for basal and luminal cytokeratins. (B) Mammosphere quantification and (C) representative images from co-cultured NMuMG-RFP and E1KD-GFP cells as well as (D & E) NMuMG cells supplied with increasing amounts of E1KD conditioned media (error bars represent mean +/- SD; n=10; ****p <0.0001, One-way Anova.

The Secreted Cytokine ILEI is Necessary for TGFβ/hnRNP E1-Mediated EMT and BCSC formation

Previously, we identified the secreted cytokine interleukin-like EMT inducer (ILEI) as a member of a cohort of mRNAs involved in EMT that are regulated by TGFβ/hnRNP E1 through a 3'-UTR-mediated translational silencing mechanism [61]. To examine whether TGFβ-induced expression of ILEI is necessary and/or sufficient to activate an EMT program, we introduced either scramble control or ILEI-specific shRNA constructs into the NMuMG and E1KD cell lines (referred to as NMuMG and E1KD shSCR/shILEI). Figure 4A demonstrates successful silencing of ILEI protein levels in NMuMG shILEI cells when compared to NMuMG shSCR lines after TGFβ stimulation for 24 hours, whereas E1KD shSCR cells that possess constitutive ILEI translation, lose this expression level after ILEI shRNA silencing (Fig 4A). This effect is also observed in the secretion of the mature processed 18kD ILEI protein from the various cell lines after analysis of the conditioned media (Fig 4B). To test TGFβ responsiveness in these cell lines, we assessed both morphology and EMT marker regulation after TGFβ stimulation for 24 hours. NMuMG shSCR cells undergo a morphological EMT after TGFβ treatment, indicated by elongated fibroblast-like cell morphology when examined by phase contrast microscopy, whereas NMuMG shILEI cells do not (Fig 4C). Assessment of EMT markers in these cell lines shows that the epithelial cell adhesion marker E-cadherin is down-regulated in NMuMG shSCR cells after 24h TGFβ stimulation but maintained in NMuMG shILEI cells after the same treatment (Fig 4D). A change in expression pattern is also observed in the E1KD cell lines

where E1KD shSCR cells that lack E-cadherin restore E-cadherin upon ILEI silencing (Fig 4D). The mesenchymal markers N-cadherin and alpha-smooth muscle actin (α-SMA) show opposite trends compared to E-cadherin in the NMuMG and E1KD populations, whereby ILEI levels dictate the relative expression patterns of these markers (Fig 4D). These data collectively demonstrate that ILEI translation/secretion through TGFβ/hnRNP E1 is important for induction of EMT in mammary epithelial cell populations.

Mammosphere assays were used to determine whether ILEI is responsible for BCSC self-renewal in E1KD cells. As shown, TGFβ pre-treatment induces mammosphere formation in NMuMG shSCR control cells, which is attenuated in shRNA-ILEI-silenced NMuMG cells (Fig 4E). Similarly, E1KD shSCR cells that display constitutive self-renewal and mammosphere formation properties lose this phenotype upon ILEI knockdown (Fig 4F). To test the contribution of ILEI in the conditioned media derived from E1KD shSCR/ILEI cells on mammosphere formation, we assayed spheroid growth of NMuMG cells in the presence of either E1KD shSCR or E1KD shILEI conditioned media (Fig 4G). We show that only the conditioned media derived from E1KD shSCR cells is able to induce mammosphere growth in the NMuMG cell lines relative to positive control E1KD cells. We show that supplementing pure rILEI in the mammosphere formation assay of E1KD shILEI cells is able to partially rescue their spheroid formation capacity relative to positive control E1KD shSCR cells (Fig. 4H). Collectively, these data suggest that ILEI secretion is necessary for inducing the self-renewal properties in BCSCs regulated by TGFβ/hnRNP E1.

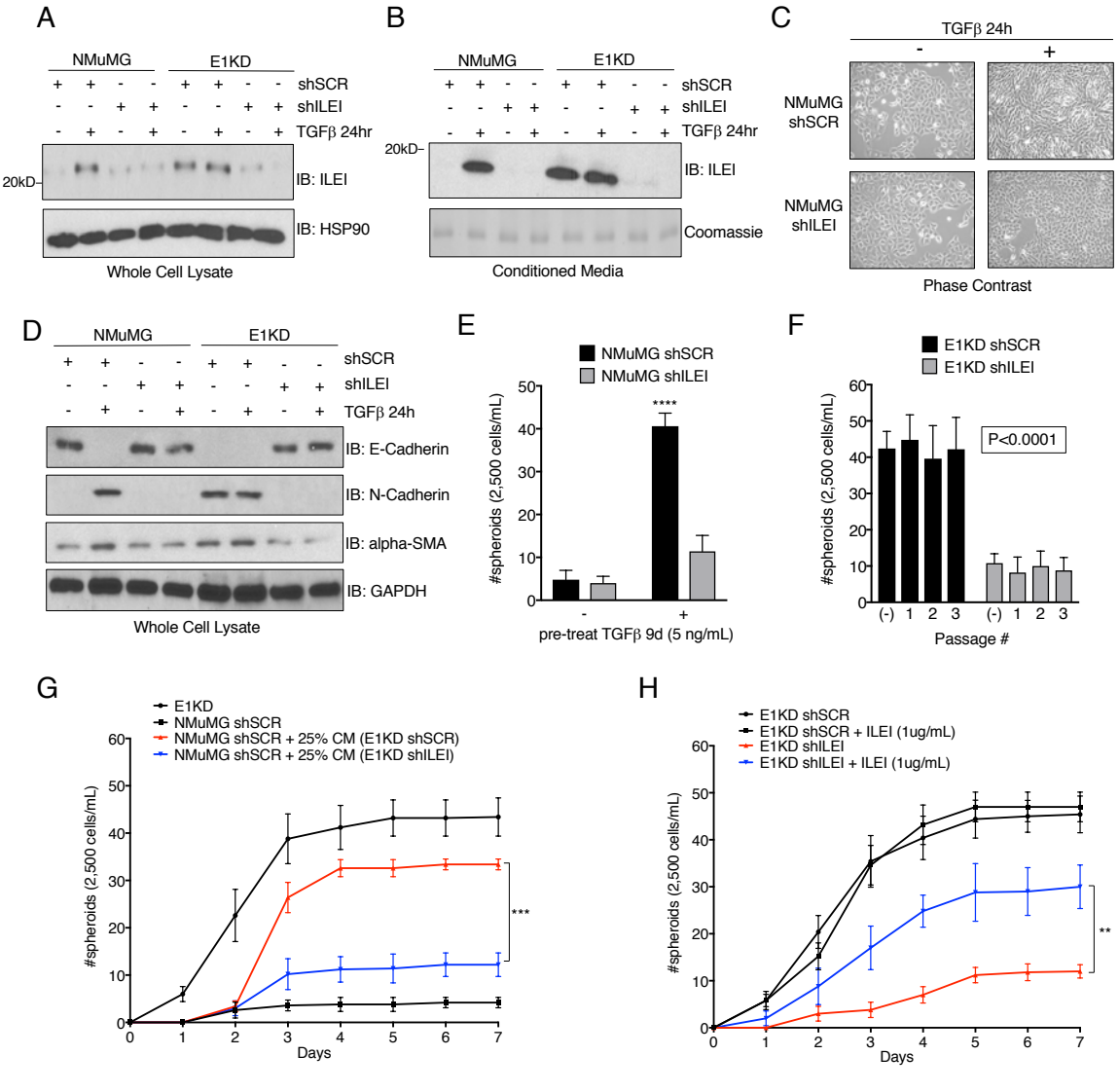

Fig 4. The Secreted Cytokine ILEI is Necessary for TGFβ/hnRNP E1-Mediated EMT and BCSC formation (figure legend next page)

Fig 4. The Secreted Cytokine ILEI is Necessary for TGFβ/hnRNP E1-Mediated EMT and BCSC formation. Immunoblot analysis of either (A) whole cell lysates or (B) conditioned media from NMuMG and E1KD cells stably transduced with either scramble control shRNA (shSCR) or ILEI knock-down shRNA (shILEI) in the presence or absence of TGFβ (5ng/ml) for 24 hours. Coomassie staining was used as a loading control for conditioned media. (C) Phase contrast images of NMuMG shSCR and NMuMG shILEI cells in the presence and absence of TGFβ stimulation for 24 hours. (D) Immunoblot analysis of EMT markers in whole cell lysates derived from NMuMG/E1KD shSCR and NMuMG/E1KD shILEI cells in the presence and absence of TGFβ stimulation for 24 hours. (E) Quantification of mammosphere formation by TGFβ pre-treatment (5ng/mL) in NMuMG cells stably transduced with either scramble control shRNA (shSCR) or ILEI knock-down shRNA (shILEI) (error bars represent mean +/- SD; n=5; ****p<0.0001, unpaired Student's t-test). (F) Quantification of mammosphere formation and self-renewal in E1KD cells stably transduced with either scramble control shRNA or ILEI knock-down through several passages (error bars represent mean +/- SD; n=5, p <0.0001 for all passages, paired Student's t-tests between correlative passage numbers). (G) Mammosphere formation by NMuMG shSCR cells supplemented with conditioned media derived from either E1KD shSCR or E1KD shILEI cells (25% total volume) with E1KD mammosphere growth used as a positive control (error bars represent mean +/- SD, n=5; ***p=0.0002, 2-way ANOVA). (H) Quantification of mammosphere formation in E1KD shSCR/shILEI cells in the presence and absence of purified recombinant ILEI (error bars represent mean +/- SD; n=5; **p=0.0013, 2-way ANOVA).

BCSC phenotypes in hnRNP E1-silenced cells are driven by ILEI

To further investigate the contribution of ILEI to stemness potential of E1KD cell populations, we further analyzed E1KD shSCR/shILEI cells for stemness characterization. Upon silencing, The E1KD shSCR/shILEI cell lines display constitutive mesenchymal morphologies in both the presence and absence of TGFβ (Fig 5A). These data suggest that ILEI knockdown is sufficient to block TGFβ-mediated EMT but is insufficient to induce a MET program within the mesenchymal E1KD pool. To test the contribution of ILEI to stemness potential in a human cell line, we utilized shRNA-mediated silencing of ILEI in human basal epithelial A549 cells and performed oncosphere assays (Fig 5B-C). We demonstrate that ILEI silencing significantly abrogates constitutive spheroid formation capacity of A549 cells, confirming ILEI as an important factor in both

murine and human stem cell phenotypes. Analysis of the stemness markers BMI1 and Nanog support the mammosphere self-renewal experiments and reveal an upregulation of these factors in E1KD cells when compared to NMuMG cells (Fig 5E). This observation in E1KD cells is ILEI-dependent, as siRNA-mediated silencing of ILEI induces the loss of BMI and Nanog levels (Fig 5F).

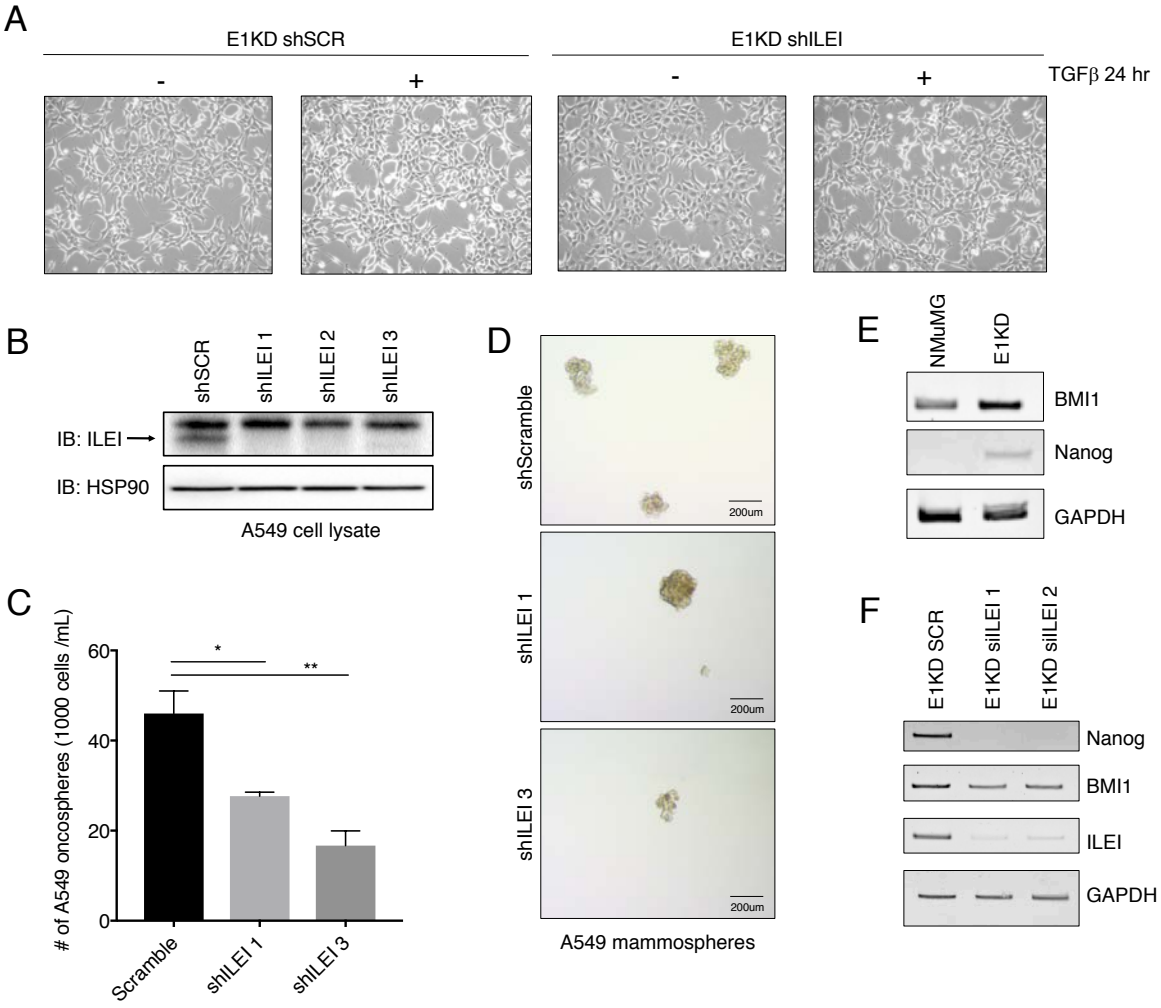

Fig 5. BCSC phenotypes in hnRNP E1-silenced cells are driven by ILEI. (A) Phase contrast images of NMuMG E1KD shSCR and NMuMG E1KD shILEI cells in the presence and absence of TGFβ stimulation for 24 hours. (B) Immunoblot analysis demonstrating ILEI knockdown with three shILEI constructs compared to shSCR in A549 cells. (C) Oncosphere quantification after 10 days of growth in minimal media for A549 shSCR and two shILEI cell lines (error bars represent mean +/- SD; n=5; *p<0.05, **p<0.01 unpaired Student's t-test). (D) Representative images for A549 oncospheres quantified in Fig 5c. (E) Semi-quantitative PCR for BMI1 and Nanog in NMuMG and E1KD cells. (F) Semi-quantitative PCR for BMI1, Nanog, and ILEI RNA levels in E1KD cells silenced for ILEI.

ILEI Protein Levels Correlate with Mammary Tumor Progression

To further investigate the association between ILEI and human malignancy, we probed a series of cancer cell lines that represent different subtypes of breast carcinoma populations with various levels of metastatic potential. Human SUM cell lines were derived from patients with breast malignancies [102]. Figure 6A demonstrates that ILEI is upregulated in a correlative manner in both human and murine metastatic populations (E1KD, 4T1, SUM44, MDA-MB-231) when compared to non-metastatic cell lines (NMuMG, SUM149, SUM190, SUM150, MCF10). Furthermore, using human breast tissue microarrays from the Biorepository and Tissue Analysis core at MUSC, we correlated ILEI expression with tumorigenesis in human patients. Both pre-malignant and primary tumor samples demonstrate a significant increase in IHC score compared to normal breast tissue (Fig 6B-C). Similarly, tumors found within the lymph node have significantly higher levels of ILEI compared to normal lymph node tissue (Fig 6D). Using only patient samples that contained matched breast tissue tumors and lymph node tumors, we could see a significant increase in ILEI expression at the metastatic site compared to the primary tumor site (Fig 6E). These data indicate that ILEI signaling is involved in tumorigenesis of mammary epithelial cells in human patients.

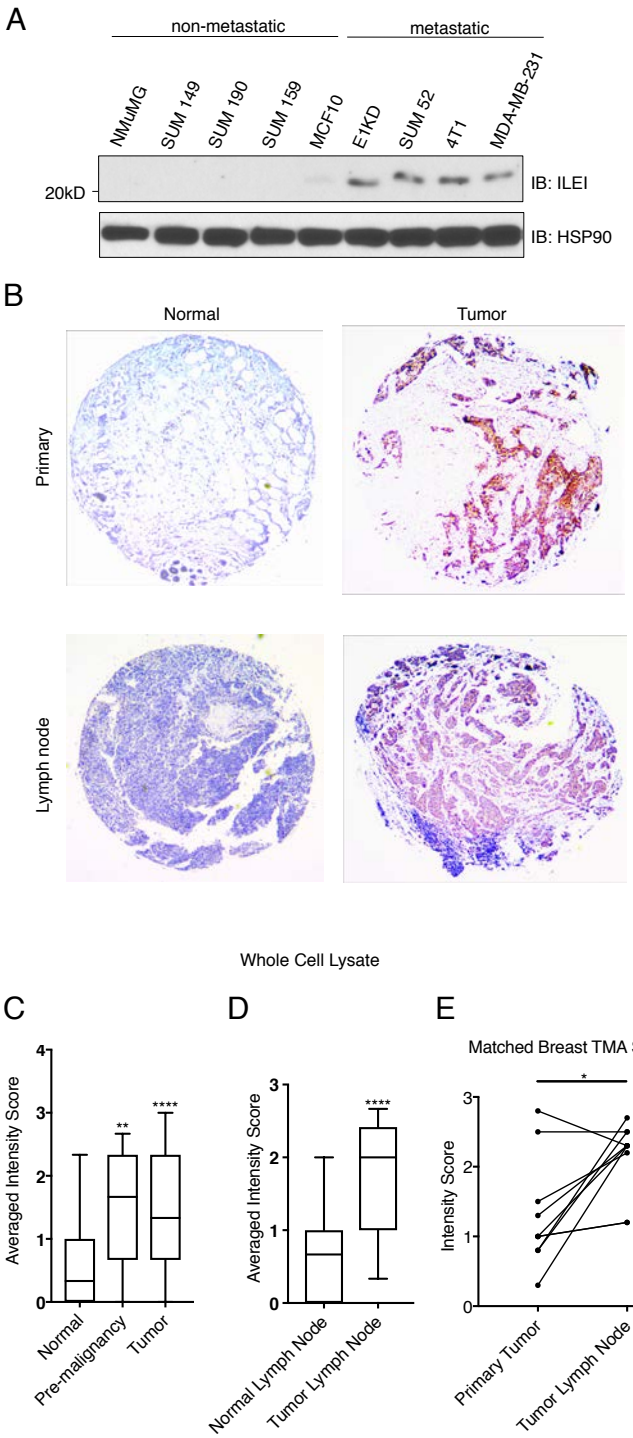

Fig 6. ILEI Protein Levels Correlate with Mammary Tumor Progression. (A) Immunoblot analysis of basal ILEI levels in both murine and human cell lines that display altered metastatic potential. (B) Representative images taken at 5x magnification of normal breast, tumor breast, normal lymph node or tumor lymph node TMAs after immunohistochemistry analysis of ILEI. (C) Quantification of IHC scores for all normal breast tissue, pre-malignant tissue and tumor tissue samples (box plot represents intensity score distribution minimum to maximum; ****p<0.0001, **p<0.01, unpaired Student's t-test). (D) Quantification of IHC scores for all normal lymph node tissue, and tumor lymph node tissue samples (box plot represents intensity score distribution minimum to maximum; ****p<0.0001, unpaired Student's t-test). (E) Plot showing matched primary tumor and lymph node tumor patient samples (n=8, *p=0.013, paired Student's t-test).

Table 3. Clinicopathological features of breast cancer TMA specimens.

Sample ID	Age	Vital Status	Days between Surgery and Date of last contact/Death	Recurrence	Days between Surgery and Recurrence	Histological Type	Staging	ILEI IHC score (Tumor)	ILEI IHC score (Pre-Mal)	ILEI IHC score (Lymph Node)
1389	61	alive	2799	yes	806	Invasive ductal carcinoma	T2N1aMX	1.5	2.5	2.2
2501	73	alive	1811	no		Infiltrating lobular, NOS	T2N0MX	1.3	N/A	N/A
3565	62	alive	1312	unknown	unknown	Invasive ductal carcinoma	T1N0MX	2.2	1.5	N/A
4555	68	alive	841	unknown	unknown	Invasive ductal carcinoma	T1cN0MX	1.0	N/A	2.3
1459	64	alive	2666	unknown	unknown	Infiltrating ductal, NOS	T1bN0MX	1.3	2.2	N/A
1335	32	alive	2713	no		Invasive ductal carcinoma	T3N3aMX	0.8	0.7	2.7
1356	50	alive	2916	no		Invasive ductal carcinoma	T3N1cMX	1.3	N/A	2.3
1373	69	alive	3022	yes	0 (prior surgery for DCIS)	Invasive ductal carcinoma	T1N1MX	2.5	2.3	2.5
1420	58	dead	474	yes	373	Invasive ductal carcinoma	T2N1MX	0.3	N/A	2.3
4215	63	alive	1132	no		Infiltrating lobular, NOS	T2N0MX	2.5	N/A	N/A
1968	75	dead	749	yes	485	Invasive ductal carcinoma	T2N2aMX	1	N/A	1.2
2601	52	dead	1558	yes	1101	Invasive lobular carcinoma	T1aN1MX	2.5	N/A	Missing/damaged specimen
1351	45	dead	235	yes	178	Invasive ductal carcinoma	T3N2MX	2	N/A	1.5
1360	60	alive	2887	yes	1802	Papillary carcinoma	T2N0MX	0.5	0.8	N/A
4368	49	alive	1036	no		Invasive ductal carcinoma	T1aN0MX	2.7	N/A	N/A
4664	47	unknown	unknown	unknown	unknown	Invasive ductal carcinoma	T1bN0MX	1.7	N/A	N/A
1484	44	dead	784	yes	326	Invasive ductal carcinoma	unknown	1	N/A	1.2
4594	79	alive	582	no		Invasive carcinoma	T3N1aMX	0.8	N/A	2.5
4065	49	alive	1004	unknown	unknown	Invasive ductal carcinoma	T2N2aMX	2.8	N/A	2.3
1441	80	alive	2679	no		Infiltrating ductal, mucinous (colloid)	T2N0MX	1	2.3	N/A
1773	53	alive	2365	no		Invasive ductal carcinoma	unknown	1	N/A	N/A
5010	63	alive	468	no		Invasive ductal carcinoma	T1cN0MX	1.5	1.5	N/A
5076	31	alive	388	no		Invasive ductal carcinoma	T1cN0MX	0	1	N/A
5108	42	alive	386	no		Invasive ductal carcinoma	T1aN0MX	0	2.2	N/A
4673	59	alive	574	no		Infiltrating lobular, NOS	T1cN0MX	2.5	0	N/A
4684	66	alive	534	no		Invasive ductal carcinoma	T2N0MX	2.7	0.8	N/A
4692	45	alive	492	no		Invasive ductal carcinoma	T1cN1aMX	2.8	0.3	N/A
5317	60	alive	182	no		Invasive lobular carcinoma	T1bNXMX	1.8	N/A	N/A
5428	63	alive	197	diagnosis		Invasive lobular carcinoma	T2N0MX	1.2	N/A	N/A
5615	51	alive	11	no		Invasive ductal carcinoma	T2N0	2.5	N/A	N/A
5116	49	alive	142	unknown		Invasive ductal carcinoma	T1cN1MX	0.2	N/A	N/A
5126	51	alive	498	no		Invasive lobular carcinoma	T2N1aMX	1.8	N/A	N/A
5219	79	alive	491	no		Invasive lobular carcinoma	T2N0MX	1.5	N/A	N/A

ILEI Binds to the Cytokine Receptor LIFR

Little is known regarding ILEI's mechanism of action. We utilized a yeast-two hybrid screen to identify potential ILEI binding partners using the ILEI coding sequence as bait and a HeLa cDNA library as prey. Among the 60 candidate interacting partners was the cytokine receptor LIFR precursor (Fig 7A). To demonstrate ILEI binding to the cell surface, we [I^{125}]-radiolabeled recombinant ILEI and performed crosslinking experiments using the non-permeable, non-reducible chemical cross-linker BS3. Complexed, radiolabeled control [I^{125}]-rLIF and experimental [I^{125}]-rILEI and were both observed at molecular weights in excess of 250kDa compared to the free ligand, which migrates at approximately 20kDa (Fig 7B). In addition to binding the cell surface in a similar manner as rLIF (Fig 7C), [I^{125}]-rILEI binding could be out-competed using 50X-fold unlabeled rILEI protein, demonstrating the specificity of the interaction (Fig 7D). Additionally, we immunoprecipitated LIFR from E1KD cells following rILEI treatment and BS3 crosslinking. Both ILEI and LIFR were detected by immunoblot analysis after LIFR immunoprecipitation. Due to the irreversibility of the BS3 cross-linker, both ILEI and LIFR were observed to shift to a molecular weight larger than LIFR alone and consistent with complex formation (Fig 7E). Finally, transfection of either empty vector or a FLAG-tagged LIFR construct in HEK293 cells (Fig 7F) allows for radiographic detection of ILEI binding to LIFR after the addition of [I^{125}]-rILEI and immunoprecipitation with a LIFR antibody. The positive control [I^{125}]-rLIF was also observed to co-precipitate with LIFR (Fig 7G).

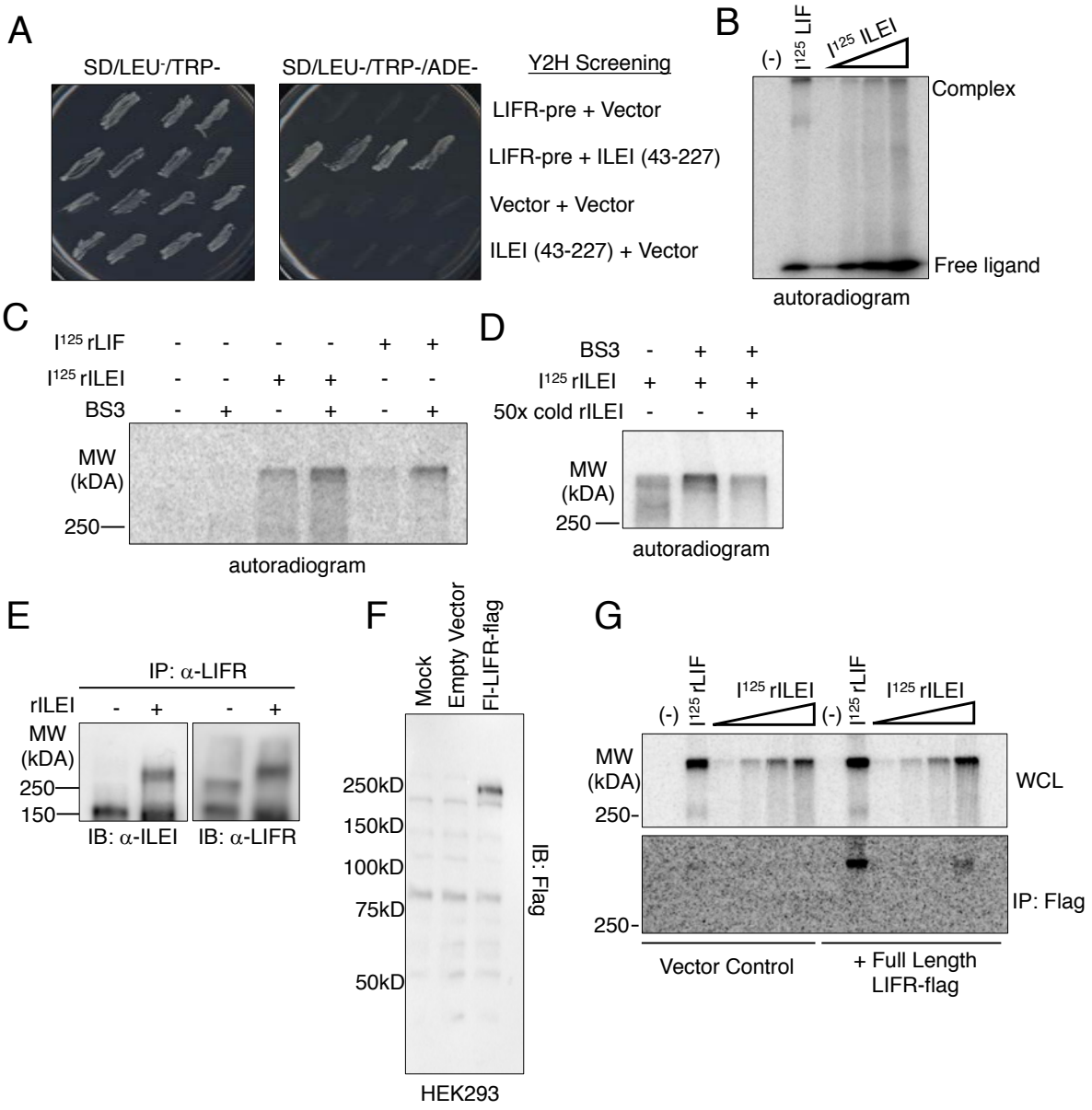

Fig 7. ILEI Binds to the Cytokine Receptor LIFR. (A) Yeast 2-hybrid of ILEI 43-227 probed against a HELA cDNA library demonstrating activation of adenine reporter and colony growth corresponding to mature ILEI interacting with LIFR precursor. (B) Immunoblot showing free ligand from whole cell lysate after ^{125}I ligand incubation and BS3. (C) BS3 cross-linking in HEK293 cells in the presence or absence of 625pM ^{125}I-rILEI and ^{125}I-LIF. Radiolabeled BSA was used in control lanes. (D) Cold-competition assay of radiolabeled ^{125}I-rILEI with or without 50x cold recombinant rILEI. Indicated samples were BS3 cross-linked to the surface of HEK293 cells and separated by SDS-PAGE. (E) Immunoprecipitation of LIFR in HEK293 cells in the presence and absence of 10nM rILEI followed by immunoblot for either rILEI or LIFR. All lanes were crosslinked with BS3. (F) Immunoblot analysis of FLAG-LIFR overexpression in HEK293 cells. (G) Overexpression of full-length FLAG-tagged LIFR or vector control followed by ^{125}I-rLIF (625pM) and ^{125}I-rILEI (100pM-2nM) stimulation with BS3 crosslinking. Cell lysates were immunoprecipitated with Flag antibody and separated on an 8% SDS-PAGE gel.

TGFβ/hnRNP E1-mediated BCSC formation requires both ILEI and LIFR

Since LIFR serves as a receptor for several cytokines involved in self-renewal, we postulated that it may serve as the extracellular receptor mediating ILEI signaling and BCSC phenotypes. Indeed, TGFβ signaling and/or hnRNP E1 knockdown in NMuMG cells induces the upregulation of LIFR protein, suggesting a potential role of the receptor in TGFβ-induced EMT/BCSC formation (Fig 8A). We utilized shRNA-mediated silencing of LIFR in both NMuMG and E1KD cell lines in order to investigate any differential BCSC formation capabilities dependent on either TGFβ stimulation or hnRNP E1 knockdown (Fig 8B-C). We observed attenuated mammosphere formation and self-renewal capacity when compared to scramble control cells, phenocopying ILEI's effect on mammosphere formation. Furthermore, we observed mammosphere rescue when rILEI was added to E1KD cells silenced for ILEI, as shown previously (Fig 8D). Alternatively, mammosphere formation was not rescued when rILEI was incubated with E1KD cells silenced for LIFR (E1KD shLIFR), suggesting that ILEI is functioning through LIFR to mediate the self-renewal phenotype (Fig 8D). We also transiently silenced ILEI and LIFR with targeted siRNAs in E1KD cells to test their mammosphere formation capacity both constitutively as well as after co-incubation with purified rILEI (Fig 78E-F). As expected, either shRNA or siRNA-mediated knockdown of ILEI and LIFR results in attenuated self-renewal properties. Only cells silenced for ILEI are able to regain this phenotype when supplied with recombinant rILEI. Another functional activity assay used to demonstrate stemness is monitoring aldehyde dehydrogenase (ALDH) activity. We observed an increase in aldehyde dehydrogenase activity in

the E1KD cells when compared to NMuMG cells. This increase was reduced upon downregulation of both ILEI and LIFR protein levels (Fig 8G), further confirming the role of both ILEI and LIFR in the cancer stem cell phenotype.

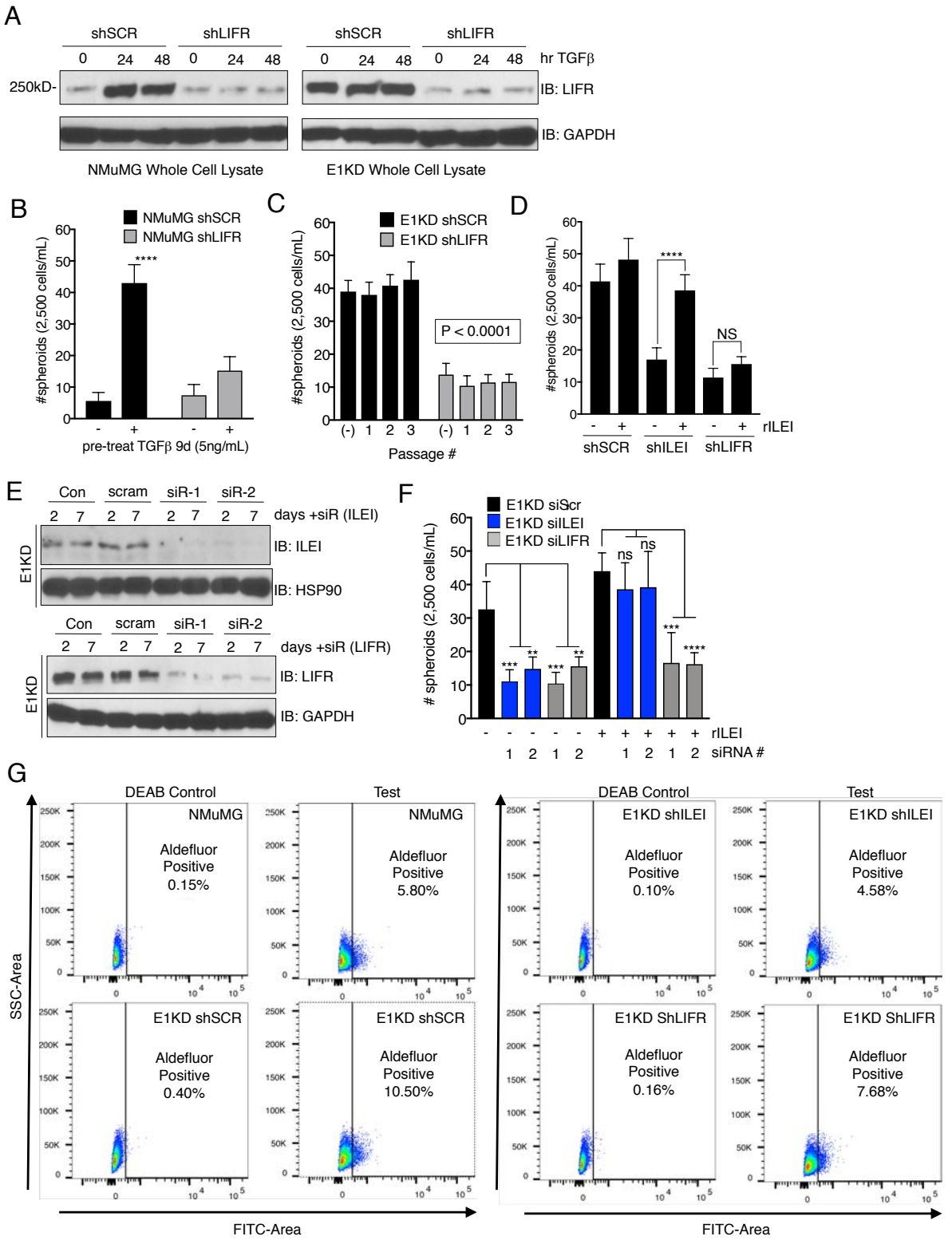

Fig 8. TGFβ/hnRNP E1-mediated BCSC formation requires both ILEI and LIFR (full figure legend next page).

Fig 8. TGFβ/hnRNP E1-mediated BCSC formation requires both ILEI and LIFR. (A) Immunoblot analysis of LIFR levels in TGFβ treated NMuMG and E1KD shSCR versus shLIFR cells. (B) Mammosphere assay of NMuMG cells stably transduced with either scramble control or LIFR knock-down shRNA (shLIFR) in the presence and absence of 9-day TGFβ pre-treatment (5ng/mL) (error bars represent mean +/- SD; n=5; ****p<0.0001, unpaired Student's t-test). (C) Quantification of mammosphere formation and self-renewal in E1KD cells stably transduced with either scramble control shRNA or LIFR knock-down (error bars represent mean +/- SD; n=5; p<0.0001 for all passages, paired Student's t-tests between correlative passage numbers). (D) Quantification of mammosphere formation in E1KD shSCR/shILEI/ shLIFR cells in the presence and absence of 10nM purified recombinant ILEI (error bars represent mean +/- SD; n=5; ****p<0.0001, unpaired Student's t-test). (E) Immunoblot analysis of ILEI and LIFR levels in E1KD cells transiently transfected with siRNA molecules. (F) Quantification of mammosphere formation in E1KD siSCR/ siILEI/ siLIFR cells in the presence and absence of 10nM purified recombinant ILEI (error bars represent mean +/- SD; n=5; **p<0.01, ***p<0.001, ****p<0.0001, unpaired Student's t-test). (G) FACS analysis of NMuMG, E1KD shSCR, E1KD shILEI, and E1KD shLIFR cells using the ALDEFLUOR Assay as described by the manufacturer and analyzed using FlowJo Software.

ILEI Induces STAT3 Signaling and BCSC formation through the Activation of LIFR

Downstream of LIFR activation, STAT3 is known to contribute to maintenance and self-renewal of stem cells [103]. To determine whether ILEI-induced LIFR activation resulted in phosphorylation of STAT3, we first monitored phospho-STAT3 at position Y705 (pSTAT3) in NMuMG and E1KD cells with and without TGFβ. Treatment with TGFβ for 24 hours induces pSTAT3 signaling in normal mammary epithelial cells (NMuMG). This activation is lost with both ILEI and LIFR protein reduction (Fig 9A-B). As shown, E1KD cells, which exhibit basal stem cell properties, possess constitutive pSTAT3 in the absence of TGFβ, and silencing of ILEI or LIFR in these cells results in a decrease in constitutive pSTAT3 levels (Fig 9A-B). Moreover, the addition of increasing concentrations of rILEI to E1KD shILEI cells for 30 minutes showed a corresponding increase in pSTAT3 (Fig. 9C). To test endogenous LIFR activation, we treated either control E1KD

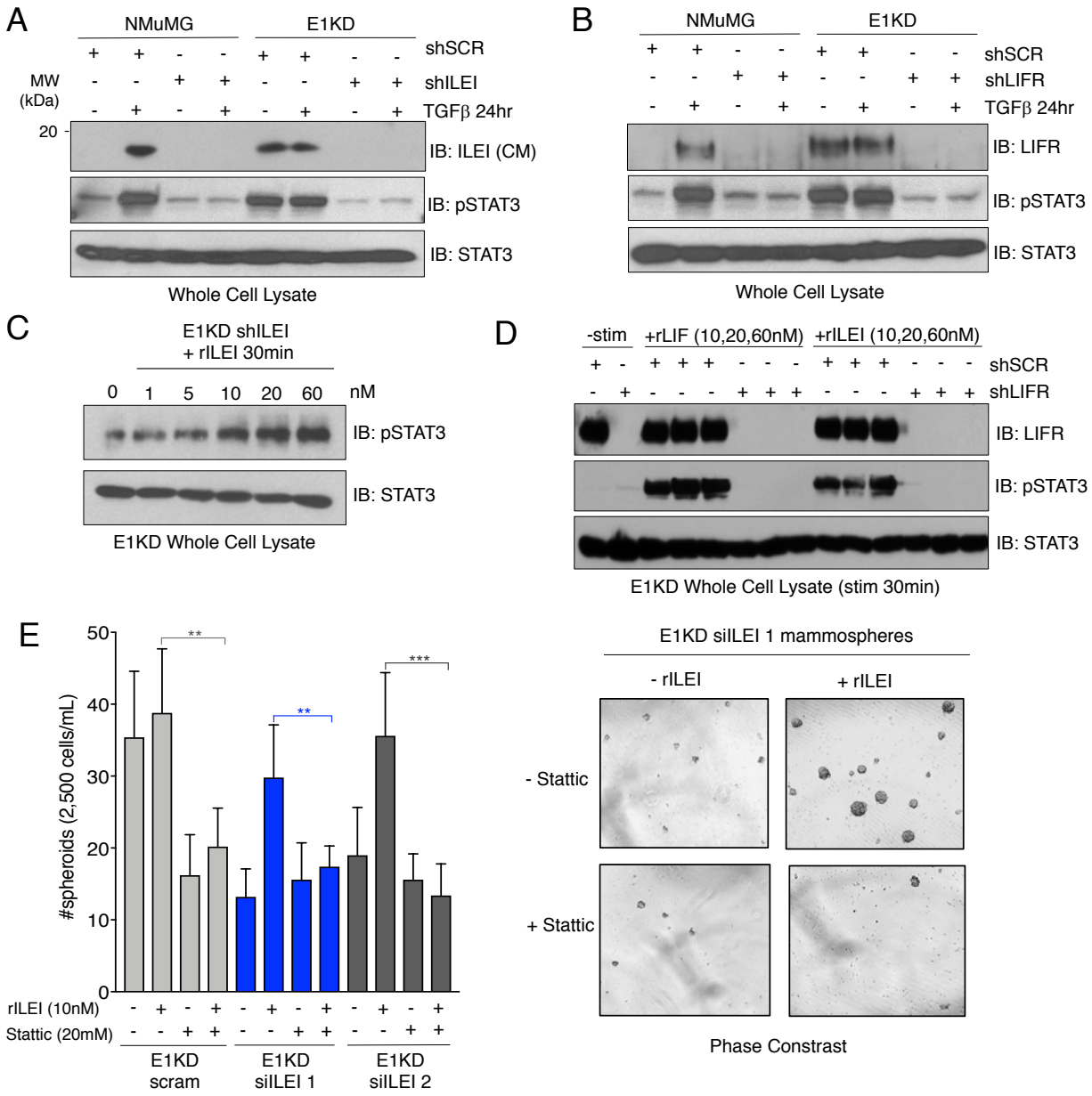

Fig 9. ILEI Induces STAT3 Signaling and BCSC formation through the Activation of LIFR (full figure legend next page).

shSCR cells or shLIFR cells with ILEI and LIF. Only E1KD cells that contain LIFR are responsive to ILEI and LIF through the subsequent activation of STAT3, demonstrating that LIFR mediates ILEI signaling (Fig 9D). In order to determine whether STAT3 activation is important for ILEI-mediated self-renewal phenotypes

Fig 9. ILEI Induces STAT3 Signaling and BCSC formation through the Activation of LIFR. (A) Immunoblot analysis of basal pSTAT3 levels in NMuMG and E1KD cells stably transduced with control shSCR shRNA, as well as shRNA targeting either ILEI or (B) LIFR. Cells were stimulated with TGFβ (5ng/mL) for 24 hours where indicated. (C) Stimulation of E1KD shILEI cells with the indicated concentration of recombinant ILEI for 30 minutes. Lysates were probed for phosphorylated STAT3 protein. (D) E1KD cells or E1KD shLIFR cells treated with increasing concentration of rLIF and rILEI for 30 minutes. Lysates were probed for LIFR, pSTAT3, and total STAT3. (E) Mammosphere assay using E1KD cells treated with two siRNA molecules against ILEI and rescued with rILEI treatment at 10nM. The STAT3 inhibitor Stattic was added at 20μM where indicated (error bars represent mean +/- SD; n=5; **p<0.01, ***p<0.001, unpaired Student's t-test). Right panels show phase contrast images of E1KD siILEI 1 spheroids in the presence and absence of ILEI and/or Stattic.

in E1KD cells, we utilized small molecule inhibitor of STAT3 activation termed Stattic. Figure 9E demonstrates that inhibition of STAT3 signaling significantly abrogates E1KD spheroid formation ability. The loss of this phenotype upon STAT3 inhibition cannot be rescued by rILEI treatment, suggesting that ILEI-mediated BCSC phenotypes are dependent upon LIFR and STAT3 (Fig 9E).

Overexpression of LIFR in mammary epithelial cells results in enhanced ILEI sensitivity

In order to investigate ILEI/LIFR interactions in cells, we generated two constructs of LIFR containing either the full-length receptor (FL-LIFR) or a truncation of the extracellular cytokine binding region (MU-LIFR) (Fig 10A). These constructs were overexpressed in NMuMG cells, which do not maintain high levels of endogenous LIFR (Fig 10B). While we could not detect an increase in basal pSTAT3 levels in the transfectants compared to E1KD cells, most likely due to the absence of ILEI translation (Fig 10C), we did observe activation of pSTAT3 in cells overexpressing the FL-LIFR, and not the MU-LIFR cells, following a 30 minute incubation with rILEI (Fig 10D). Further, co-immunoprecipitation analyses revealed that a 30 minute stimulation of cells overexpressing the FL-LIFR, and not the MU-

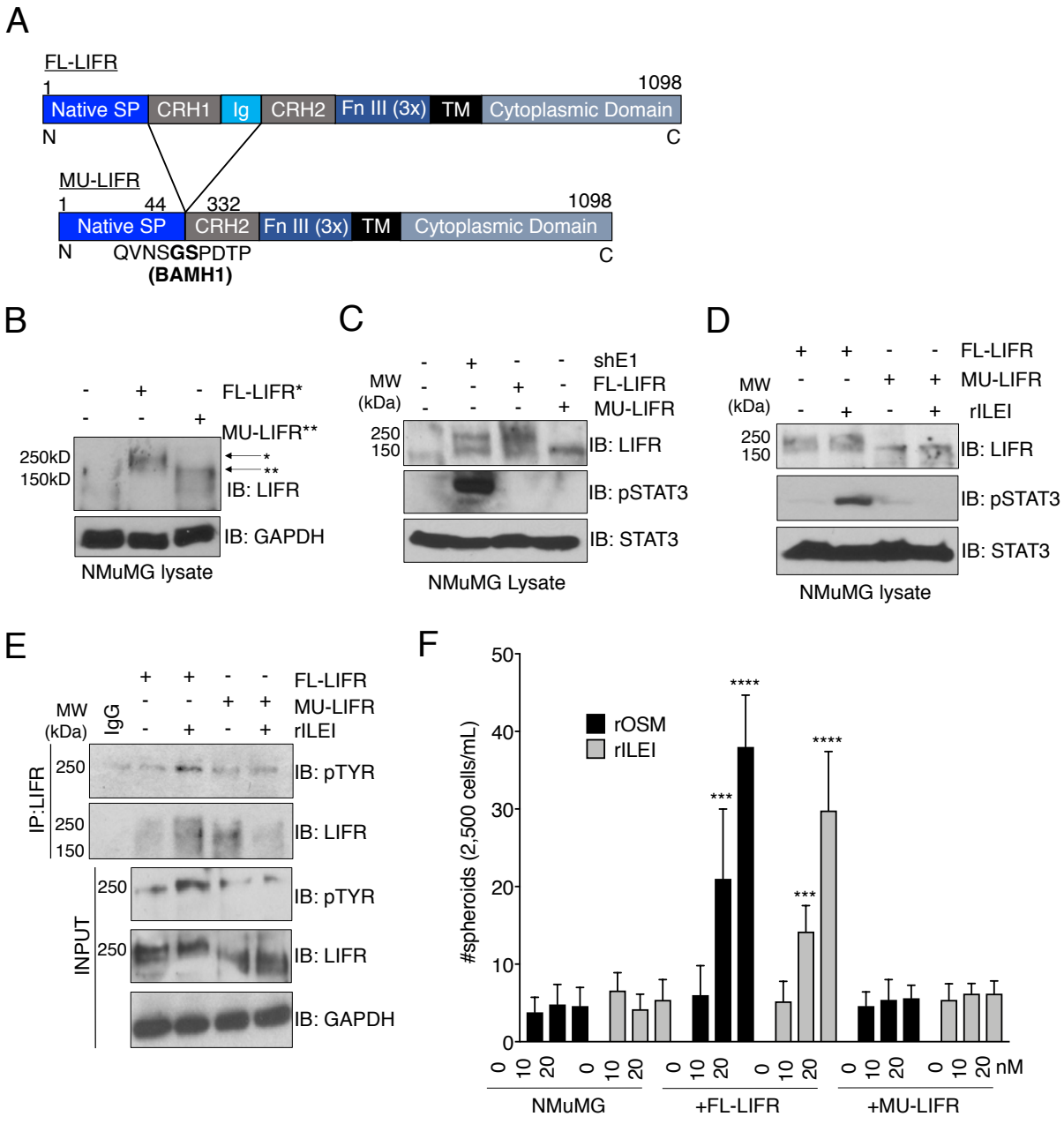

Fig 10. Overexpression of LIFR in mammary epithelial cells results in enhanced ILEI sensitivity (full figure legend next page).

Fig 10. Overexpression of LIFR in mammary epithelial cells results in enhanced ILEI sensitivity. (A) Construct diagram of FL-LIFR and mutated LIFR (MU-LIFR) lacking the cytokine binding region. Regions include the native signal peptide, cytokine receptor homology domains 1 and 2, Ig-like domain, Fibronectin type III repeat, transmembrane and cytoplasmic domains. (B) Overexpression of FL-LIFR and MU-LIFR constructs in NMuMG cells. (C) Immunoblot analysis of basal STAT3 activation in NMuMG cells overexpressing either FL-LIFR or MU-LIFR compared to parental NMuMG and E1KD cells. (D) Immunoblot analysis of STAT3 activation in response to rILEI (20nM) for 30 minutes in either NMuMG FL-LIFR or MU-LIFR cells. (E) Immunoprecipitation of LIFR after rILEI stimulation (20nM) for 30 minutes in NMuMG cells overexpressing either FL-LIFR or MU-LIFR followed by immunoblot analysis. (F) Quantification of mammosphere formation in NMuMG FL/MU-LIFR cells in the presence or absence of rOSM/rILEI pre-treatment for 7 days (error bars represent mean +/- SD; n=5; ****p<0.0001, ***p<0.001, unpaired Student's t-test).

LIFR, with rILEI promoted tyrosine phosphorylation of LIFR (Fig 10E). These results demonstrate that ILEI induces Jak/STAT signaling through the extracellular activation of the LIF receptor. We performed mammosphere assays to observe ILEI/LIFR signaling as it relates to epithelial cell self-renewal with the NMuMG FL/MU-LIFR cell lines in the presence of long-term ILEI treatment. The LIFR ligand OSM, recently shown to induce CSC phenotypes through pSTAT3 activation, was used as a positive control [104]. Figure 5k demonstrates that neither rILEI nor rOSM induce mammosphere formation in parental NMuMG cells. However, expression of FL-LIFR, but not the MU-LIFR, confers mammosphere formation capabilities to these cells, demonstrating that the cytokine-binding region of the receptor is necessary to elicit downstream biological phenotypes controlled by ILEI signaling (Fig 10F). Collectively, these data demonstrate that ILEI initiates STAT3 signaling through LIFR and this mechanism is necessary for BCSC phenotypes in mammary epithelial cells.

ILEI/LIFR Signaling Contributes to Mammary Stemness, Tumorigenesis, and Metastasis *in vivo*

To elucidate the *in vivo* potential of E1KD cells, we performed mammary fat-pad reconstitution experiments. Cleared fat-pads from 3-week old NOD/SCID female mice, were injected with either NMuMG-RFP or E1KD-GFP cells. 6 weeks post-injection, fat pads were isolated and analyzed by Carmine staining and imaged for fluorescent signals. E1KD-GFP cells, but not the NMuMG-RFP parental cells, were able to reconstitute the ductal network of cleared fat pads as observed with Carmine stain and GFP fluorescence (Fig 11A), demonstrating the pluripotent nature of the NMuMG cell line upon hnRNP E1 protein reduction. GFP expression in the ductal outgrowth validates that the *de novo* ductal tree growth is a result of E1KD cell injections and not failed clearance of the endogenous ductal tree. RFP signal was not observed in the NMuMG injected fat pads.

We have previously shown that E1KD cells, but not wild type NMuMG cells, are tumorigenic and metastatic when injected into the mammary fat-pad of NOD SCID mice[59,60]. To determine the contribution ILEI/LIFR signaling to these results, we performed similar mammary fat pad injections with either control E1KD shSCR, shILEI, and shLIFR cells and monitored tumor formation and metastatic disease. Female NOD/SCID mice were injected in the mammary fat pad region with dose-dependent concentrations ranging from 1k-100k cells. We demonstrate quantitatively that there is a significant alteration in tumor volume over time that is observed over multiple cell concentrations (Fig 11B). Similarly, we detected significant alterations in final tumor weight and tumor initiating cell frequency (TIC,

calculated using Extreme Limiting Dilution Analysis (ELDA) [105]) between control E1KD shSCR cells and the E1KD shILEI/LIFR lines (Fig 11C).

To investigate whether there was a difference in metastatic spread to the lungs from these experiments, we harvested lungs at the time of tumor extraction and performed H&E staining to identify metastases. Our data indicate that there is an aberration of metastatic lesions between the control E1KD shSCR lungs and the E1KD shILEI/LIFR lungs. Representative images show lungs with the largest metastatic burden obtained from each cell line (Fig 11D). Lungs extracted from mice injected with E1KD shSCR cells showed an average metastatic lesion area of 4.99% where the corresponding lungs from E1KD shILEI and shLIFR injected mice had an average metastatic area of 0.49% and 2.03%, respectively (Fig.10D, right graph).

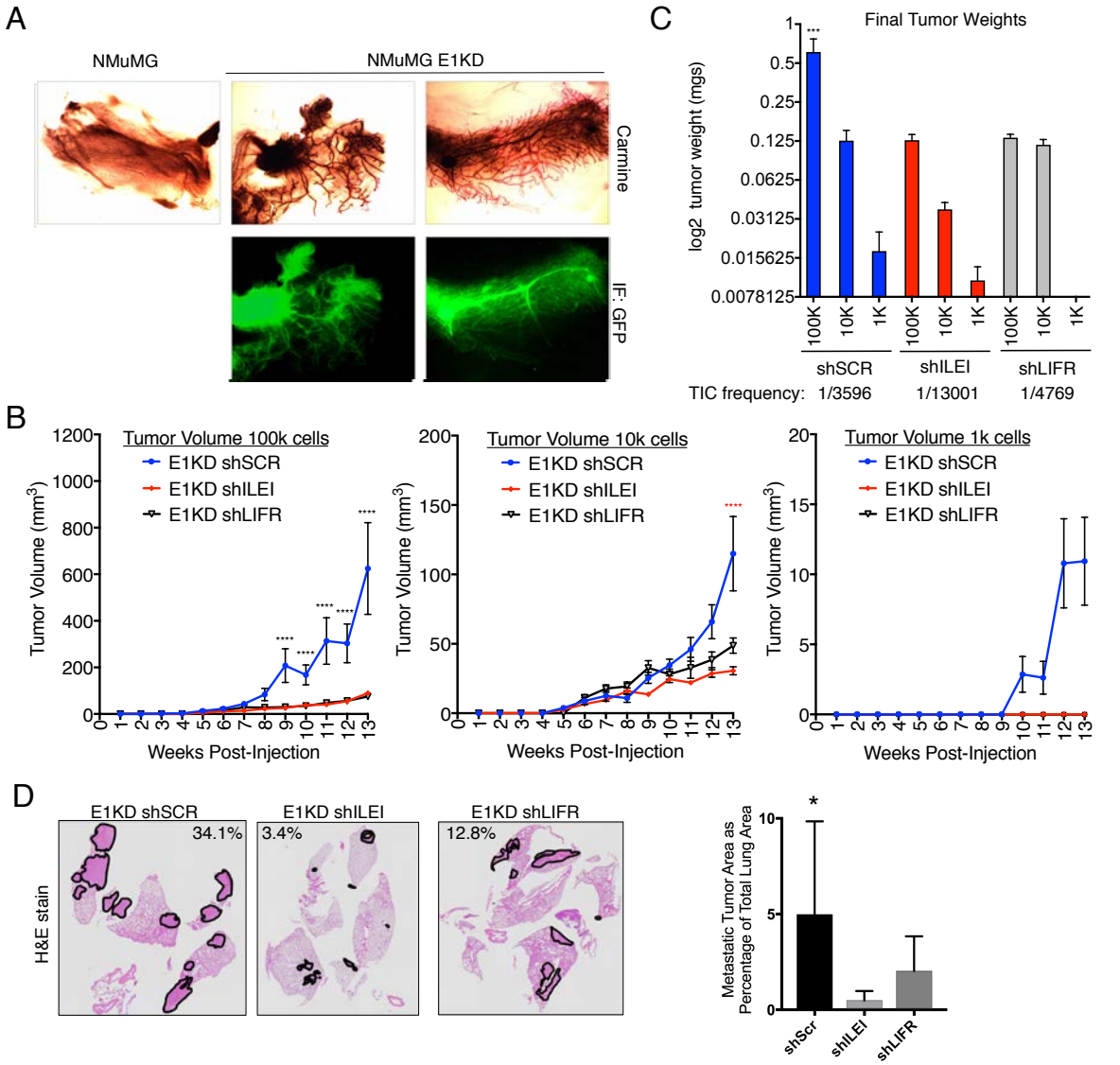

Fig 11. ILEI/LIFR Signaling Contributes to Mammary Stemness, Tumorigenesis, and Metastasis *in vivo*. (A) Mammary fat-pad reconstitution assay of NMuMG-GFP and E1KD-GFP cells orthotopically implanted into the cleared fat-pad of 3-week old female NOD/SCID mice. (B) Quantification of tumor volume over time in female NOD/SCID mice injected with E1KD shSCR, shILEI, and shLIFR cells at concentrations of 1k, 10k, and 100k cells per injection into the mammary fat-pad (error bars represent mean +/- SEM n≥4; ****p<0.0001, 2-way ANOVA; shSCR is significant compared to shILEI and shLIFR in 100k cell injections, shSCR is significant compared to shILEI in 10k cell injections). (C) Final mammary tumor weight quantification from female NOD/SCID mice injected with 1k, 10k, and 100k E1KD shSCR, shILEI, and shLIFR cells into the mammary fat-pad with a TIC frequency displayed for each condition (error bars represent mean +/- SEM, n≥4, ***p=0.0002, One-way Anova; E1KD shSCR 100k condition is significant when compared to the shSCR 10k and 1k conditions, as well as all shILEI and shLIFR conditions). (D) H&E staining of metastatic area in lungs of female NOD/SCID mice injected with E1KD shSCR, shILEI, and shLIFR cells into the mammary fat-pad. Representative images show lungs with the largest metastatic burden for each cell condition. Metastatic area percentage is shown for these images as well as quantification in right graph (error bars represent mean +/- SD; n=5; *p<0.05).

LEI/LIFR signaling contributes to tumor initiation

Previously, we observed changes in LIFR expression levels from low levels in the NMuMG cells to high levels in NMuMG cells silenced for hnRNP E1 (Fig 7A). Corresponding to our NMuMG versus E1KD data, in HMLE cells, the mesenchymal cell population displays increased levels of LIFR when compared to the epithelial cell population (Fig 12A). To further examine LIFR levels in tumorigenesis, we utilized a progression series developed in the lab and assessed the relative quantity of LIFR expression in our BCSC model (E1KDs) as compared to the resulting tumors from these cells [106]. This model was initiated using the NMuMG normal mammary cell line after hnRNP E1 knockdown. E1KD cells injected into the mammary fat pad of NOD/SCID mice form both primary mammary tumors (M1P) and lung metastases (L1P), from which cells were isolated and cultured in puromycin selection [106]. Interestingly, E1KD cells have significantly upregulated LIFR protein (Fig 8A & 12B) compared to the wild type NMuMG cell line, yet tumor outgrowth at both the primary and metastatic sites have lost expression of the LIFR gene product (Fig. 11B). ILEI levels in the conditioned media of the progression series increase (Fig 12C). As discussed below, LIFR expression could be important in tumor initiation and the breast cancer stem cell phenotype yet be downregulated during tumor outgrowth. Indeed, as observed in both primary tumors and metastatic tumors derived from the MMTV-PyMT breast cancer tumor model, LIFR levels are decreased overall in the tumor tissue (Fig 12D). IHC staining in these tumors for LIFR and ILEI, in addition to H&E staining, indicate that despite low overall levels of LIFR, there are distinct cells within the

cancer growth that maintain LIFR expression and could potentially act as BCSCs. ILEI expression is observed in all areas where LIFR expression is seen (Fig 12D).

Our *in vivo* analyses indicate that hnRNP E1 is an important factor controlling *in vivo* stemness properties within the mammary epithelium. We further show that the tumorigenic properties harbored by cells lacking hnRNP E1, which has been established previously [59,60], is mediated by ILEI and LIFR. The current model depicts an undiscovered signaling pathway that controls EMT and stemness properties regulated by TGFβ. We collectively demonstrate that TGFβ-induced ILEI expression and activation of LIFR through the hnRNP-E1 mechanism of EMT induction is responsible for enhanced tumorigenesis and CSC formation *in vitro* and *in vivo*.

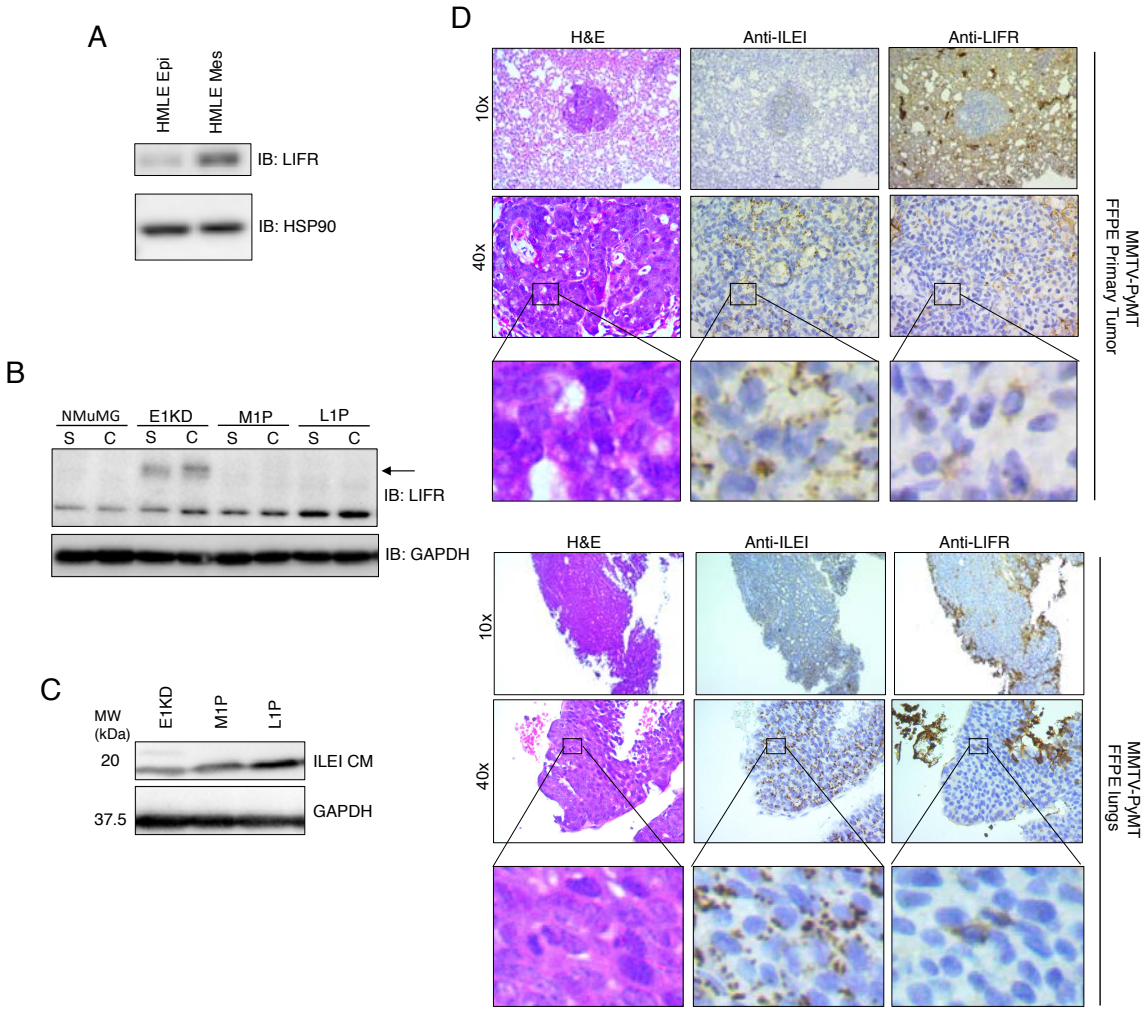

Fig 12. ILEI/LIFR signaling contributes to tumor initiation. (A) Immunoblot analysis of LIFR levels in epithelial and mesenchymal HMLE cells. (B) Immunoblot analysis of LIFR in NMuMG, E1KD, and E1KD cells injected into NOD/SCID fat pads and cultured from mouse primary tumor formation (M1P) and lung metastases (L1P). (C) Immunoblot analysis of ILEI from conditioned media of E1KD, M1P, and L1P cells. (D) Sections of FFPE primary tumors and lungs from MMTV-PyMT mice stained for H&E or IHC for ILEI and LIFR and imaged at 10x or 40x magnification.

3.3 Discussion

The dual roles of TGFβ signaling as a tumor-suppressor in normal epithelial cells and early-stage cancers, as well as tumor-promoter in advanced tumors stands as a complex paradigm of tumor development and spread [34,35]. Given its role in EMT induction and CSC formation during late stages of tumorigenesis, well-defined insight into these TGFβ-regulated processes is vital for the development of new-targeted therapies. Here, we have delineated a non-canonical TGFβ/hnRNP-E1-driven mechanism of CSC formation and tumorigenesis through the progenitor factor ILEI and the cytokine receptor LIFR. We demonstrate that TGFβ induces the expression and secretion of ILEI, through an hnRNP E1 translational mechanism, resulting in the activation of LIFR and downstream STAT3 signaling to mediate enhanced stemness and tumorigenic properties (Figure 8).

BCSCs serve as valuable therapeutic targets due to their ability to self-renew and differentiate to generate heterogeneity in the bulk tumor population, as well as display resistance to chemotherapeutic agents [50,89]. The emergence of tumor-initiating cancer stem cells (CSCs) has been identified across several cancer types including breast cancer, melanoma, and leukemia [50]. Various lines of evidence indicate that cell transformation caused by TGFβ-mediated EMT may be partially involved in BCSC formation during epithelial tumorigenesis [41,51,58]. Additionally, BCSCs rely on signaling pathways related to embryonic development and inflammatory signaling responses to maintain their stem-like properties, including Wnt/β-catenin, NOTCH, and importantly, Jak/STAT [103]. Signaling through the Jak/STAT pathway promotes proliferation, invasion, angiogenesis,

and metastasis [107]. Several groups have demonstrated the role of STAT3 in aiding stem cell/mesenchymal properties in cell populations originated from epithelial derived cancers including self-renewal and tamoxifen resistance [108,109].

Our evaluation of TGFβ-mediated EMT and BCSC formation through hnRNP E1 regulation has revealed insightful evidence of STAT pathway activation through an ILEI signaling axis. Modulation of ILEI in epithelial NMuMG cells or mesenchymal NMuMG cells knocked down for hnRNP E1 results in abrogated EMT and self-renewal capacity upon TGFβ stimulation *in vitro*. We demonstrate that either silencing of hnRNP E1 or sustained translation of ILEI by TGFβ stimulation is both necessary for EMT induction as well as CSC formation *in vitro*. These observations prompted an investigation into candidate effector molecules that aid in the ILEI signaling pathway to further understand its role in BCSC formation. Utilizing yeast-two-hybrid screening with a cDNA library derived from HeLA cell mRNA, we identified an interaction between ILEI and a precursor of the cytokine receptor LIFR. LIFR serves as a signaling platform for several cytokines and functions together with its co-receptor gp130, and in some instances with other ligand-specific co-receptors [98]. Activation of LIFR through ligand-binding induces a multitude of signaling pathways including JAK/STAT, AKT, and ERK [98]. These modalities have been established to converge and orchestrate a complex signaling network that results in the maintenance, pluripotency and self-renewal properties observed in embryonic stem cells (ESCs) [69]. Interestingly, it has been demonstrated that the assortment of ligands for LIFR elicit individual responses from this receptor [110]. For example, OSM and LIF can induce similar, yet distinct,

activation of STAT1, STAT3, ERK and JNK in T47D breast tumor cells [111]. In neuronal cells, CNTF and LIF result in different activation of downstream pathways due to variances in localization of receptor subunits to lipid rafts in the membrane [112]. Therefore, due to a complex network of co-receptors and regulators associated with the LIF receptor, further investigation comparing ILEI to previously identified LIFR ligands and the discovery of any co-receptors will be necessary to understand the ILEI/LIFR signaling pathway, and an important next step for targeted drug development.

The seeding of metastases and tumor heterogeneity requires intricate programming and over-activation/suppression of several signaling pathways [113]. ILEI has been established as an oncogenic cytokine responsible for both EMT and tumorigenesis [66]. Despite a clear function for STAT3 signaling in BCSCs, some reports describe LIFR as a metastasis suppressor [74,76,77,108]. Conflicting studies showed that high levels of LIFR in melanoma are associated with increased migration and poor prognosis in patients, and in prostate cancer epigenetic activation of LIFR is correlated with metastasis [78,79]. Despite the apparent discrepancies, we believe that our data along with the findings from Johnson et al. provide an interesting explanation [75]. Consistent with LIFR and STAT3's role in cancer stem cell maintenance, migration and invasion, LIFR protein levels are low in the normal mammary epithelial cells (NMuMG cells), yet high in our hnRNP E1 knockdown cells with a BCSC phenotype (Fig 8A). Most interestingly, when the primary tumors and metastatic lesions derived from NMuMG E1KD cells are extracted from NOD SCID mice and analyzed by western, LIFR levels are reduced

in both the primary and metastatic tumor cells when compared to E1KD cells (Fig 12B). This suggests that LIFR is playing important roles in maintenance of the cancer stem cells and in tumor formation yet may be inhibitory to tumor outgrowth both at the primary and secondary sites depending on the cellular context.

Similarly, Johnson et al. found that LIFR protein levels regulate the dormancy state of breast cancer cells disseminated to the bone [75]. In particular, LIFR protein reduction induced proliferation of the metastatic lesions in bone from cells that would otherwise remain dormant. Upon downregulation of LIFR, specific reduction in the mRNA of several dormancy and cancer stem cell genes was observed. Hypoxia was also shown to reduce LIFR protein levels, thereby down-regulating stem cell associated genes to promote metastatic growth and an exit from the dormancy state. Conversely, valproic acid induced expression of LIFR and consistently induced dormancy and cancer stem cell associated genes [75]. In our NMuMG E1KD cells, reducing LIFR inhibits the tumor initiating potential of our cells, and therefore reduces the tumorigenicity and metastatic potential of this system. Based on these findings, we believe that the ILEI/LIFR complex plays an important role in the maintenance of cancer stem cells at distant sites and may affect the switch from a dormant state to active metastatic growth. Herein, we have established a detailed mechanism by which TGFβ induces BCSC phenotypes during EMT induction.

Chapter 4

TGFβ induces LIFR transcription through positive feedback activation of ILEI/STAT3 signaling in breast cancer stem cell populations

4.1 Introduction

The tall cytokine receptor tyrosine kinase Leukemia Inhibitory Factor Receptor (LIFR) functions through high-affinity ligand-binding to a subset of the IL-6 family of secreted cytokines such as leukemia inhibitory factor (LIF), cardiotrophin-1 (CT-1), ciliary neurotrophic factor (CNTF), and oncostatin M (OSM) [64,71,98,114,115]. Ligand-binding to LIFR rapidly induces TYK2/JAK phosphorylation followed by subsequent cross-phosphorylation of opposing TYK2/JAKs on a nearby co-receptors such as gp130 which enables complex formation [98,116]. The LIFR ligands CT-1 and CNTF also contain ligand-specific "alpha" receptors, further complexing the variety of mechanisms that LIFR signaling entails [98,117]. Activation of several major cell-regulatory pathways including the Jak/STAT, Erk/MAPK, and Akt/PI3K signaling is regulated by LIFR [69,73,116,118]. This wide variety of signaling modalities may explain why LIFR is detected on most tissues and is involved in many important cell biological processes including inflammation, bone-remodeling, reproduction, cardiac function, neuromuscular function, the hematopoietic system, and embryonic stem cell (ESC) homeostasis [65,98,115,119–122]. In the context of cancer progression, LIFR has been implicated in both the enhancement and repression of oncogenesis, metastatic progression, and dormancy phenotypes [74,75,100].

During metastatic progression, TGFβ promotes EMT, similarly to other TGFβ responses, through type I (TβRI) and type II (TβRII) Ser/Thr receptor kinases

and integrates canonical Smad, as well as non-Smad, signaling and requires activation of the PI3K/Akt pathway [9,32,123]. While it is well established that the EMT process is regulated at the transcriptional level through factors such as Zeb1/2, Snail, and Slug, we have recently demonstrated that regulation of gene expression at the post-transcriptional level plays an important role in TGFβ-mediated EMT [59,60,124,125]. Recently, we have characterized a TGFβ regulatory pathway mediating EMT and BCSC formation that is controlled, through both transcriptional and translational mechanisms, by the RNA binding protein, heterogeneous nuclear ribonucleoprotein E1 (hnRNP E1) [59,60]. This hnRNP E1-regulated pathway initiates an autocrine signaling pathway that is not operative in normal epithelial cells but that is activated once cells have undergone an EMT or in cells in which hnRNP E1 has been silenced [59,126]. The ligand of this pathway, ILEI is regulated through a non-canonical TGFβ signaling pathway by 3'-UTR-mediated translational silencing at the mRNA level by hnRNP E1 [59,60]. TGFβ stimulation or silencing of hnRNP E1 increases ILEI translation and induces an EMT program that correlates to enhanced invasion and migration [59,60,106]. We also identified LIFR as the ILEI receptor and demonstrated that ILEI/LIFR signals through Stat3 to drive both TGFβ-mediated EMT and BCSC formation[126]. Further, reduction of either ILEI or LIFR protein levels results in reduced tumor growth, fewer tumor initiating cells and reduced metastasis within the hnRNP E1 knock-down cell populations *in vivo* [126].

During our characterization of ILEI/LIFR signaling, we observed that increases in ILEI expression, induced through either TGFβ stimulation or hnRNP E1 knock-down, led to enhanced LIFR protein expression levels [126]. Indeed,

stimulating normal murine mammary gland epithelial (NMuMG) cells with ILEI does not elicit downstream signaling pathways without the presence of either endogenous or exogenously overexpressed LIFR [126]. Herein, we aimed to understand how TGFβ/hnRNP E1 induces LIFR upregulation and whether this mechanism is important for the cellular phenotypes driven by the ILEI/LIFR signaling axis. We determined that TGFβ transcriptional transactivates LIFR expression through both canonical Smad3 and non-canonical ILEI-Stat3 mechanisms, and that disruption of either TGFβ/Smad and/or TGFβ/ILEI/Stat3 pathways alters LIFR transcription and BCSC formation. Collectively, our results are suggestive of a ligand-induced positive feedback loop controlled by TGFβ that triggers LIFR transcription through two distinct signaling arms.

4.2 Results

TGFβ induces LIFR expression through canonical SMAD3 and non-canonical ILEI/STAT3 signaling

We have shown that TGFβ stimulation or knock-down of hnRNP E1 results in mammary EMT induction followed by an increase in stemness potential that is driven by ILEI and LIFR [126]. While ILEI has been demonstrated to promote mammary tumorigenesis and metastasis, studies on LIFR function have demonstrated its dual-functionality as both a tumor-suppressive and tumor-enhancing gene in breast malignancy. To examine LIFR expression levels we performed RT-PCR and immunoblot analysis of Normal Murine Mammary Gland epithelial cells (NMuMG) or Human Mammary Epithelial cells (HMLE) in the presence and absence of TGFβ (Fig 13A). LIFR transcription and translation are

upregulated with TGFβ treatment in both cell populations (Fig 13A). We also probed for Smad3 and Stat3 activation and demonstrate that Smad3 is activated (phosphorylated) within1-3 h of TGFβ stimulation, while Stat3 is activated at 6 h and sustained for up to 72 h upon TGFβ treatment in both cell lines (Fig 13A). These kinetics of Smad3 and Stat3 activation in response to TGFβ are in agreement with previous results [123,126,127]. Concomitant with Smad3/Stat3 signaling, LIFR mRNA and protein levels are elevated after 24 hours of TGFβ stimulation. We next examined TGFβ-mediated LIFR upregulation in the 4T1 mouse breast cancer progression model and demonstrate elevated LIFR levels and Stat3 activation concomitant with the increased metastatic potential of the 4T1 cells compared to the 67NR and 4T07 cells (Fig 13A; right panel) [128]. To quantitatively monitor LIFR transcriptional responses we performed qPCR experiments in NMuMG cell lines treated with TGFβ (Fig 13B) and confirm that LIFR is upregulated by 3 h. To determine the contribution of Smad3 and Stat3 signaling in LIFR induction, we transiently silenced Smad3 and Stat3 using control or sequence specific siRNAs (Fig 13C-D). We demonstrate that TGFβ upregulation of LIFR requires both Smad3 and Stat3 activation, as silencing of either results in abrogated LIFR transcription and translation (Fig 13C-D). To confirm these observations, we next employed selective Smad3 and Stat3 inhibitors. The Smad3 inhibitor (SIS3) blocks Smad3 phosphorylation, while the Stat3 inhibitor (Stattic) abrogates Stat3 phosphorylation, dimerization, and nuclear localization [129,130]. Our results (Fig 13E-G) demonstrate that NMuMG cells remain viable in the presence of the inhibitors over a 24 h treatment, and that inhibition of either Smad3 or Stat3

abrogates LIFR upregulation in response to TGFβ. Collectively, these data demonstrate that TGFβ induces LIFR transcriptional upregulation dependent on both Smad3 and Stat3 signaling in mammary epithelial cells.

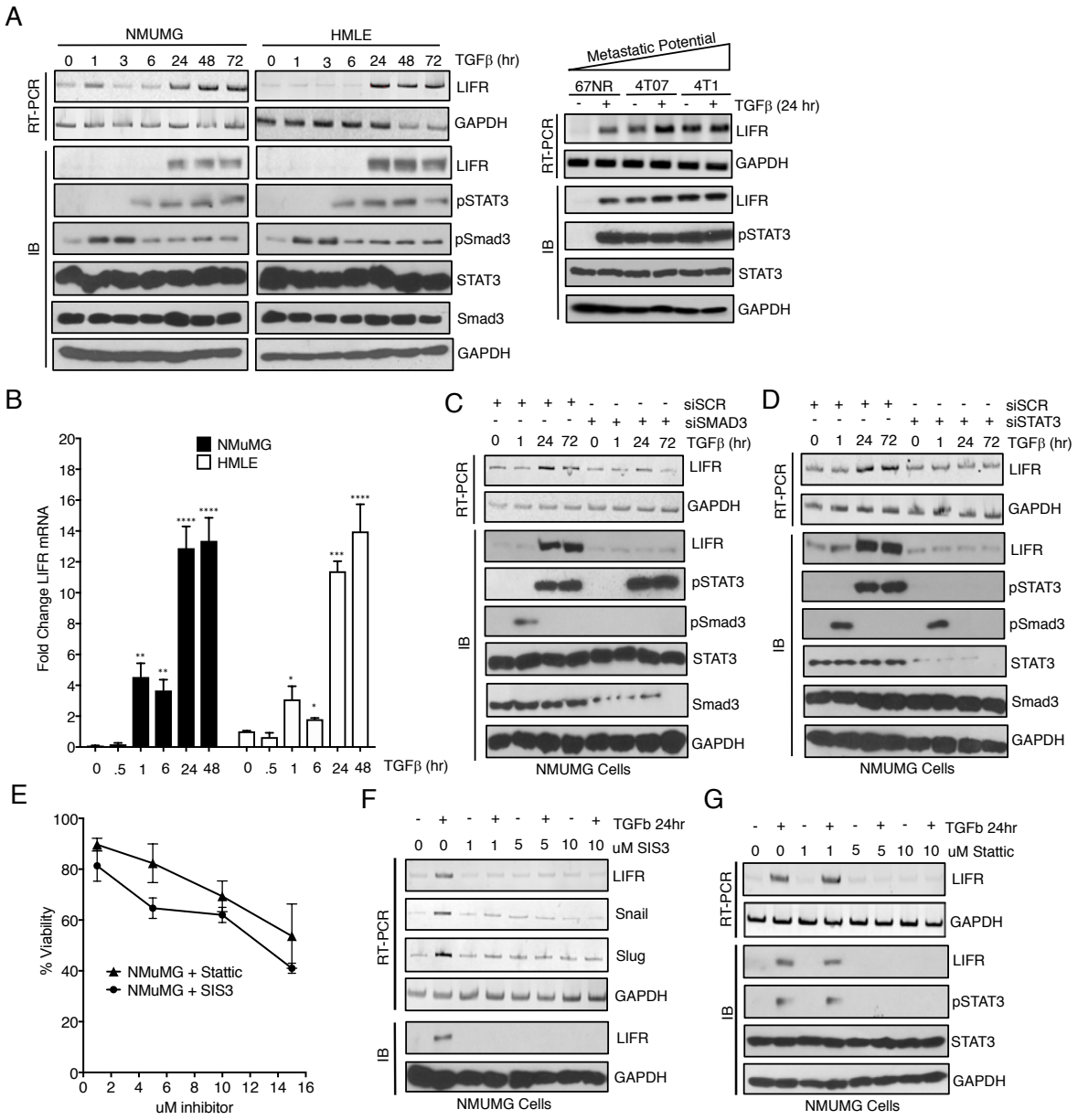

Fig 13. TGFβ induces LIFR upregulation through coordinated SMAD3/STAT3 activation. (A) RT-PCR and immunoblot analysis of (left) NMuMG and HMLE cells stimulated with TGFβ (5ng/mL) from 0 to 72 hours and (right) the 67NR tumor progressions series from 0 to 24 hours. (B) Quantitative PCR (qPCR) analysis of NMuMG and HMLE cells stimulated with TGFβ from 0 to 72 hours (error bars represent mean +/- SD; n=5; ****p <0.0001, unpaired Student's t-test). (C) RT-PCR and immunoblot analysis of NMuMG cells transiently transfected with control siRNA (siSCR) or siRNA targeting Smad3 (siSMAD3) and (D) Stat3 (siSTAT3). (E) Cell Viability analysis by MTT in NMuMG cells incubated with the small-molecule inhibitors SIS3 (Smad3i) and Stattic (Stat3i) for 24 hours. (F-G) RT-PCR and immunoblot analysis of NMuMG cells incubated with TGFβ in the presence and absence of SIS3 and Stattic.

TGFβ-mediated LIFR upregulation is dependent on hnRNP E1 and ILEI

We have previously shown that ILEI/LIFR signaling is required for TGFβ-mediated EMT and BCSC formation in breast epithelium and that ILEI is translationally upregulated following TGFβ stimulation and/or functional silencing of hnRNP E1 [59,61]. To determine whether ILEI plays a role in the upregulation of its own receptor, we utilized NMuMG and NMuMG cells silenced using siRNA for ILEI and/or hnRNP E1. NMuMG cells silenced for ILEI (siILEI) do not show an upregulation of LIFR after TGFβ treatment (Fig 14A). Interestingly, Smad3 activation is unaltered in NMuMG siILEI cells but downstream Stat3 activation is diminished upon TGFβ treatment (Fig 14A). This suggests that ILEI mediates TGFβ-induced LIFR upregulation through Stat3 signaling. In order to test whether the addition of purified recombinant ILEI (rILEI) rescues LIFR upregulation after 6 h of TGFβ treatment, we utilized NMuMG siILEI cells and stimulated with TGFβ (Fig 14B). We show that the addition of rILEI after TGFβ stimulation is sufficient to rescue LIFR transcription and Stat3 activation (Fig 14B). We next investigated the relative contribution of hnRNP E1 to LIFR induction in NMuMG cells stably attenuated for hnRNP E1 expression (E1KD) that display high tumorigenicity and stemness properties *in vitro* and *in vivo* [59,60,106,126]. In these E1KD cells we observed constitutive LIFR, ILEI, and phospho-Stat3 levels (Fig 14C). Of note, Smad3 activation is unaltered in hnRNP E1 attenuated E1KD cells suggesting that it is upstream of hnRNP E1 and ILEI (Fig 14C). Next, we utilized siRNAs against either control scramble (siSCR), ILEI (siILEI), and LIFR (siLIFR) in E1KD cells to determine whether recombinant ILEI could rescue LIFR levels and constitutive

Stat3 activation (Fig 14D). The data demonstrate a significant loss of pStat3 and LIFR levels in siILEI and siLIFR cells respectively, and that treatment with rILEI can rescue pStat3 but not LIFR expression (Fig 14D), suggesting that ILEI signaling through LIFR is required for auto-induction of its own receptor. These results demonstrate that LIFR upregulation by TGFβ is dependent on hnRNP E1 and ILEI.

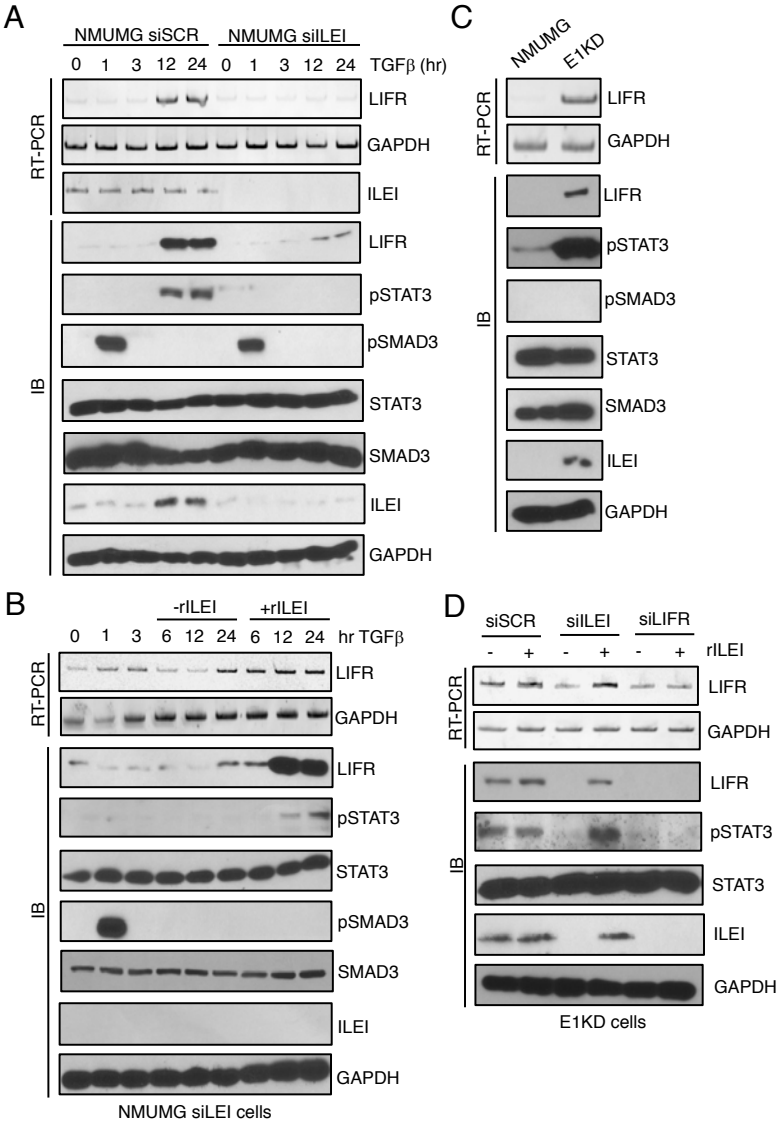

Fig 14. TGFβ-mediated LIFR upregulation is dependent on ILEI translation through the functional silencing of hnRNP E1. (A) RT-PCR and immunoblot analysis of NMuMG cells transiently transfected with control siRNA (siSCR) or siRNA targeting ILEI (siILEI) in the presence and absence of TGFβ from 0 to 24 hours. (B) RT-PCR and Immunoblot analysis of NMuMG siILEI cells in the presence and absence of TGFβ from 0 to 24 hours as well as recombinant ILEI (rILEI) from 6 to 24 hours. (C) RT-PCR and immunoblot analysis of NMuMG cells and NMuMG cells stably silenced for hnRNP E1 (E1KD). (D) RT-PCR and immunoblot analysis of NMuMG E1KD cells transiently transfected with either control siRNA (siSCR), siRNA targeting ILEI (siILEI), or siRNA targeting LIFR (siLIFR) in the presence and absence of rILEI (10nM) from 0 to 24 hours.

TGFβ induction of LIFR and BCSC formation requires both Smad3 and Stat3 signaling

TGFβ is a potent inducer of EMT and BCSC properties [59,126]. To determine the function of Smad3 and Stat3 to TGFβ/ILEI/LIFR-mediated stemness in mammary epithelial cells, we utilized siRNAs guided to Smad3 and Stat3 in both NMuMG and E1KD cells (Fig 15A-B). We stimulated NMuMG/E1KD cells transiently silenced for Smad3 and Stat3 with TGFβ for 24 h and monitored LIFR transcription (Fig 15C). As shown, Smad3 and Stat3 silencing abrogates TGFβ-mediated LIFR transcription in NMuMG cells (Fig 15C, left graph). However, only Stat3 inhibition significantly decreases constitutive LIFR transcriptional upregulation in E1KD cells (Fig 15C, right graph). This suggests that E1KD cells rely on Stat3 in order to mediate basal LIFR upregulation, while NMuMG cells stimulated with TGFβ require both activated Smad3 and Stat3 to induce LIFR. Using a mammosphere assay to monitor self-renewal and BCSC properties *in vitro* (Fig 15D-E), we next demonstrate that NMuMG cells rely on TGFβ pre-treatment as well as Smad3/Stat3 activation for mammosphere growth (Fig 15D, left graph). E1KD cells do not require TGFβ pre-treatment and rely solely on activated Stat3 for mammosphere growth (Fig 15D, right graph; images of spheres in Fig 15E). We previously show that hnRNP E1 silencing and ILEI translation are necessary for TGFβ-mediated BCSC formation [126]. To determine whether rILEI can rescue mammospheres growth of E1KD siILEI cells attenuated for Smad3 (siSmad3) or Stat3 (siStat3), we cultured cells with or without rILEI (Fig 3F). We show that only Stat3 silencing, and not Smad3 attenuation, impacts the ability of rILEI to rescue

the constitutive mammosphere growth of E1KD cells (Fig 3F). The data show that TGFβ induction of LIFR and BCSC formation relies on both Smad3 and Stat3, while cells silenced for hnRNP E1 only rely on ILEI and Stat3.

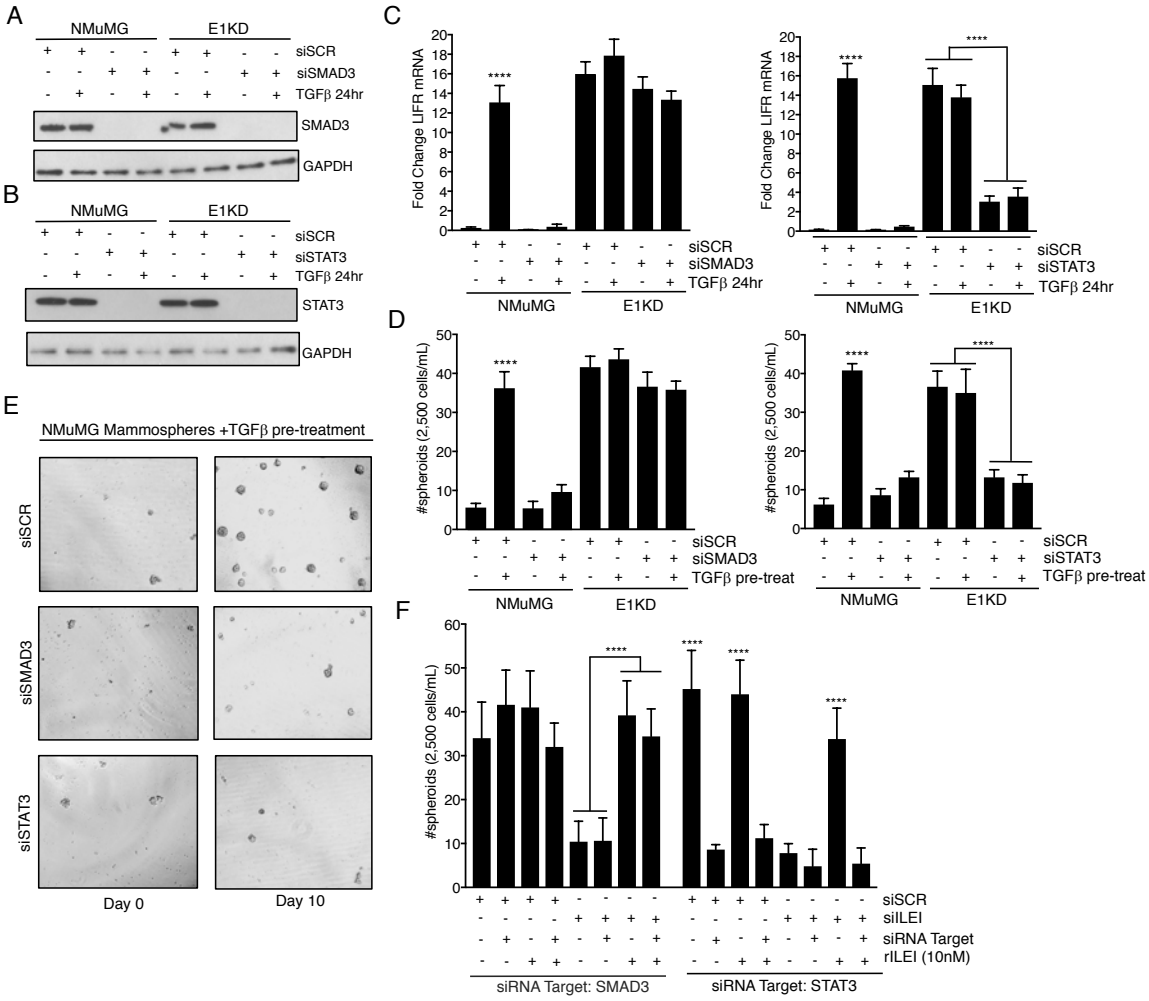

Fig 15. **TGFβ-mediated LIFR upregulation through SMAD3 and ILEI/STAT3 signaling mediates stemness properties in mammary epithelial cells.** (A) RT-PCR and immunoblot analysis of NMuMG and NMuMG E1KD cells transiently transfected with either control siRNA (siSCR), siRNA targeting Smad3 (siSMAD3) or (B) Stat3 in the presence and absence of TGFβ (5ng/mL) from 0 to 24 hours. (C) Quantitative PCR (qPCR) analysis of NMuMG and NMuMG E1KD cells transiently transfected with either control siRNA (siSCR), siRNA targeting Smad3 (siSMAD3) or Stat3 (siSTAT3) in the presence and absence of TGFβ from 0 to 24 hours (error bars represent mean +/- SD; n=5; ****p <0.0001, unpaired Student's t-test). (D) Mammosphere assay quantitation and (E) images of NMuMG cells transiently transfected with either control siRNA (siSCR), siRNA targeting Smad3 (siSMAD3) or Stat3 (siSTAT3) in the presence and absence of TGFβ from 0 to 24 hours (error bars represent mean +/- SD; n=5; ****p <0.0001, unpaired Student's t-test). (F) Mammosphere assay quantitation and (E) images of NMuMG E1KD cells transiently transfected with either control siRNA (siSCR), siRNA targeting ILEI (siILEI), Smad3 (siSMAD3) or Stat3 (siSTAT3) in the presence and absence of rILEI (10nM) from 0 to 24 hours (error bars represent mean +/- SD; n=5; ****p <0.0001, unpaired Student's t-test).

4.3 Discussion

TGFβ has been extensively studied for its dual roles in breast cancer tumorigenesis and metastasis [35,141]. During homeostasis and early events of metastasis, TGFβ serves as a tumor-suppressor factor. However, during late stages of metastasis, the TGFβ signaling network is highly altered to facilitate pro-tumorigenic and survival phenotypes [35,141]. Out of the several cellular phenotypes controlled by TGFβ signaling, many advances have demonstrated the importance of EMT programs during mammary tumorigenesis. While a multitude of investigators link EMT to disease, this process is ultimately a broad classification of molecular switches that dictate the transition from non-invasive epithelial cells to highly migratory mesenchymal populations that resemble stem cells [51,52]. It is therefore important to delineate specific factors that mediate disease-associated EMT and BCSC formation.

We have extensively shown the importance of TGFβ in the induction of mammary EMT programs that is dependent on translational regulation of ILEI by hnRNP E1 [59–61,126]. We have recently shown that ILEI functions through the cytokine receptor LIFR to induce BCSC phenotypes and *in vivo* tumorigenesis through activation of STAT3 signaling [126]. LIFR serves as a signaling platform for several ligands and has been shown to be involved in developmental pathways through its binding to several cytokines [70,112,115,122]. Like the TGFβ pathway, LIFR is implicated as both pro-tumorigenic as well as tumor suppressive [74,75,77,126]. This may be due to its ubiquitous expression profile and promiscuity to bind several ligands in several cell types. A key observation made by our previous work is that

TGFβ induces LIFR upregulation during EMT and BCSC formation in NMuMG cells [126]. Concomitantly, NMuMG E1KD cells display constitutive LIFR expression and STAT3 activation through ILEI. These data suggest that LIFR upregulation by TGFβ is dependent on hnRNP E1 function [126]. Two major points to address arose from these collective works; (1) What is causing LIFR upregulation by TGFβ and (2) is this phenomenon is ILEI dependent?

Herein, we have elucidated a mechanism of TGFβ-mediated LIFR upregulation through feed-forward signaling by ILEI/LIFR activation that relies on an initial early trigger of canonical TGFβ/SMAD3 signaling. Our initial studies of ILEI function involved first stimulating NMuMG cells with ILEI and probing for any signaling pathways that may be upregulated (Data not published). These experiments did not provide any meaningful hits as all pathways examined (MAPK/Erk, PI3K/Akt, JAK/STAT) were not activated by ILEI. These results hinted at the possibility that TGFβ signaling is critical not only for ILEI translation through functional hnRNP E1 silencing, but also for its downstream signaling [59]. This prompted us to investigate early canonical TGFβ signals that may "drive" ILEI functional output. Since TGFβ signaling has been extensively shown to modulate gene transcription through the regulatory SMAD proteins, we decided to test whether SMAD signaling played a role in long-term TGFβ-mediated LIFR upregulation [24]. We chose SMAD3 due to studies showing its effect on TGFβ-mediated EMT and tumorigenesis [142]. Indeed, inhibition of either SMAD3 or STAT3 signaling by siRNA or inhibitor studies resulted in altered LIFR upregulation by TGFβ (Fig 13). These results provided preliminary insight into what may be

“driving” LIFR upregulation due to previous results showing the inability of ILEI to induce STAT3 activation when stimulating wild-type NMuMG cells (not published). We determined that the basal LIFR expression in NMuMG cells is not sufficient to mediate ILEI signals. This point is demonstrated further by the fact that overexpressing LIFR in NMuMG cells results in STAT3 activation when treated with rILEI.

To look at the effect of SMAD3/STAT3 abrogation in the context of hnRNP E1 and ILEI, only STAT3 silencing produced a significant alteration in both downstream LIFR upregulation as well as BCSC phenotype acquisition (Figs 14 and 15). These results further support the hypothesis that TGFβ/SMAD signaling drives the upregulation of LIFR, while hnRNP E1 silencing and ILEI/LIFR signaling maintains LIFR upregulation and BCSC formation. We postulated that the TGFβ effect initially produces LIFR levels through SMAD signaling while simultaneously inducing ILEI translation. The kinetically coordinated manner of this process (SMAD3 activation occurs at 1 hour while ILEI translation occurs roughly 6 hours post treatment) suggests that once ILEI has been secreted, an adequate concentration of LIFR has been upregulated by TGFβ/SMAD3 which then allows the ILEI/LIFR pathway to commence. It is indeed possible to assume that the E1KD cells are producing TGFβ that is playing a partial role in pushing this mechanism, but the reliance of these cells on TGFβ to drive ILEI/LIFR signaling is significantly diminished when compared to NMuMG cells containing hnRNP E1. These data collectively demonstrate that TGFβ induces both the ligand (ILEI) and

receptor (LIFR) mediating downstream BCSC formation in mammary epithelial cells through coordination of two separate signaling pathways

Chapter 5

Conclusions and Future Perspectives

The collective work shown herein demonstrates a novel signaling axis whereby TGFβ induces the translation of a ligand (ILEI) and the transcription of its cognate receptor (LIFR). The biology of TGFβ has been studied extensively by several groups and has been established as a pleotropic cytokine with several functions in both promoting and suppressing tumorigenesis [34,35]. In the context of mammary epithelial cancers, TGFβ has been shown to induce tumor formation through its misregulation of EMT programs [36,61,144]. EMT is utilized during organ development and tissue remodeling but becomes misregulated during tumorigenesis and metastasis [36,38,39,51]. EMT has also been extensively shown to control stem cell phenotypes in breast cancer cells that ultimately dictates tumor heterogeneity and chemoresistance [38,51,88] . Since TGFβ-mediated EMT is integral for both normal developmental processes as well as cellular homeostasis, it is a highly difficult challenge to mitigate its overall function strictly in the context of disease. Indeed, misregulated TGFβ signaling is observed in many pathologies including but not limited to vascular dysplasia, fibrosis, atherosclerosis, and immune disorders [9]. These challenges necessitate investigation into disease-specific mechanisms of TGFβ downstream of its initial signaling ques.

Our lab has studied a non-canonical TGFβ signaling pathway extensively involved in both skin and breast malignancies [126,145]. These mechanisms involved

differential regulation of EMT programs by TGFβ through transcript-selective translation of important mRNAs with EMT-related functions such as Dab2 and ILEI [59,60]. ILEI has been previously established as an important factor in mediating EMT and tumorigenesis by several groups [66,67,126]. Similar to TGFβ, ILEI also plays roles in normal developmental processes as well as other pathologies such as Alzheimer's [68,93]. Given the plethora of downstream cellular phenotypes governed by ILEI signaling, it is necessary to interrogate the mechanistic processes that participate in ILEI signaling once it has been translationally upregulated by TGFβ. The goal of this project was to uncover mechanistic insight into the ILEI signaling pathway through a series of biochemical, cell and molecular techniques. Although many functional outputs have been associated with ILEI, little progress had been made due to the inability to produce bioactive protein for cellular studies. Through experimental screening of ILEI constructs from several sources that may produce activity, we uncovered subtle molecular changes that facilitate the proteins ability to signal through its dimerization by means of intermolecular disulfide bridges (Fig 1). Indeed, the x-ray structure of ILEI represents the protein as a dimeric species that "domain swaps"[81]. It is interesting however that only roughly 5-10% of secreted ILEI is dimeric, which holds true with recombinant protein in solution while in the absence of a reducing agent such as beta mercaptoethanol (Fig 1). These observations pose many questions on ILEI structure and function, as it would be presumed biologically and evolutionarily that the active dimeric molecule would outcompete the monomeric species in solution. In order to "enrich" the dimer species, we relied on simple manipulations surrounding the preparation,

purification, and storage of the protein. We observed that incubating the pure protein derived from *E.coli* at 37 degrees overnight not only shifted the monomer/dimer ratio from roughly 90:10 to 60:40, we discovered that the more dimeric species elicited signaling activity by activation of STAT3 at 30 minutes post stimulation in E1KD cells and NMuMG cells overexpressing LIFR. These results made intuitive sense to us since performing long-term biologic experiments such as mammospheres formation assays with monomeric ILEI (90:10) yielded a biological response. We postulated therefore that the incubation period of ILEI within these biologic assays allows for proper dimerization and downstream function. The isolation of biologically activate ILEI proved to be a rate-limiting step in the process of understanding its mechanism in EMT, tumorigenesis and metastasis.

In order to understand mechanisms that elicit STAT3 activation by secreted ILEI, we first aimed to compile ILEI interaction partners by yeast-two-hybrid screening. We mined through the ILEI interactome by this screen to decipher potential extracellular receptors that were enriched in this analysis. Indeed, one of the hits corresponded to the LIFR precursor (Fig 7A). Intuitively, one would not expect to observe a cytokine/receptor interaction within the nuclei of yeast cells. However, we used this screen as a hint for possible candidates that could be tested downstream through simple *in vitro* experiments to identity an ILEI effector molecule expressed on the cell surface of mammalian cells. Previous studies in our lab demonstrated a possible correlation of ILEI and hnRNP E1 to STAT3 activation. Given these observations coupled the current understanding of LIFR as

an extracellular receptor with several ligands and functional roles in embryonic stem cell biology through STAT3 activation, we postulated it may serve as the ILEI receptor. Through extensive analysis using si/shRNA guidance, protein-protein binding, and cell signaling studies, we validated LIFR as the receptor for ILEI. This axis is responsible for TGFβ-mediated cancer stem cell phenotypes and tumorigenesis *in vitro* and *in vivo*. These studies demonstrated a novel cytokine signaling pathway controlled by TGFβ. As with any line evidence of this nature, there are more questions that arise than there are answers. One phenomenon that was observed within this work was the upregulation of both ILEI as well as LIFR after either TGFβ signaling (24hr) or functional silencing of hnRNP E1 (Fig 8B). These results correlated to a previous observation that treating NMuMG cells with ILEI produced no STAT3 activation or BCSC properties. ILEI-mediated STAT3 activation through LIFR is only observed when either hnRNP E1 is silenced or full-length LIFR is overexpressed in NMuMG cells (Fig 9C-D). In order to fully understand the ILEI signaling pathway through LIFR, it became evident that there is an additional mechanism controlling the upregulation of LIFR through TGFβ signaling and/or hnRNP E1 silencing.

Our observations concerning TGFβ/hnRNP E1-mediated LIFR upregulation at the protein level led to further investigation into this phenomenon. We first observed that this effect was not only translational but transcriptional (Fig 13A) Through refined analysis of the kinetics pertaining to TGFβ signaling, we decided to explore the contribution of the early canonical SMAD signaling pathway to our mechanism of downstream ILEI/STAT3 signaling. Our data indicate that TGFβ

induces LIFR upregulation at early time points (1-6 hr) as well as later time points (24-72 hr) (Fig 13A). We decided to test the contribution of SMAD3 to this mechanism due to its extensive role in TGFβ-mediated EMT [123,142]. Our hypothesis was that early SMAD3 activation was inducing the upregulation of LIFR that then became available for ILEI to signal through and further induce LIFR through enhanced STAT3 activity. We were able to demonstrate that upon TGFβ stimulation in NMuMG cells, SMAD3 and STAT3 levels are necessary for both long-term LIFR upregulation as well as BCSC formation *in vitro* (Fig 15). Interestingly, E1KD cells only relied on STAT3 to display basal LIFR upregulation as well as constitutive BCSC properties (Fig. 15). These results culminate in the importance of ILEI in mediating downstream BCSC phenotypes through its interaction with LIFR. Without ILEI present, NMuMG cells do not upregulate LIFR upon long-term TGFβ stimulation. This is also true in the E1KD cell populations where ILEI silencing diminishes constitutive LIFR upregulation and BCSC phenotypes. Therefore, ILEI is activating a positive feedback loop once it has interacted with LIFR and activated downstream STAT3-mediated LIFR transcription. In order for this loop to initiate, we postulate that TGFβ must signal SMAD3 to "kickstart" the upregulation of LIFR in order to ILEI to take over and begin the feed-forward loop. BCSCs have been established as drivers of tumorigenesis and drug resistance [56,89]. Although this project is primarily mechanistic in nature, we have observed that silencing of hnRNP E1 leads to the inability of mammary fat-pad reconstitution *in vivo*. Furthermore, we show *in vivo* that silencing of ILEI or LIFR in basally tumorigenic E1KD cells significantly

abrogates their ability to form tumors and metastasize to the lung. The collective work presented within reveals a novel feed-forward mechanism of BCSC formation that relies on TGFβ-mediated upregulation of a ligand (ILEI) and its extracellular receptor (LIFR).

Mechanistic insight into the TGFβ/ILEI/LIFR signaling axis has presented revealed several questions that guide future investigations. For instance, it has been well established that transcription factors such as the SMADs and STATs contain additional co-factors that aid in their DNA-binding and regulatory functions [146–149]. Previous studies have demonstrated the signaling kinetics of SMAD3 and STAT3 in response to TGFβ signaling, whereby SMAD3 activation is immediate upon stimulation and STAT3 activation is constitutive at later time points [123,126]. We postulated that differential SMAD3/STAT3 signaling kinetics may coordinate an axis whereby LIFR transcription is initiated by immediate SMAD3 activation and maintained downstream by ILEI/LIFR signaling. These hypotheses were intended to answer the question of what drives ILEI signaling, since stimulation of NMuMG cells with ILEI provided no activation of STAT3 due to low LIFR expression in these cell populations (Data not shown). These results indicated that there has to be a TGFβ-responsive signal that drives LIFR upregulation in order for ILEI to mediate its signaling cascade. These results pose a question of what dictates the specificity of these sites as it pertains to LIFR upregulation. From the aspect of the ILEI/LIFR signaling axis, there are many future perspectives that can be attained from high-resolution structural analysis of the complex. Since LIFR is a promiscuous receptor that binds several ligands and forms complexes with various co-receptors, it is

undoubtedly possible that ILEI coordinates a complex containing additional co-factor receptors [98]. Under the pretense of drug discovery purposes, it is critical to understand the ILEI/LIFR complex at the molecular level in order for the development of targeted therapies that antagonizes its formation and downstream signaling. Although ILEI may function during homeostasis through LIFR for developmental and progenitor purposes, we predict that targeting ILEI/LIFR in breast cancer patients is more precisely targeted versus attempting to neutralize TGFβ. In other words, targeting TGFβ will harbor significantly more off-target effects compared to targeting a downstream pathway controlled by TGFβ that is more functionally fine-tuned. These future directions will indeed guide the probable development of small-molecules or antibody therapies that will neutralize the ILEI/LIFR interaction in breast cancer patients.

In conclusion, we have delineated a mechanism of TGFβ-mediated BCSC formation through ILEI and LIFR. We show that this mechanism is tightly controlled by coordinated canonical SMAD3 signaling as well as downstream ILEI-driven STAT3 activation through LIFR binding. TGFβ/SMAD3 initiates both the upregulation of ILEI (translational) and LIFR (transcriptional), while ILEI and LIFR subsequently control LIFR transcription and BCSC phenotypes through STAT3. These findings will serve as a potential therapeutic platform for metastatic breast cancer.

Chapter 6

References

1. Facts, C. Cancer Facts & Figures 2018. (2018).
2. Sotiriou, C. & Pusztai, L. Gene-Expression Signatures in Breast Cancer. *N. Engl. J. Med.* (2009). doi:10.1056/NEJMra0801289
3. Weigelt, B., Baehner, F. L. & Reis-Filho, J. S. The contribution of gene expression profiling to breast cancer classification, prognostication and prediction: A retrospective of the last decade. *Journal of Pathology* (2010). doi:10.1002/path.2648
4. Dai, X. *et al.* Breast cancer intrinsic subtype classification, clinical use and future trends. *American Journal of Cancer Research* (2015). doi:www.ajcr.us/ISSN:2156-6976/ajcr0014158
5. Onitilo, A. A., Engel, J. M., Greenlee, R. T. & Mukesh, B. N. Breast cancer subtypes based on ER/PR and Her2 expression: Comparison of clinicopathologic features and survival. *Clin. Med. Res.* (2009). doi:10.3121/cmr.2008.825
6. Moses, H. & Barcellos-Hoff, M. H. TGF-β Biology in Mammary Development and Breast Cancer. *Cold Spring Harb. Perspect. Biol.* **3**, a003277 (2011).
7. Daniel, C. W., Robinson, S. & Silberstein, G. B. The role of TGF-beta in patterning and growth of the mammary ductal tree. *J. Mammary Gland Biol. Neoplasia* **1**, 331–41 (1996).
8. Esquivel-Velázquez, M. *et al.* The Role of Cytokines in Breast Cancer

Development and Progression. *J. Interf. Cytokine Res.* (2015). doi:10.1089/jir.2014.0026

9. Blobe, G. C., Schiemann, W. P. & Lodish, H. F. Role of Transforming Growth Factor β in Human Disease. *N. Engl. J. Med.* (2000). doi:10.1056/NEJM200005043421807
10. Huminiecki, L. *et al.* Emergence, development and diversification of the TGF- signalling pathway within the animal kingdom. *BMC Evol. Biol.* (2009). doi:10.1186/1471-2148-9-28
11. Massagué, J. TGFβ signalling in context. *Nature Reviews Molecular Cell Biology* (2012). doi:10.1038/nrm3434
12. Piek, E., Heldin, C. H. & Ten Dijke, P. Specificity, diversity, and regulation in TGF-beta superfamily signaling. *FASEB J.* (1999). doi:10.1890/13-0290.1
13. Sporn, M. B., Roberts, A. B., Wakefield, L. M. & de Crombrugghe, B. Some recent advances in the chemistry and biology of transforming growth factor-beta. *J. Cell Biol.* **105**, 1039 LP-1045 (1987).
14. Assoians, R. K., Komoriya, A., Meyers, C. A., Miller, D. M. & Sporn, M. B. Transforming Growth Factor-ß in Human Platelets. *J. Biol. Chem.* (1983). doi:10.1016/j.molstruc.2014.01.078
15. Frolik, C. a, Dart, L. L., Meyers, C. a, Smith, D. M. & Sporn, M. B. Purification and initial characterization of a type beta transforming growth factor from human placenta. *Proc. Natl. Acad. Sci. U. S. A.* (1983). doi:10.1073/pnas.80.12.3676

16. Roberts, A. B. *et al.* Purification and Properties of a Type β Transforming Growth Factor from Bovine Kidney. *Biochemistry* (1983). doi:10.1021/bi00294a002

17. Beta, T. G. F.-. Some Recent Advances in the Chemistry and Biology of Transforming Growth Factor- Beta. **105**, 1039–1045 (1987).

18. Poniatowski, L. A., Wojdasiewicz, P., Gasik, R. & Szukiewicz, D. Transforming growth factor beta family: Insight into the role of growth factors in regulation of fracture healing biology and potential clinical applications. *Mediators of Inflammation* (2015). doi:10.1155/2015/137823

19. Kothapalli, D., Frazier, K. S., Welply, A., Segarini, P. R. & Grotendorst, G. R. Transforming growth factor beta induces anchorage-independent growth of NRK fibroblasts via a connective tissue growth factor-dependent signaling pathway. *Cell growth Differ.* (1997). doi:10.1162/106454603322221531

20. Wakefield, L. M., Smith, D. M., Flanders, K. C. & Sporn, M. B. Latent transforming growth factor-β from human platelets. A high molecular weight complex containing precursor sequences. *J. Biol. Chem.* (1988).

21. Watabe, T. & Miyazono, K. Roles of TGF-β family signaling in stem cell renewal and differentiation. *Cell Research* (2009). doi:10.1038/cr.2008.323

22. Annes, J. P. Making sense of latent TGFbeta activation. *J. Cell Sci.* (2003). doi:10.1242/jcs.00229

23. Zilberberg, L. *et al.* Specificity of latent TGF-β binding protein (LTBP) incorporation into matrix: Role of fibrillins and fibronectin. *J. Cell. Physiol.*

(2012). doi:10.1002/jcp.24094

24. Schmierer, B. & Hill, C. S. TGFβ-SMAD signal transduction: Molecular specificity and functional flexibility. *Nature Reviews Molecular Cell Biology* (2007). doi:10.1038/nrm2297

25. Shi, Y. & Massagué, J. Mechanisms of TGF-β signaling from cell membrane to the nucleus. *Cell* (2003). doi:10.1016/S0092-8674(03)00432-X

26. Hill, C. S. Transcriptional control by the SMADs. *Cold Spring Harbor Perspectives in Biology* (2016). doi:10.1101/cshperspect.a022079

27. Mullen, A. C. & Wrana, J. L. TGF-β family signaling in embryonic and somatic stem-cell renewal and differentiation. *Cold Spring Harb. Perspect. Biol.* (2017). doi:10.1101/cshperspect.a022186

28. Mullen, A. C. *et al.* Master transcription factors determine cell-type-specific responses to TGF-β signaling. *Cell* (2011). doi:10.1016/j.cell.2011.08.050

29. Whyte, W. A. *et al.* Master transcription factors and mediator establish super-enhancers at key cell identity genes. *Cell* (2013). doi:10.1016/j.cell.2013.03.035

30. Mulder, K. M. & Morris, S. L. Activation of p21(ras) by transforming growth factor β in epithelial cells. *J. Biol. Chem.* (1992).

31. Edlund, S. Transforming Growth Factor-beta -induced Mobilization of Actin Cytoskeleton Requires Signaling by Small GTPases Cdc42 and RhoA. *Mol. Biol. Cell* (2002). doi:10.1091/mbc.01-08-0398

32. Bakin, A. V., Tomlinson, A. K., Bhowmick, N. A., Moses, H. L. & Arteaga,

C. L. Phosphatidylinositol 3-kinase function is required for transforming growth factor β-mediated epithelial to mesenchymal transition and cell migration. *J. Biol. Chem.* (2000). doi:10.1074/jbc.M005912200

33. Zhang, Y. E. Non-Smad pathways in TGF-β signaling. *Cell Research* (2009). doi:10.1038/cr.2008.328

34. Lebrun, J.-J. The Dual Role of TGFβ in Human Cancer: From Tumor Suppression to Cancer Metastasis. *ISRN Mol. Biol.* **2012**, 381428 (2012).

35. Akhurst, R. J. & Derynck, R. TGF-beta signaling in cancer--a double-edged sword. *Trends Cell Biol.* **11**, S44-51 (2001).

36. Kalluri, R. & Weinberg, R. A. The basics of epithelial-mesenchymal transition. *J. Clin. Invest.* **119**, 1420–8 (2009).

37. Larue, L. & Bellacosa, A. Epithelial-mesenchymal transition in development and cancer: role of phosphatidylinositol 3' kinase/AKT pathways. *Oncogene* **24**, 7443–54 (2005).

38. Acloque, H., Adams, M. S., Fishwick, K., Bronner-Fraser, M. & Nieto, M. A. Epithelial-mesenchymal transitions: The importance of changing cell state in development and disease. *Journal of Clinical Investigation* (2009). doi:10.1172/JCI38019

39. Nieto, M. A., Huang, R. Y. Y. J., Jackson, R. A. A. & Thiery, J. P. P. EMT: 2016. *Cell* (2016). doi:10.1016/j.cell.2016.06.028

40. Gheldof, A. & Berx, G. Cadherins and Epithelial-to-Mesenchymal Transition. *Prog. Mol. Biol. Transl. Sci.* **116**, 317–336 (2013).

41. Richards, E. J. *et al.* Long non-coding RNAs (LncRNA) regulated by

transforming growth factor (TGF) β: LncRNA-hit-mediated TGFβ-induced epithelial to mesenchymal transition in mammary epithelia. *J. Biol. Chem.* **290**, 6857–67 (2015).

42. Yao, D., Dai, C. & Peng, S. Mechanism of the Mesenchymal–Epithelial Transition and Its Relationship with Metastatic Tumor Formation. *Mol. Cancer Res.* **9**, 1608 LP-1620 (2011).

43. Zhou, B. B. S. *et al.* Tumour-initiating cells: Challenges and opportunities for anticancer drug discovery. *Nature Reviews Drug Discovery* (2009). doi:10.1038/nrd2137

44. Singh, S. K. *et al.* Identification of human brain tumour initiating cells. *Nature* (2004). doi:10.1038/nature03128

45. Schatton, T. *et al.* Identification of cells initiating human melanomas. *Nature* (2008). doi:10.1038/nature06489

46. Al-Hajj, M., Wicha, M. S., Benito-Hernandez, A., Morrison, S. J. & Clarke, M. F. Prospective identification of tumorigenic breast cancer cells. *Proc. Natl. Acad. Sci.* **100**, 3983–3988 (2003).

47. Hope, K. J., Jin, L. & Dick, J. E. Acute myeloid leukemia originates from a hierarchy of leukemic stem cell classes that differ in self-renewal capacity. *Nat. Immunol.* (2004). doi:10.1038/ni1080

48. Reya, T., Morrison, S. J., Clarke, M. F. & Weissman, I. L. Stem cells, cancer, and cancer stem cells. *Nature* **414**, 105 (2001).

49. Choi, D. S., Rosato, R. R. & Chang, J. C. Breast cancer stem cells. in *Molecular Pathology of Breast Cancer* (2016). doi:10.1007/978-3-319-

41761-5_10

50. Kreso, A. & Dick, J. E. Evolution of the cancer stem cell model. *Cell Stem Cell* **14**, 275–91 (2014).

51. Mani, S. A. *et al.* The epithelial-mesenchymal transition generates cells with properties of stem cells. *Cell* **133**, 704–15 (2008).

52. Ye, X. *et al.* Distinct EMT programs control normal mammary stem cells and tumour-initiating cells. *Nature* **525**, 256–60 (2015).

53. Lamouille, S., Xu, J. & Derynck, R. Molecular mechanisms of epithelial–mesenchymal transition. *Nat. Rev. Mol. Cell Biol.* **15**, 178 (2014).

54. Morel, A. P. *et al.* Generation of breast cancer stem cells through epithelial-mesenchymal transition. *PLoS One* (2008). doi:10.1371/journal.pone.0002888

55. Oskarsson, T., Batlle, E. & Massagué, J. Metastatic Stem Cells: Sources, Niches, and Vital Pathways. *Cell Stem Cell* **14**, 306–321 (2014).

56. Eyler, C. E. & Rich, J. N. Survival of the Fittest: Cancer Stem Cells in Therapeutic Resistance and Angiogenesis. *J. Clin. Oncol.* **26**, 2839–2845 (2008).

57. Abdullah, L. N. & Chow, E. K.-H. Mechanisms of chemoresistance in cancer stem cells. *Clin. Transl. Med.* **2**, 3 (2013).

58. Asiedu, M. K., Ingle, J. N., Behrens, M. D., Radisky, D. C. & Knutson, K. L. TGFbeta/TNF(alpha)-mediated epithelial-mesenchymal transition generates breast cancer stem cells with a claudin-low phenotype. *Cancer Res.* **71**, 4707–19 (2011).

59. Chaudhury, A. *et al.* TGF-beta-mediated phosphorylation of hnRNP E1 induces EMT via transcript-selective translational induction of Dab2 and ILEI. *Nat. Cell Biol.* **12**, 286–93 (2010).

60. Hussey, G. S. *et al.* Identification of an mRNP complex regulating tumorigenesis at the translational elongation step. *Mol. Cell* **41**, 419–31 (2011).

61. Hussey, G. S. *et al.* Establishment of a TGFβ-induced post-transcriptional EMT gene signature. *PLoS One* **7**, e52624 (2012).

62. Zhu, Y. *et al.* Cloning, expression, and initial characterization of a novel cytokine-like gene family. *Genomics* **80**, 144–50 (2002).

63. Kishimoto, T. IL-6: From its discovery to clinical applications. *Int. Immunol.* (2010). doi:10.1093/intimm/dxq030

64. Bruce, A. G., Linsley, P. S. & Rose, T. M. Oncostatin M. *Prog. Growth Factor Res.* (1992). doi:10.1016/0955-2235(92)90029-H

65. Song, J. H., Houde, A. & Murphy, B. D. Cloning of leukemia inhibitory factor (LIF) and its expression in the uterus during embryonic diapause and implantation in the mink (Mustela vison). *Mol. Reprod. Dev.* (1998). doi:10.1002/(SICI)1098-2795(199809)51:1<13::AID-MRD2>3.0.CO;2-Z

66. Waerner, T. *et al.* ILEI: a cytokine essential for EMT, tumor formation, and late events in metastasis in epithelial cells. *Cancer Cell* **10**, 227–39 (2006).

67. Lahsnig, C. *et al.* ILEI requires oncogenic Ras for the epithelial to mesenchymal transition of hepatocytes and liver carcinoma progression. *Oncogene* **28**, 638–50 (2009).

68. Katahira, T., Nakagiri, S., Terada, K. & Furukawa, T. Secreted factor FAM3C (ILEI) is involved in retinal laminar formation. *Biochem. Biophys. Res. Commun.* **392**, 301–6 (2010).

69. Hirai, H., Karian, P. & Kikyo, N. Regulation of embryonic stem cell self-renewal and pluripotency by leukaemia inhibitory factor. *Biochem. J.* **438**, 11–23 (2011).

70. Aghajanova, L. Leukemia inhibitory factor and human embryo implantation. in *Annals of the New York Academy of Sciences* (2004). doi:10.1196/annals.1335.020

71. HEINRICH, P. C. *et al.* Principles of interleukin (IL)-6-type cytokine signalling and its regulation. *Biochem. J.* **374**, 1 LP-20 (2003).

72. Leonard, W. J. & O'Shea, J. J. JAKS AND STATS: Biological Implications. *Annu. Rev. Immunol.* **16**, 293–322 (1998).

73. Fahmi, A. *et al.* p42/p44-MAPK and PI3K are sufficient for IL-6 family cytokines/gp130 to signal to hypertrophy and survival in cardiomyocytes in the absence of JAK/STAT activation. *Cell. Signal.* **25**, 898–909 (2013).

74. Chen, D. *et al.* LIFR is a breast cancer metastasis suppressor upstream of the Hippo-YAP pathway and a prognostic marker. *Nat. Med.* **18**, 1511–7 (2012).

75. Johnson, R. W. *et al.* Induction of LIFR confers a dormancy phenotype in breast cancer cells disseminated to the bone marrow. *Nat. Cell Biol.* **18**, 1078–1089 (2016).

76. Luo, Q. *et al.* LIFR functions as a metastasis suppressor in hepatocellular

carcinoma by negatively regulating phosphoinositide 3-kinase/AKT pathway. *Carcinogenesis* **36**, 1201–12 (2015).

77. Ma, D. *et al.* Leukemia inhibitory factor receptor negatively regulates the metastasis of pancreatic cancer cells in vitro and in vivo. *Oncol. Rep.* **36**, 827–36 (2016).

78. Guo, H., Cheng, Y., Martinka, M. & McElwee, K. High LIFr expression stimulates melanoma cell migration and is associated with unfavorable prognosis in melanoma. *Oncotarget* **6**, 25484–98 (2015).

79. Lv, S. *et al.* Histone methyltransferase KMT2D sustains prostate carcinogenesis and metastasis via epigenetically activating LIFR and KLF4. *Oncogene* **37**, 1354–1368 (2018).

80. Csiszar, A. *et al.* Interleukin-like epithelial-to-mesenchymal transition inducer activity is controlled by proteolytic processing and plasminogen-urokinase plasminogen activator receptor system-regulated secretion during breast cancer progression. *Breast Cancer Res.* **16**, 433 (2014).

81. Johansson, P. *et al.* FAM3B PANDER and FAM3C ILEI represent a distinct class of signaling molecules with a non-cytokine-like fold. *Structure* (2013). doi:10.1016/j.str.2012.12.009

82. Howley, B. V, Hussey, G. S., Link, L. A. & Howe, P. H. Translational regulation of inhibin βA by TGFβ via the RNA-binding protein hnRNP E1 enhances the invasiveness of epithelial-to-mesenchymal transitioned cells. *Oncogene* **35**, 1725–35 (2016).

83. James, P., Halladay, J. & Craig, E. A. Genomic libraries and a host strain

designed for highly efficient two-hybrid selection in yeast. *Genetics* (1996).

84. Brill, B., Boecher, N., Groner, B. & Shemanko, C. S. A sparing procedure to clear the mouse mammary fat pad of epithelial components for transplantation analysis. *Lab. Anim.* **42**, 104–10 (2008).

85. Liu, F., Gu, L.-N., Shan, B.-E., Geng, C.-Z. & Sang, M.-X. Biomarkers for EMT and MET in breast cancer: An update. *Oncol. Lett.* **12**, 4869–4876 (2016).

86. Yates, L. R. *et al.* Genomic Evolution of Breast Cancer Metastasis and Relapse. *Cancer Cell* **32**, 169–184.e7 (2017).

87. Yu, M. *et al.* Circulating breast tumor cells exhibit dynamic changes in epithelial and mesenchymal composition. *Science* **339**, 580–4 (2013).

88. Tsai, J. H., Donaher, J. L., Murphy, D. A., Chau, S. & Yang, J. Spatiotemporal regulation of epithelial-mesenchymal transition is essential for squamous cell carcinoma metastasis. *Cancer Cell* **22**, 725–36 (2012).

89. Velasco-Velázquez, M. A., Homsi, N., De La Fuente, M. & Pestell, R. G. Breast cancer stem cells. *Int. J. Biochem. Cell Biol.* **44**, 573–7 (2012).

90. Lessard, J. & Sauvageau, G. Bmi-1 determines the proliferative capacity of normal and leukaemic stem cells. *Nature* **423**, 255–60 (2003).

91. Chiou, S.-H. *et al.* Positive correlations of Oct-4 and Nanog in oral cancer stem-like cells and high-grade oral squamous cell carcinoma. *Clin. Cancer Res.* **14**, 4085–95 (2008).

92. Tomita, H., Tanaka, K., Tanaka, T. & Hara, A. Aldehyde dehydrogenase 1A1 in stem cells and cancer. *Oncotarget* **7**, 11018–32 (2016).

93. Hasegawa, H., Liu, L., Tooyama, I., Murayama, S. & Nishimura, M. The FAM3 superfamily member ILEI ameliorates Alzheimer's disease-like pathology by destabilizing the penultimate amyloid-β precursor. *Nat. Commun.* **5**, 3917 (2014).

94. Määttä, J. A. *et al.* Fam3c modulates osteogenic cell differentiation and affects bone volume and cortical bone mineral density. *Bonekey Rep.* **5**, 787 (2016).

95. Korkaya, H. *et al.* Activation of an IL6 inflammatory loop mediates trastuzumab resistance in HER2+ breast cancer by expanding the cancer stem cell population. *Mol. Cell* **47**, 570–84 (2012).

96. Kim, S.-Y. *et al.* Role of the IL-6-JAK1-STAT3-Oct-4 pathway in the conversion of non-stem cancer cells into cancer stem-like cells. *Cell. Signal.* **25**, 961–9 (2013).

97. Ginestier, C. *et al.* CXCR1 blockade selectively targets human breast cancer stem cells in vitro and in xenografts. *J. Clin. Invest.* **120**, 485–97 (2010).

98. Nicola, N. A. & Babon, J. J. Leukemia inhibitory factor (LIF). *Cytokine Growth Factor Rev.* **26**, 533–44 (2015).

99. Yue, X., Wu, L. & Hu, W. The regulation of leukemia inhibitory factor. *Cancer cell Microenviron.* **2**, (2015).

100. Li, X. *et al.* LIF promotes tumorigenesis and metastasis of breast cancer through the AKT-mTOR pathway. *Oncotarget* **5**, 788–801 (2014).

101. Wahl, G. M. & Spike, B. T. Cell state plasticity, stem cells, EMT, and the

generation of intra-tumoral heterogeneity. *NPJ breast cancer* **3**, 14 (2017).

102. Forozan, F. *et al.* Molecular cytogenetic analysis of 11 new breast cancer cell lines. *Br. J. Cancer* **81**, 1328–34 (1999).
103. Matsui, W. H. Cancer stem cell signaling pathways. *Medicine (Baltimore).* **95**, S8–S19 (2016).
104. Junk, D. J. *et al.* Oncostatin M promotes cancer cell plasticity through cooperative STAT3-SMAD3 signaling. *Oncogene* **36**, 4001–4013 (2017).
105. Hu, Y. & Smyth, G. K. ELDA: Extreme limiting dilution analysis for comparing depleted and enriched populations in stem cell and other assays. *J. Immunol. Methods* **347**, 70–78 (2009).
106. Howley, B. V, Link, L. A., Grelet, S., El-Sabban, M. & Howe, P. H. A CREB3-regulated ER-Golgi trafficking signature promotes metastatic progression in breast cancer. *Oncogene* **37**, 1308–1325 (2018).
107. Thomas, S. J., Snowden, J. A., Zeidler, M. P. & Danson, S. J. The role of JAK/STAT signalling in the pathogenesis, prognosis and treatment of solid tumours. *Br. J. Cancer* **113**, 365–71 (2015).
108. Wang, T. *et al.* JAK/STAT3-Regulated Fatty Acid β-Oxidation Is Critical for Breast Cancer Stem Cell Self-Renewal and Chemoresistance. *Cell Metab.* **27**, 136–150.e5 (2018).
109. Wang, X. *et al.* STAT3 mediates resistance of CD44(+)CD24(-/low) breast cancer stem cells to tamoxifen in vitro. *J. Biomed. Res.* **26**, 325–35 (2012).
110. Ishihara, K. & Hirano, T. Molecular basis of the cell specificity of cytokine action. *Biochim. Biophys. Acta* **1592**, 281–96 (2002).

111. Underhill-Day, N. & Heath, J. K. Oncostatin M (OSM) cytostasis of breast tumor cells: characterization of an OSM receptor beta-specific kernel. *Cancer Res.* **66**, 10891–901 (2006).

112. Port, M. D., Gibson, R. M. & Nathanson, N. M. Differential stimulation-induced receptor localization in lipid rafts for interleukin-6 family cytokines signaling through the gp130/leukemia inhibitory factor receptor complex. *J. Neurochem.* **101**, 782–93 (2007).

113. Gerlinger, M. *et al.* Intratumor heterogeneity and branched evolution revealed by multiregion sequencing. *N. Engl. J. Med.* **366**, 883–892 (2012).

114. Skiniotis, G., Lupardus, P. J., Martick, M., Walz, T. & Garcia, K. C. Structural Organization of a Full-Length gp130/LIF-R Cytokine Receptor Transmembrane Complex. *Mol. Cell* (2008). doi:10.1016/j.molcel.2008.08.011

115. Pennica, D. *et al.* Expression cloning of cardiotrophin 1, a cytokine that induces cardiac myocyte hypertrophy. *Proc. Natl. Acad. Sci.* (1995). doi:10.1073/pnas.92.4.1142

116. Stahl, N. *et al.* Association and activation of Jak-Tyk kinases by CNTF-LIF-OSM-IL-6 β receptor components. *Science (80-.).* (1994). doi:10.1126/science.8272873

117. Boulanger, M. J. & Garcia, K. C. Shared cytokine signaling receptors: structural insights from the gp130 system. *Adv. Protein Chem.* **68**, 107–46 (2004).

118. Oh, H. *et al.* Activation of phosphatidylinositol 3-kinase through

glycoprotein 130 induces protein kinase B and p70 S6 kinase phosphorylation in cardiac myocytes. *J. Biol. Chem.* (1998). doi:10.1074/jbc.273.16.9703

119. Walker, E. C. *et al.* Oncostatin M promotes bone formation independently of resorption when signaling through leukemia inhibitory factor receptor in mice mice. *J. Clin. Invest.* (2010). doi:10.1172/JCI40568
120. Rao, M. S. *et al.* Leukemia inhibitory factor mediates an injury response but not a target-directed developmental transmitter switch in sympathetic neurons. *Neuron* (1993). doi:10.1016/0896-6273(93)90229-K
121. Matsuda, T. *et al.* STAT3 activation is sufficient to maintain an undifferentiated state of mouse embryonic stem cells. *EMBO J.* (1999). doi:10.1093/emboj/18.15.4261
122. Niwa, H., Burdon, T., Chambers, I. & Smith, A. Self-renewal of pluripotent embryonic stem cells is mediated via activation of STAT3. *Genes Dev.* (1998). doi:10.1101/gad.12.13.2048
123. Wang, G., Matsuura, I., He, D. & Liu, F. Transforming growth factor-β-inducible phosphorylation of Smad3. *J. Biol. Chem.* (2009). doi:10.1074/jbc.M809281200
124. Postigo, A. A., Depp, J. L., Taylor, J. J. & Kroll, K. L. Regulation of Smad signaling through a differential recruitment of coactivators and corepressors by ZEB proteins. *EMBO J.* (2003). doi:10.1093/emboj/cdg226
125. Naber, H. P. H., Drabsch, Y., Snaar-Jagalska, B. E., ten Dijke, P. & van Laar, T. Snail and Slug, key regulators of TGF-β-induced EMT, are

sufficient for the induction of single-cell invasion. *Biochem. Biophys. Res. Commun.* (2013). doi:10.1016/j.bbrc.2013.04.037

126. Woosley, A. N. *et al.* TGFβ promotes breast cancer stem cell self-renewal through an ILEI/LIFR signaling axis. *Oncogene* (2019). doi:10.1038/s41388-019-0703-z
127. Liu, R. Y. *et al.* JAK/STAT3 signaling is required for TGF-β-induced epithelial- mesenchymal transition in lung cancer cells. *Int. J. Oncol.* (2014). doi:10.3892/ijo.2014.2310
128. Heppner, G. H., Miller, F. R. & Shekhar, P. V. M. Nontransgenic models of breast cancer. *Breast Cancer Research* (2000). doi:10.1186/bcr77
129. Jinnin, M. Characterization of SIS3, a Novel Specific Inhibitor of Smad3, and Its Effect on Transforming Growth Factor-beta1-Induced Extracellular Matrix Expression. *Mol. Pharmacol.* (2005). doi:10.1124/mol.105.017483
130. Schust, J., Sperl, B., Hollis, A., Mayer, T. U. & Berg, T. Stattic: A Small-Molecule Inhibitor of STAT3 Activation and Dimerization. *Chem. Biol.* (2006). doi:10.1016/j.chembiol.2006.09.018
131. Dreos, R., Ambrosini, G., Groux, R., Perier, R. C. & Bucher, P. The eukaryotic promoter database in its 30th year: Focus on non-vertebrate organisms. *Nucleic Acids Res.* (2017). doi:10.1093/nar/gkw1069
132. Mathelier, A. *et al.* JASPAR 2016: A major expansion and update of the open-access database of transcription factor binding profiles. *Nucleic Acids Res.* (2016). doi:10.1093/nar/gkv1176
133. Massagué. How cells read TGF-beta signals. *Nat. Rev. Mol. cell Biol.*

(2000).

134. Neradil, J. & Veselska, R. Nestin as a marker of cancer stem cells. *Cancer Science* (2015). doi:10.1111/cas.12691

135. Zhou, Z. *et al.* RNA Binding Protein Nanos2 Organizes Post-transcriptional Buffering System to Retain Primitive State of Mouse Spermatogonial Stem Cells. *Dev. Cell* (2015). doi:10.1016/j.devcel.2015.05.014

136. Dravis, C. *et al.* Sox10 Regulates Stem/Progenitor and Mesenchymal Cell States in Mammary Epithelial Cells. *Cell Rep.* (2015). doi:10.1016/j.celrep.2015.08.040

137. Jeter, C. R., Yang, T., Wang, J., Chao, H. P. & Tang, D. G. Concise Review: NANOG in Cancer Stem Cells and Tumor Development: An Update and Outstanding Questions. *Stem Cells* (2015). doi:10.1002/stem.2007

138. Ramsay, R. G. & Gonda, T. J. MYB function in normal and cancer cells. *Nature Reviews Cancer* (2008). doi:10.1038/nrc2439

139. Fang, X. *et al.* Twist2 contributes to breast cancer progression by promoting an epithelial-mesenchymal transition and cancer stem-like cell self-renewal. *Oncogene* (2011). doi:10.1038/onc.2011.181

140. Jiao, X. *et al.* c-Jun induces mammary epithelial cellular invasion and breast cancer stem cell expansion. *J. Biol. Chem.* (2010). doi:10.1074/jbc.M110.100792

141. Bierie, B. & Moses, H. L. Gain or loss of TGFβ signaling in mammary carcinoma cells can promote metastasis. *Cell Cycle* (2009).

doi:10.4161/cc.8.20.9727

142. Roberts, A. B. *et al.* Smad3 is key to TGF-β-mediated epithelial-to-mesenchymal transition, fibrosis, tumor suppression and metastasis. *Cytokine and Growth Factor Reviews* (2006). doi:10.1016/j.cytogfr.2005.09.008

143. Noguchi, K. *et al.* Interleukin-like EMT inducer regulates partial phenotype switching in MITF-low melanoma cell lines. *PLoS One* (2017). doi:10.1371/journal.pone.0177830

144. MIYAZONO, K. Transforming growth factor-β signaling in epithelial-mesenchymal transition and progression of cancer. *Proc. Japan Acad. Ser. B* (2009). doi:10.2183/pjab.85.314

145. Noguchi, K. *et al.* Interleukin-like EMT inducer (ILEI) promotes melanoma invasiveness and is transcriptionally up-regulated by upstream stimulatory factor-1 (USF-1). *J. Biol. Chem.* (2018). doi:10.1074/jbc.RA118.003616

146. Reiter, F., Wienerroither, S. & Stark, A. Combinatorial function of transcription factors and cofactors. *Current Opinion in Genetics and Development* (2017). doi:10.1016/j.gde.2016.12.007

147. Miyazono, K. I. *et al.* Hydrophobic patches on SMAD2 and SMAD3 determine selective binding to cofactors. *Sci. Signal.* (2018). doi:10.1126/scisignal.aao7227

148. Yoon, J. H. *et al.* Phosphorylation status determines the opposing functions of Smad2/Smad3 as STAT3 cofactors in T<inf>H</inf>17 differentiation. *Nat. Commun.* (2015). doi:10.1038/ncomms8600

149. Giraud, S. *et al.* Functional interaction of STAT3 transcription factor with the coactivator NcoA/SRC1a. *J. Biol. Chem.* (2002). doi:10.1074/jbc.M111486200